Report no. changed (Mar 2006): SM-307-UU

SACLANTCEN MEMORANDUM
serial no.: SM-307

SACLANT UNDERSEA RESEARCH CENTRE MEMORANDUM

CELTIC DUET
A JOINT SACLANTCEN/NRL SHALLOW-WATER SEA TRIAL IN CELTIC SEA DURING JULY 1992: DATA SUMMARY

Dale D. Ellis, F. Desharnais, R.H. Clarke, R. Hollett, E. Baglioni and A. Legner

October 1996

SACLANT Undersea Research Centre
Viale San Bartolomeo 400
19138 San Bartolomeo (SP), Italy

tel: +39-187-540.111
fax: +39-187-524.600

e-mail: library@saclantc.nato.int

NORTH ATLANTIC TREATY ORGANIZATION

CELTIC DUET
A Joint SACLANTCEN / NRL Shallow-Water Sea Trial in the Celtic Sea during July 1992: Data Summary

Dale D. Ellis, F. Desharnais, R.H. Clarke,
R. Hollett, E. Baglioni and A. Legner

The content of this document pertains to work performed under Project 05 of the SACLANTCEN Programme of Work. The document has been approved for release by The Director, SACLANTCEN.

David L. Bradley
Director

intentionally blank page

CELTIC DUET
A Joint SACLANTCEN / NRL Shallow-Water Sea Trial in the Celtic Sea during July 1992: Data Summary

Dale D. Ellis, F. Desharnais, R.H. Clarke*, R. Hollett, E. Baglioni and A. Legner

Executive Summary: In July 1992 a joint shallow-water sea trial was conducted in the Celtic Sea by the SACLANT Undersea Research Centre and the US Naval Research Laboratory. The purpose was to obtain monostatic and bistatic reverberation measurements, with supporting transmission loss and environmental measurements. Three sites were chosen: one where small sand waves were deemed to be present, a second where there were large sand ridges, and a third where thin sediment over a chalk bottom was expected. Two ships were used, the NRV *Alliance*, and the USNS *Bartlett*. Both ships were equipped with towed arrays, towed acoustic projectors, vertical arrays and supporting equipment for environmental measurements. The Naval Research Laboratory designation of this trial was SWAMP-III; the original SACLANTCEN designation was AAG 92/3, or OGOPOGO-II. A follow-on SACLANTCEN sea trial obtained additional propagation and geo-acoustic measurements, which have been described in other SACLANTCEN reports.

The emphasis of this report is the description of the experiments, the ship tracks, and environmental inputs. A summary of the waverider analysis carried out at Imperial College in the UK is included. Some acoustic results are shown, describing checks on the data quality and illustrating representative data for propagation, ambient noise and reverberation.

Data from the sea trial have been exported for acoustic research to the US (Naval Research Labratory, and Applied Research Laboratories at Penn State University), Canada (Defence Research Establishment Atlantic), and the UK (Imperial College).

*) Imperial College of Science, Technology and Medicine, London, UK

intentionally blank page

CELTIC DUET
A Joint SACLANTCEN / NRL Shallow-Water Sea Trial in the Celtic Sea during July 1992: Data Summary

Dale D. Ellis, F. Desharnais, R.H. Clarke*, R. Hollett, E. Baglioni, and A. Legner

Abstract: In July 1992 a joint shallow-water sea trial was conducted in the Celtic Sea by the SACLANT Undersea Research Centre and the US Naval Research Laboratory. The purpose was to obtain monostatic and bistatic reverberation measurements, with supporting transmission loss and environmental measurements. Three sites were chosen: one where small sand waves were deemed to be present, a second where there were large sand ridges, and a third where thin sediment over a chalk bottom was expected. Two ships were used, the NRV *Alliance*, and the USNS *Bartlett*. Both ships were equipped with towed arrays and towed projectors. Both ships had vertical arrays and supporting equipment for environmental measurements. A follow-up sea trial obtained additional propagation and geo-acoustic measurements. The report describes the experiments, the ship tracks, and environmental inputs. Some results are shown, including a summary of the waverider analysis carried out at Imperial College in the UK. A few acoustic results are shown, describing checks on the data quality and illustrating representative data for propagation, ambient noise and reverberation.

Keywords: reverberation, ambient noise, propagation, sea-surface spectra, sound speed profiles

*) Imperial College of Science, Technology and Medicine, London, UK

Contents

1 Introduction

The Celtic Duet Trial took place on the European continental shelf, the Southwestern Approaches of the English Channel to the south and west of the UK, during July 1992. The two participating laboratories were the SACLANT Undersea Research Centre and the US Naval Research Laboratory (NRL) in Washington, DC. The main purpose of the trial was to obtain calibrated monostatic and bistatic reverberation data, with supporting propagation and environmental measurements. The ultimate goal is to validate shallow-water sonar models and understand the underlying scattering processes.

Two vessels were used, the NRV *Alliance* and the USNS *Bartlett*. Each vessel carried a towed projector, towed horizontal array, and a deployable vertical moored array. Three sites were investigated (Fig. 1). Site A has a hard flat bottom of about 100 m depth. Site B has a bottom consisting of pronounced sand ridges aligned in almost perfect one-dimensional corrugations. Site C has a mixed chalk and compacted sediment bottom.

The primary sound sources used during the trial were projectors, sending CW, FM, and other pulses and wave trains. Most of the experiments were conducted near 400 Hz, but the Centre's source was occasionally operated at frequencies from 300 Hz up to 1280 Hz. At Site B, explosive charges were used during one experiment. Various tracks were used by the two ships, including triangular, radial, and pentagonal runs.

Transmission loss and time spreading measurements were made using an echo-repeater. Several CW transmission loss tows were made to determine propagation loss, fluctuations, and spectral spreading.

Throughout the trial the *Alliance* IMS (Information Management System) monitored the sea state, wind speed and direction and the ship's position, speed and heading. The sound-speed profiles were monitored by taking conductivity, temperature, and depth measurements (CTDs) at the beginning and end of each run. Expendable bathy-thermographs (XBTs) were taken at intervals. There was a classic summer profile of two regions of constant sound speed, the higher sound speed region lying over the lower and separated by a thermocline between 20 and 50 m. At Sites B and C, a waverider buoy was deployed to obtain the sea surface spectra. Acoustic Doppler current profiling measurements were made throughout the trial to monitor the high tidal currents expected in the region. Some *Bartlett* environmental information is also included, including XBTs, navigational information, and bathymetry.

The bottom profile (bathymetry) was monitored continuously using the ships' echo sounders. A Uniboom seabed profiler survey was conducted at Site A. A follow-on cruise by the SACLANTCEN Seabed Acoustics Group obtained additional seabed information, and the seabed characteristics have been analysed [1].

2
Cruise Information

This section contains a description of the experiments, the environmental information obtained, and the equipment used in the sea trial. Details are presented in Appendices A, B, and C.

2.1. EXPERIMENTS

Table 1 outlines the date and start and finish times in UTC (Coordinated Universal Time) of each experiment conducted during the experimental trial Celtic Duet (AAG 92-3), with reference to the site where each experiment occurred. The three sites - A, B and C - are described in the Cruise Plan, Cruise Report, and *Alliance* Cruise Log. Some of the experiments were executed by SACLANTCEN only (with NRV *Alliance*), and others were executed in collaboration with the Naval Research Laboratory (USNS *Bartlett*). The run numbers in Table 1 are code names associated with each acoustic or non-acoustic experiment; different names were used by SACLANTCEN and NRL. Some runs involved NRL and the *Bartlett* only; these experiments are not listed here. Figure 2 supplements Table 1 as it briefly summarizes the main hardware deployments for each day of the experimental trial.

Table 1 *Experiment summary for the experimental trial Celtic Duet*

Experiment	Start: (Day) UTC	Finish: (Day) UTC	Site	*Alliance* Run #s	*Bartlett* Run #s
Bathymetry survey	(4) 2140	(5) 0049	A	BATHY1	
Ping transmission - radial tracks	(5) 0810	(5) 2000	A	A1	106A-F, 107A-F
Ping transmission - triangular tracks	(6) 0825	(6) 1910	A	A2	108A-C, 109A-D, 110A
CW tone transmission	(6) 1945	(6) 2015	A	CW1	
Bathymetry survey	(7) 0310	(8) 0730	B	BATHY2	
Transmission loss and reverberation with pings	(8) 1200	(9) 0440	B	TLB	

Table 1 (continued)

Experiment	Start: (Day) UTC	Finish: (Day) UTC	Site	*Alliance* Run #s	*Bartlett* Run #s
CW tone transmission	(8) 1612	(8)1725	B	CW2	
Ping transmission - triangular tracks	(9) 0845	(9) 1645	B	B1	
SUS charge run	(10) 1330	(10) 1900	B	B2SUS	203A-F
Ping transmission - triangular tracks	(11) 0825	(11) 1900	B	B2	204A-E, 205A-C, 206 A-D
CW tone transmission	(11)1843	(11) 1924	B	CW3	
Ping transmission - parallel tracks	(12) 0925	(12) 1900	B	B3	207A-K
Ping transmission - radial tracks	(13) 0855	(13) 1835	B	B4	208A-B, 209A-F
Bathymetry survey	(14) 2135	(15) 0510	C	BATHY3	
Ping transmission - radial tracks	(15) 1115	(15) 1820	C	C1	301A-F, 302A-D
Bathymetry survey	(15) 2200	(16) 0615	C	BATHY4	
Ping transmission - triangular tracks	(16) 0930	(16) 1640	C	C2	304A-C, 305A-C
Ping transmission - triangular tracks	(17) 0830	(17) 1930	C	C3	308A-F, 309A-C
Reverberation polygon	(18) 1025	(18) 2030	C	POLYG1	
Reverberation polygon	(20) 0805	(20) 1825	A	POLYG2	
Uniboom survey	(20) 2020	(21) 1100	A	UNIBOOM	

The experiments are briefly described below. Track plots for each of the experiments are given in Appendix A.

4-5 July: Bathymetric survey (BATHY1)

The bathymetric survey covered an area of 4 by 4 n. mi. at Site A. The *Alliance* track is shown in Fig. A-1. The bathymetric information collected with the echo-sounder during the bathymetry surveys is shown in the next section (Ship, Weather and Sea Information). No acoustic data were collected.

5 July: Ping transmission - radial tracks (A1)

Both ships towed a horizontal array and a projector for monostatic and bistatic reverberation measurements. The acoustic signals were pulses and wave trains of various frequencies (see Section 2.6). The *Alliance* and *Bartlett* tracks are shown in Fig. A-2. The *Alliance* sent pings during the outgoing leg, and the *Bartlett* sent pings during the incoming leg.

6 July: Ping transmission - triangular tracks (A2)

Both vessels towed their sound source and horizontal array. The sound sources transmitted alternately every three minutes. The ships' tracks are shown in Fig. A-3; the gap in the *Bartlett* track is due to a lack of navigation data between 9:15 and 12:00 UTC.

6 July: First CW tone transmission (CW1)

At the end of the preceding experiment, the *Bartlett* source transmitted a CW tone at 350.31 Hz which *Alliance* recorded on its horizontal array. The ships' tracks are shown in Fig. A-4. The acoustic data were recorded for a period of 30 min.

7-8 July: Bathymetric survey (BATHY2)

An extensive bathymetric survey by *Alliance* over Site B lasted for more than 24 hours. The *Alliance* track is shown in Fig. A-5, and the echo-sounder data are shown in the next section. The purpose was to determine the peaks and troughs of the ridges for deployment of the vertical arrays in later experiments.

8 July: Second CW tone transmission (CW2)

The *Alliance* source transmitted a CW tone at 375 Hz which was recorded on the vertical array. Acoustic data were recorded for a period of 73 min. during two periods. For the first period the track is shown in Fig. A-6; the second CW period was included in the next experiment (TLB), in track Fig. A-7.

8-9 July - Transmission loss and reverberation (TLB)

This was an experiment to obtain long-range transmission loss, received by NRL. At short ranges (less than 10 n. mi.) the data were also received on the SACLANTCEN vertical array. The tracks of both vessels are shown in Fig. A-7. During the outgoing leg, the

Alliance source transmitted multiple CW tones for transmission loss measurements. During the incoming leg, the *Alliance* source transmitted pings with a three-minute repetition rate for reverberation measurements.

9 July: Ping transmission - triangular tracks (B1)

During this experiment, *Alliance* deployed both the vertical and horizontal arrays, and the sound source. *Bartlett* also deployed the NRL sound source and horizontal array. The sources sent pings alternately every four minutes. The tracks are shown in Fig. A-8.

10 July: SUS charge run (B2SUS)

Alliance deployed its vertical array and *Bartlett* deployed its horizontal array. *Alliance* dropped SUS charges at 10 min. intervals along the 210° and 030° legs of the track shown in Fig. A-9. *Alliance*'s speed was 10 kn during the SUS drops, while *Bartlett*'s speed was 4 kn.

11 July: Ping transmission - triangular tracks (B2)

Alliance deployed both arrays (vertical and horizontal) and its sound source. *Bartlett* deployed its sound source and horizontal array. Both sources transmitted pings alternately every 4 minutes. The tracks are shown in Fig. A-10.

11 July: Third CW tone transmission (CW3)

At the end of the previous experiment, the *Alliance* source transmitted a CW tone at 375 Hz which was recorded on the vertical array. The tracks are shown in Fig. A-11. The acoustic data were recorded for a period of 30 min.

12 July: Ping transmission - parallel tracks (B3)

Both vessels deployed their sound source and horizontal array. The vessels followed parallel tracks, as shown in Fig. A-12, while the *Alliance* sound source transmitted pings every four minutes. Occasional CW tones were sent. *Bartlett*'s sound source was not working during this period.

13 July: Ping transmission - radial tracks (B4)

Both vessels deployed their sound source and horizontal array. The vessels followed opposite tracks, as shown in Fig. A-13, while the *Alliance* sound source transmitted pings every four min.

14-15 July: Bathymetric survey (BATHY3)

A bathymetric survey was conducted by *Alliance* over Site C, during the night of 14 to 15 July. The *Alliance* track is shown in Fig. A-14.

15 July: Ping transmission - radial tracks (C1)

Both vessels deployed their sound source and horizontal array. The vessels followed opposite tracks, as shown in Fig. A-15.

15-16 July: Bathymetric survey (BATHY4)

This bathymetric survey was the second one executed by *Alliance* over Site C, during the night of 15 to 16 July. The *Alliance* track is shown in Fig. A-16.

16 July: Ping transmission and echo-repeater experiment - triangular tracks (C2)

Alliance deployed both vertical and horizontal arrays, and sound source. The vertical array was noisy due to the shallow water, so data were recorded for only part of the time. *Bartlett* also deployed their sound source and horizontal array. The tracks are shown in Fig. A-17. On the outgoing leg, *Bartlett* sent pings every 3 or 4 minutes, and *Alliance* echo-repeated every second ping. On the anti-parallel leg, the sources sent pings alternately. On the incoming leg, *Alliance* sent the pings, and *Bartlett* echo-repeated every second ping.

17 July: Ping transmission - triangular tracks (C3)

Alliance and *Bartlett* deployed their horizontal arrays and sound sources. The sources sent pings alternately. The ships' tracks are shown in Fig. A-18. The apparent jumps in *Alliance*'s track are due to occasional updating of the inertial navigation fixes. The *Alliance* GPS was not working, for this or subsequent experiments. The gap in the *Bartlett* track is due to the unavailability of navigational data between 15:10 and 16:00.

18 July: Reverberation polygon (POLYG1)

Alliance deployed its sound source and horizontal array at site C, and made a 5-sided polygonal track (Fig. A-19) for reverberation measurements, sending several pings at various frequencies and array apertures. *Bartlett* did not participate in this experiment.

20 July: Reverberation polygon (POLYG2)

Alliance deployed its sound source and horizontal array at site A, and made a second reverberation polygon (Fig. A-20), similar to the site C experiment on 18 July. *Bartlett* did not participate in this experiment.

20-21 July: Uniboom survey (UNIBOOM)

Alliance deployed the Uniboom equipment, and made a bottom survey following the track shown in Fig. A-21. The data were recorded on the straight parts of the track only. The *Alliance* GPS was not working.

2.2. SHIP, WEATHER AND SEA INFORMATION

This section describes some of the information collected by the non-acoustic sensors on board *Alliance* and *Bartlett*. Figures in Appendix B include, for each experiment as defined in Table 1 and for each vessel participating in the experiment:

1. water depth (m) along the track;
2. sea state;
3. wind speed (knots);
4. wind direction (°T) corrected for ship motion;
5. ship speed (knots); and
6. ship direction (°T).

The water depth readings from *Alliance* have occasional spikes that have not been edited.

The sea state readings are entered manually into the non-acoustic data management system, and if no update is entered at any given time, the previous reading is kept. Delays in updating the sea state are possible, although one expects the sea state to lag a change in wind speed anyway.

Although the vessels had different tracks, they were usually close to each other. For this reason, the water depth along the *Alliance* track and the *Bartlett* track are expected to be slightly different, but the wind speed and direction should be similar. However, the wind speed sensor on *Alliance* is badly located (behind the main mast), therefore the wind readings for *Alliance* are biased when the wind direction is close to the ship heading. This bias is evident in several cases where the correlation is excellent between the corrected wind direction and ship heading (for example in Fig. B-3, run A2). In such a case, the wind speed is usually underestimated. Also, if the wind is from astern, the wind speed will sometimes be over-estimated due to turbulence behind the mast. For this reason, the wind readings from *Alliance* should be used with care.

Ship and wind directions toward the north produce vertical lines in the display, caused by fluctuations between small positive bearings and bearings just less than 360°.

2.3. XBTs AND CTDs

Soundings were taken of the conductivity, temperature, and depth (CTDs) at the beginning and end of each run. Expendable bathythermographs (XBTs) were deployed occasionally. During the trial, *Alliance* deployed 48 XBTs, 1 expendable conductivity-temperature-depth probe (XCTD), and produced 18 CTD records. *Bartlett* deployed 53 XBTs. Table 2 summarizes the measurements from each site, and indicates where figures of the sound speed profiles can be found.

Appendix C contains details of the profiles. The tables summarize the information for each record: launch platform, record number, date/time of launch, and latitude/longitude/site of launch. Figures C-1 to C-16 show the sound speed profiles. A maximum of 10 profiles was included in each figure for clarity, and a single scale was used for ease of comparison. Note that the XBTs apparently extend deeper than the bottom because the depth reading is time-function based on the rate of fall. The tables in Appendix C should be consulted to determine the actual water depth.

The profiles are typical of the area for the summer season. A fairly shallow warm layer is present at the surface of the ocean, overlaying a steep thermocline. The depth of the minimum sound speed is around 20-30 m at site A, 40-60 m at site B, and 30-40 m at site C. The sound speeds below the minimum are slightly lower at sites B and C than at site A, which is the most shallow site. Overall, the sound speed profiles are similar within each area, independent of the type of probe or of the platform.

Table 2 *Origin of sound speed profiles and figure organization*

Site	Platform	Probe type	Profile #	Figure #
A	*Alliance*	XCTD	1	C-1
A	*Alliance*	CTD	1-3, 18, 19	C-2
A	*Alliance*	XBT	44-48	C-3
A	*Bartlett*	XBT	1-9	C-4
A	*Bartlett*	XBT	10-17	C-5
B	*Alliance*	XBT	1-10	C-6
B	*Alliance*	XBT	11-20	C-7
B	*Alliance*	XBT	21-29	C-8
B	*Alliance*	CTD	4-10 (except 5)	C-9
B	*Bartlett*	XBT	18-26	C-10
B	*Bartlett*	XBT	27-35	C-11
C	*Alliance*	XBT	30-36	C-12
C	*Alliance*	XBT	37-43	C-13
C	*Alliance*	CTD	11-17	C-14
C	*Bartlett*	XBT	36-45	C-15
C	*Bartlett*	XBT	46-55	C-16

2.4. BOTTOM INFORMATION

The three sites were selected for the cruise on the basis of bottom topography and expected bottom type. Acoustic information obtained from previous propagation and ambient noise investigations in the area was also available. Site A was chosen because it was relatively flat, and there was evidence of regions with small sand waves [2]. Site B was chosen for the long ridging sand waves, which should show directional effects in propagation and scattering. The ridges, running NE-SW, can be seen in Fig. 3, and the striking periodicity of them can be seen from a portion of the echo-sounder survey perpendicular to the crests (Fig. 4). Site C was chosen for its thin sediment cover over a chalk bottom. The intent was to look for a strong frequency dependence in scattering and propagation, as Ellis and Chapman [3, 4] had reported for propagation over a similar area. However, broadband experiments were not conducted, since the use of SUS charges was deemed inappropriate: 18 m SUSs would detonate close to the ship, and the 100 m water depth left too small a depth margin for the 90 m SUSs.

2.4.1. *Bottom characteristics*

The SACLANTCEN Seafloor Acoustic Group (SAG) explored the bottom characteristics at three sites in the area of the *Celtic Duet* cruise. Figure 3 shows the positions, where Uniboom measurements were carried out during our cruise and in course of a subsequent experiment by the SAG Group. Much of the following interpretation is from Max *et al.* [1].

Site A

The bottom at Site A has a very flat erosional surface. The composition of the upper bottom layers varies within the area as shown in Fig. 5. North of 49°30' N the bottom is composed of chalk and to the south the bottom is composed of an essentially conformable Paleocene sequence of clay, sand, and calcareous beds overlying a basal hard, white limestone. There is a narrow transition zone between the two different bottoms.

The area also has patches of high reflectivity. Multiple fathometer returns were visible in the NRL low-frequency echo sounder; see Fig. 19 of Max *et al.* [1].

Site B

The bottom at Site B is relatively smooth, but not flat, the predominant bottom features being long NE-SW asymmetric sand waves (with the steeper slope toward the NW). The surface of the large dunes was eroded during the rise of sea level. Gravel and coarse sand may cover the top of the sand waves, although the lower areas probably have fine-grained sediments. There may also be shallow, coarse-grained patches in the lower areas.

Underneath the sand waves, upper Tertiary and Plio-Pleistocene sands and gravels can be found, often with thin limy and limestone partings and beds. Troughs between the sand waves may show this unlithified sediment at the surface.

Site C

Site C has a chalk bottom with a thin, patchy sediment cover. The bottom is flat, with a relief of the order of less than 1 m, with some upstanding chalk features often not completely covered by sediments. On top of the chalk is an acoustically darker, rippled sediment, probably formed from coarse sand and gravel, which is locally buried by an acoustically lighter, infilling sand disposed in long streaks and irregular shaped patches. Recent sediment thickness is not known in detail, but is reported as thin, and thinning toward the west.

The acoustic properties of chalk can be estimated as V_p = 2.2–2.6 km/s, V_s = 1.1–1.5 km/s, and high attenuation. The sediment thickness can be modelled as between 10 and 50 cm of a coarse sandy layer with a porosity of greater than 50%. Underneath is coarse gravel resting on relatively fresh chalks or basement terrane. Unconsolidated mud within both the sand and gravel would probably have acoustic properties similar to water in porosity alone. At lower frequencies, it may prove unnecessary to model any sediment at all, although the sea bottom may be somewhat more reflective than presumed from the physical properties of the underlying bottom materials.

2.4.2. Acoustic properties

Previous measurements had given some idea of the acoustic parameters in nearby areas. Ellis and Chapman [3, 4] determined acoustic models of the bottom to fit propagation loss measurements in areas similar to sites B and C. Buckingham and Jones [5] have also obtained estimates of the critical angle, and hence average bottom sound speeds, from analysis of ambient noise data at a number of nearby or similar sites. Caiti and Max [6] calculated the properties of chalk for an area similar to Site A.

At Site A the properties of chalk north of 49°30' N are estimated to be similar to those of Caiti and Max given in Table 3, except that the shear speed may be lower near the water-basement interface. For an area south and west of Site A, Buckingham and Jones [5] obtained 1534 m/s for the bottom sound speed; this is consistent with the analysis of Max *et al.*, summarized in Section 2.4.1.

Table 3 *Properties of chalk by several authors*

Authors	Sound speed (m/s)		Relative density	Attenuation (dB/wavelength)	
	Compressional	Shear		Compressional	Shear
Ellis and Chapman [4]	2400	1000	2.2	0.24	1.0
Caiti and Max [6]	1720-2000	930-1050	2.2	0.6	0.3
Buckingham and Jones [5]	2044				
Max *et al.* [1]	2200-2600	1100-1500			

Chapman and Ellis [3] used a 3-layer bottom to fit measured propagation loss in a sand-ridge area similar to site B. Their values for the sediments and layer thicknesses were obtained from analyses of a survey made using a vertical incidence seismic reflection profiler [7]. Their acoustic model is given in Table 4.

Table 4 *Acoustic model for a sand ridge area (after Ellis and Chapman, [3])*

Layer thickness (m)	Sound speed (m/s)	Relative density	Attenuation (dB/wavelength)
2 m	1.9	1700	0.85
0–24m	2.0	1800	0.45
Half-space	2.2	2000	0.20

Buckingham and Jones' analysis of ambient noise data gave 1672 m/s for the average sediment speed for a location west of Site B; this is close to the 1700 m/s used by Ellis and Chapman in the upper layer.

To fit propagation losses for an area with a thin sediment cover over a chalk basement, Ellis and Chapman [4] used the value of the upper sand layer of Table 4, with the values of chalk shown in Table 3; their value of 2400 m/s for the compressional speed of chalk is higher than estimates by some other authors. Buckingham and Jones' analysis of ambient noise data gave 2044 m/s for a chalk bottom.

2.5. EQUIPMENT

A description of SACLANTCEN research equipment is given by Jones [8]. Table 5 indicates characteristics of some of the equipment used during Celtic Duet.

Table 5 *Characteristics of Alliance equipment used for Celtic Duet acoustic data collection and analysis*

Equipment	Characteristics
Vertical array	64 hydrophones 64 m aperture 0.5, 1.0 and 2.0 m subarrays 33 beams typical
Towed array	256 hydrophones 256 m aperture 0.5, 1.0 and 2.0 m subarrays 65 or 128 beams typical
Towed projector	2 pairs of elements 213 dB on axis SL at 400 Hz 211 dB on axis SL at 900 Hz
Data acquisition	6000 Hz sampling rate 2 HDDRs for backup of raw data 2 time-domain beamformers Complex band shift Optical disk storage Matched filter analysis

Figure 6 shows a typical deployment of the vertical array and waverider buoy during the trial. The vertical array had 64 hydrophones, spaced to allow 3 nested apertures of 32 hydrophones at spacings of 0.5 m, 1.0 m, and 2.0 m. Data from the 64 hydrophones were transmitted to the *Alliance* over a radio link. This link was generally satisfactory to a range of about 10 n. mi., at which time data dropouts and synchronization breaks began to occur. As the acoustic experiments were primarily near 400 Hz, the mid-frequency (1 m) aperture was used to form 33 beams, and the low-frequency aperture (2 m) was used to provide 32 hydrophones with maximum depth extent.

Figure 7 shows the towed array and towed sound source. The towed array used during this trial had 256 hydrophones, with 3 nested apertures of 128 phones at spacings of 0.5 m, 1.0 m, and 2.0 m. Two tow cables were used during the trial. The one with digital telemetry brought up signals from all 256 hydrophones to the HDDR (High Density Digital Recorder) and WARP (Wide Application Real-Time Processor) systems. The analogue cable allowed only 64 hydrophone signals to be brought up. The analogue system did not provide as high a data quality, but as it was necessary to reduce the number of HDDR tapes used, it provided a 4-fold reduction in raw data. As most of the work was near 400 Hz, at the lower end of the mid-frequency band, 65 beams were usually formed, even with the large aperture and digital telemetry. Occasionally 128 beams (forward endfire missing) were formed to obtain higher spatial resolution.

The sound source consisted of two pairs of flextensional transducers, deployed as a two-element vertical array operated in phase. The separation of the low-frequency pair was 1.9 m and the separation of the high frequency pair was 0.7 m.

For the vertical and towed arrays, the sampling frequency of the hydrophone time series was 6000 Hz. Data were recorded on the HDDRs at this rate. This sampling frequency was used in the time-domain beamformer in order to get maximum accuracy in the beams. However, once the beam time series were formed, it was only necessary to sample at 3000 Hz, as the data were generally around 400 Hz, and always below 1500 Hz. Usually only one HDDR was used for recording, leaving the other free for rewinding the previous tape and reloading a second. However, with both HDDRs working, both vertical and towed array data could be recorded simultaneously; this was occasionally done.

The data analysis consisted of taking the input data stream from the vertical or towed array, passing it through the hardware time-domain beamformer to the WARP system. Beams were equally spaced in cosine of the bearing angle, with a Hann weighting. The WARP system processed the data and wrote the results on disk. To reduce the quantity of archival storage, a complex band shift (CBS) procedure was developed for the trial (Appendix D). The complex band-shifted data were then stored on optical disks in VAX/VMS backup format.

2.6. PING TYPES

A rich variety of pulse types and wave trains were employed in this sea trial, particularly by *Bartlett*. The *Alliance* used a much reduced set of pulse types and repeated them more frequently.

Table 6a shows the main ping types used by SACLANTCEN for the reverberation measurements; BW refers to the bandwidth of the FM pulses; TB is the time-bandwidth product. The wave train WM1 consisted of pulses C9, H7, and H1 in sequence. Additional pulse types and wave trains were used occasionally; these are described in the cruise log book.

Table 6a *Characteristics of pulses most commonly transmitted by Alliance*

ID	Type	Duration (s)	Frequencies (Hz) Start-Stop	Frequencies (Hz) Centre	BW (Hz)	TB	Comments
H1	HFM	2.4	375-395	385	20	48	Upsweep
H7	HFM	8.0	364-370	367	6	48	Upsweep
C9	CW	8.0	400	400	-	1	
WM1	Mixed	18.4	364-400				C9+H7+H1

For a typical experiment with *Alliance* and *Bartlett* pinging alternately at 4-minute intervals, the sequence might be as shown in Table 6b.

For the pentagons, *Alliance* used a variety of frequencies and ping types on each leg. This required changing the array aperture and the source pair. Table 7 indicates the pulse types, the array aperture and the receiving filters used. The filter name and decimation rate refer to the complex-band-shifting procedure described in Appendix D.

Table 6b *Transmission sequence*

Time (minutes)	Source	Pulse type
0	*Alliance*	H1
4	*Bartlett*	WM1
8	*Alliance*	WM1
12	*Bartlett*	Pulse train
16	*Alliance*	H7
20	*Bartlett*	Pulse train
24	*Alliance*	WM1
28	*Bartlett*	Pulse train
32 ...	*Alliance* repeats above sequence	
36 ...	*Bartlett* repeats only WM1	

Table 7 *Characteristics of pulses and receiving characteristics for the pentagons*

ID	Type	Duration (s)	Frequencies (Hz) Start-Stop	Frequencies (Hz) Centre	Filter	Deci-mation	TB	Comments
C0	CW	8.0	365	365	F10	60	-	2-m aperture
H0	HFM	2.4	300-360	330	F60	25	144	128 beams
C9	CW	8.0	400	400	F10	60	-	1-m aperture
H12	HFM	2.4	365-425	395	F60	25	144	65 beams
C17	CW	8.0	700	700	F10	60	-	1-m aperture
H13	HFM	2.4	680-740	710	F60	25	144	128 beams
C25	CW	8.0	900	900	F10	60	-	0.5-m aperture
H22	HFM	2.4	870-930	900	F60	25	144	65 beams
C27	CW	8.0	1280	1280	F10	60	-	0.5-m aperture
H27	HFM	2.4	1200-1260	1230	F60	25	144	128 beams

3
Analysis of Sea Surface Spectra

Throughout the 16-day trial there was a persistent Atlantic swell, from around 290°. Initially the wind rose to 24 knots on July 5 and then fell away to almost flat calm on July 8, only to rise again to 24 knots on July 11. This persisted for a few days, then moderating for several days until July 17-18 when the wind was again blowing strongly at 24 knots, finally tailing off during the last few days of the trial, which finished on July 21. A Waverider buoy was deployed at Site B for the period July 8-12, and at Site C for July 15-16. Some histograms and surface-wave spectra were derived at the time from sea-surface height data transmitted from the Waverider buoy, and later were displayed and examined in greater detail. The following analysis was conducted at Imperial College, London.

3.1. INTRODUCTION

The Waverider® (Fig. 8) is a buoy which, following the movements of the water surface, measures waves by measuring the vertical acceleration of the buoy. The buoy consists of a spherical stainless steel sphere of 70cm diameter, which contains as main component an accelerometer sensor. The signal from the accelerometer is doubly integrated to yield the surface height, plus an arbitrary constant. This height information is then modulated onto a radio carrier transmitted by an aerial on top of the buoy. The receiving range is of several tens of km. The dimensions of the buoy imply that it will only respond to surface waves of the gravity type, since capillary waves have dimensions of centimetres or less. Indeed the manufacturers say that the Waverider response falls off significantly above about 0.8 Hz, as will be evident from the spectra derived from the data.

Each Waverider data record is of 20 min. duration, and gives the surface-wave height in cm. The sampling rate is 2.56 Hz, so each record contains 3,072 data points. In addition, at the beginning and end of each record there is often a calibration point which can be distinguished from real data points because the apparent wave height is some 20 m! A record is given a header such as the following:

07112125 . 1RW

which identifies the date (0711) as the 11th of July, and the start time of the record (2125) as 21:25 UTC. The trailing 1RW is an arbitrary identifier.

In all, there were 170 such 20-minute Waverider surface-wave height records taken in the course of the *Celtic Duet* trial, 117 at site B during the period 8th - 12th July, and a further 53 at site C during the period 15th - 16th July.

®Registered trademark by DATAWELL bv, Haarlem, The Netherlands

Wadhera [9] analysed 86 of the records taken at site B. His objectives were to:

- provide an onboard facility for producing a histogram and power spectrum for each record,
- compare the histograms and power spectra obtained with accepted standard models,
- interpret the histograms and power spectra in the light of the recorded wind speed.

His main conclusions were that:

- the first-order probability density function for the sea-surface height is to a good approximation normal (Gaussian) over the range of sea states from 2 to 5,
- there is no evidence of skewness in the distribution, outside that arising from statistical sampling,
- the power spectrum of the sea-surface height fits the Pierson-Moskowitz formula very well when the sea is fully developed,
- but when the wind suddenly decreases the spectrum maintains the same shape and responds by decreasing in overall intensity only very slowly.

3.2. STANDARD MODELS OF OCEAN SURFACE ROUGHNESS

It is generally accepted (see for example Brekhovskikh and Lysanov [10]) that the random height of the sea surface is to a good approximation normally (i.e. Gaussian) distributed with slight skewness (based on the work of Kinsman [11] who in 1965 analysed some 12,000 data points), and has a power spectral density known as the Pierson-Moskowitz [12] spectrum:

$$\Phi(\Omega) = \frac{0.0081\, g^2}{\Omega^5} \exp\left\{-0.74\left(\frac{\Omega_0}{\Omega}\right)^4\right\}$$

in which Ω is the radian frequency, g is the gravitational constant, and

$$\Omega_0 = \frac{g}{U}$$

where U is the wind speed in m/s, and Ω_0 is the frequency at which the spectrum peaks.

The Pierson-Moskowitz spectrum can be integrated to give the variance of the surface-wave height as

$$\sigma_h{}^2 = \int_0^\infty \Phi(\Omega)d\Omega = 2.74 \times 10^{-3}\frac{U^4}{g^2}$$

which gives

$$\sigma_h = 5.33 \times 10^{-3}\, U^2,$$

the standard deviation in metres, when U is in metres per second.

3.3. OBSERVATIONS

Figures 9a and 9b give the histogram and power spectral density respectively for the surface-wave height data record taken at 19:20 on July 11th, when the wind speed was 12 m/s (24 kn). It can be seen that the histogram is apparently well fitted by a Gaussian-shaped probability density function (p.d.f.) with the standard deviation σ_m = 63 cm of the record, and which compares well with the value σ_m = 77 cm given by the above formula in terms of the wind speed.

Wadhera [9] examined 86 such records, and applied the χ^2 test of goodness of fit to the histograms of each record to a Gaussian p.d.f. He found that only half the records validated the hypothesis (of Gaussian p.d.f. for surface height) at the 5% level, and so concluded that "the Gaussian approximation for the p.d.f. is good but not perfect". Wadhera also investigated the skewness and kurtosis (flatness) measures - which are based on the third and fourth central moments respectively - and found them to be negligible, by showing that they were not statistically significantly different from the skewness and kurtosis obtained for the output from MATLAB's [13] pseudo-random Gaussian number generator.

The power spectral density of Fig. 9b is shown in comparison with the Pierson-Moskowitz spectrum for a wind speed of 12 m/s. The agreement between the spectral density of the data and the Pierson-Moskowitz spectrum is very good, bearing in mind that the Waverider buoy's response is expected to fall off significantly above approximately 0.8 Hz.

In examining 86 spectra over a period of 5 days, during which the wind speed varied from 1 to 25 knots, Wadhera [9] confirmed that the sea must be fully developed (i.e., the wind has to blow at the intensity value used for at least a day for the Pierson-Moskowitz spectrum to be a good description of reality. In particular, if the wind suddenly drops to a very low value, the spectrum persists in much the same form as before with only gradual diminution of total energy.

4

Preliminary Acoustic Analyses

Although the bulk of this report provides environmental and navigational information, some acoustic analyses were carried out as an indication of data quality, and as a preview for later detailed analyses. The main analysis is on the CW propagation runs, but brief looks at the reverberation and ambient noise are also given.

4.1. CW RUNS

The post-trial analysis of the continuous-wave (CW) transmission loss data provided an excellent opportunity to assess the data quality, and to determine the geoacoustic parameters.

Continuous-wave (CW) acoustic transmission measurements were taken on five occasions. The first of these was run CW1 at Site A (very flat) on July 6 when the *Bartlett* towed a CW source transmitting a nominal 350 Hz at a speed of 4 kn, while the *Alliance* received the signal on the hydrophones of a horizontal towed array, on an opening range, also at 4 kn. The remaining CW runs took place at Site B, which has pronounced sand ridges on the bottom. Three of these four runs were made with the *Alliance* transmitting a CW 375 Hz tone and receiving on the moored vertical array; one with the *Alliance*'s track along the direction of the sandwave corrugations (run CW3), and two of them at right angles to the corrugations (run CW2 and part of run TLB). The final set of CW measurements was taken with both the *Bartlett* and the *Alliance* moving in parallel with each other and in a direction at right angles to the sand wave corrugations (run B3), at two fixed ranges of 4 n. mi. and 12 n. mi., with the *Alliance* transmitting a 375 Hz tone and the *Bartlett* receiving on its horizontal towed array. These data recorded on *Bartlett* would be very useful in determining transverse horizontal coherence.

4.1.1. Acoustic data quality

<u>Phase jumps on HDDR playbacks.</u>

A problem evident on the playbacks are some spikes in the data. Not nearly so obvious are phase jumps which can be seen by looking at the CBS (Complex-Band-Shifted) time series, shifted down in frequency to about 0.5 Hz (Fig. 10). These jumps can be found by unwrapping the phase (using the MATLAB [13] function `unwrap`) and looking for discontinuities. Figure 11a shows a particularly bad section; Fig. 11b shows a good section. The jump in channel 43 in Fig. 11b (solid line) from 1341 s to 1343 s looks like a real effect - such as the transmission loss going through a minimum.

Towed array tilt and depth variations

Run CW1 was intended to be a uniform radial tow; Figs. A-4 and B-5 indicate that *Alliance* carried out a manoeuvre at about 20:08, possibly to avoid a fishing vessel. Figure 12 shows the variation in depth of the two depth sensors during the tow. They are spaced 320 m apart, 32 m in front of the first hydrophone and 32 m behind the last hydrophone. The depth difference between the first and last sensor varies from 1 to 4 m, with an average difference of less than 3 m.

4.1.2. Propagation loss

Figure 13 presents an example of measured propagation loss *vs* range for Site A. The acoustic data are from the CW projector run (350.31 Hz) on 6 July. The *Alliance* and *Bartlett* tracks during the experiment are shown in Fig. A-4. *Bartlett* was towing the source and the data were recorded on the horizontal array towed by *Alliance*. The hydrophone located in the middle of the towed array was selected for the modelling. Only small acoustic variations were observed along the array.

Two different methods were used to convert the time information into ranges. The navigation data were used to extract the range between the source and the middle hydrophone as a function of time. The initial distance between source and receiver was 14.2 km and increased progressively to 20.6 km. The total track length of 6450 m is equivalent to an average speed of 8.3 knots (or 4.3 m/s). This speed was then compared to that obtained from the doppler shift of the 350.31 Hz tone. The doppler shift was very stable during the run, at 1.23 Hz on average. Because of that stability, the averaged value could be converted into an average speed of 5.26 m/s for the whole length of the track. This speed indicates that the total track length was 7900 m instead of 6450 m as indicated by navigation data. The discrepancy between the two approaches is large (18%), and it was assumed that the track length from the doppler information should be more reliable than that of the navigation data. (There was some uncertainty about the frequency transmitted by *Bartlett* at the time of the sea trial; this was investigated and is apparently not the cause of the discrepancy). The range shown in Fig. 13 was derived as follows: the initial range of 14.2 km was taken from the navigation data, and a fixed range increment was chosen to finish the track at 22.1 km, for a total distance of 7900 m (as given by the average doppler shift). Although the initial position of the track is not accurately known, the distance covered should be accurate, and therefore a small shift in range may be needed for a good match between acoustic data and modelling.

The bottom information from Section 2.4 was used to model the propagation loss as a function of range at Site A. There is some uncertainty as to which bottom parameters would best represent the bottom at the exact location of the experiment. As can be seen in Fig. 5, the CW run (which is in the west-east direction along the 49°30' parallel) is in the transition zone between the chalk bottom in the North and the gravelly sand bottom in the South. The limits of the transition area were carefully determined (and extrapolated) from the Uniboom survey data. The bottom parameters for that area should be similar to those of the chalk bottom, although it is suspected that the shear wave speed near the surface may be somewhat lower than that of the chalk bottom of Caiti and Max [6] at 60 m depth.

The initial modelling was produced with the bottom parameters of Caiti and Max [6] listed in Table 3 for chalk (surface layer). At the frequency of 350.31 Hz, the acoustic wavelength is of the order of 4 m and the near-surface sediments can have an impact on the propagation loss. For this reason the deeper layers with harder sediments were not included. The upper surface sediments were expected to be very thin, if at all present, so none were included in the model.

The source depth during the experiment was between 45 and 50 m, and the receiver depth varied between 52 and 59 m depending on the receiver location along the array, and on the time during the run. The depth of the towed array varied slightly during the run (Fig. 12). The sound speed profile in the water shows a strong thermocline from 25-30 m depth (Fig. C-1).

Preliminary modelling was done with KRAKENC [14], a range-dependent normal mode model available at SACLANTCEN. The shape of the first four modes obtained with KRAKENC is shown in Fig. 14. Both source and receiver are close to the depth of a maximum for modes 1 and 3, but close to a null for modes 2 and 4. For this reason, the source and receiver depths can have a large impact on which modes are most excited, and consequently on the final propagation loss curve.

More detailed modelling was done with SAFARI, a range-independent fast field model [15]. Several different sets of bottom parameters and of source/receiver geometries were investigated. The following conclusions were reached:

1. A compressional sound speed of 1720 m/s is realistic. A lower speed induces too much loss in the model.
2. To obtain the same propagation loss levels as in the data, the shear speed has to be much lower than the initially estimated 905 m/s. A high shear speed introduces too much loss, and it also strips off too many of the higher order modes. A low shear speed, however, gives a propagation loss structure that is very complicated with range, and does not fit the data. Intermediate values around 350 m/s offer a good compromise: some higher modes get attenuated, and the propagation loss is smoother over range. Also, average levels are similar to those of the data.
3. Attenuation values for both compressional and shear waves have a much lower impact on the final propagation loss values, as well as the density. The original estimated values were found to be satisfactory.
4. Thin layers of softer sediments were tried, without improving fits to the final propagation loss.

Figure 15 shows the propagation loss *vs* range obtained with the updated bottom model shown in Table 8. The fit between model and data shows good agreement on the overall levels, but the details of the peaks and nulls do not match well. The main problem is the inaccurately-known source depth which has a fair impact on which modes are most excited. For different source depths, the relative amplitudes of the modes result in different interference patterns as a function of range, and the resultant propagation loss curves will be quite different. The uncertainty in range in the data is also a factor to consider. The length of the track should be accurate, but absolute ranges could be shifted either way by up to 20%.

Table 8 *Bottom parameters used for propagation loss modelling*

Compressional sound speed	1720 m/s
Compressional attenuation	0.3 dB/wavelength
Shear speed	350 m/s
Shear attenuation	0.6 dB/wavelength
Density	1.82 g/cm^3

4.1.3. Vertical and horizontal coherence

The correlation between the hydrophones of the horizontal and vertical arrays was calculated. Figure 16 shows the correlation coefficient for the horizontal array at Site A, and the vertical array at Site B.

The estimated correlation length (defined as the distance at which the correlation coefficient is equal to 0.6) is 108 m horizontally, and 3.5 m vertically. The vertical correlation length is generally quite low due to the strong depth-dependent interference between the modes [16]. In the horizontal, the correlation length is much longer, although it varies according to the level of inhomogenieties in both bottom and ocean. It is unlikely that the horizontal correlation length in this experiment was degraded by the array tilt, since the average vertical distance between the first and last hydrophone was less than 3 m, which is smaller than the vertical correlation length. It should be remembered however that the two measurements (horizontal and vertical) were taken at different sites, on different days.

The effect of the different correlation lengths is shown in Fig. 17, which compares the transmission loss as a function of range/time for 3 hydrophones and for the three runs CW1, CW2, and CW3. Figure 17a shows the 5-second averaged signals from the first, middle and last hydrophones of the horizontal array (separation of 128 m between hydrophones). In Fig. 17b, the same signals are shown, but a negative delay of 24 s (128 m / 5.26 m/s) has been applied to the middle hydrophone, and twice that for the last hydrophone. The negative delay is meant to correct for the speed of the towing ship, to emphasize the good correlation between the different hydrophones. In Figs. 17c and 17d, the signals from 4 hydrophones of the vertical array are shown for runs CW2 and CW3. In both cases, the separation between the hydrophones is 1, 4 and 10 m. This shows how quickly the correlation degrades with vertical separation.

4.1.4. Spectral spreading

Spectra of the acoustic signals received on selected hydrophones were taken during the CW runs. Figure 18 shows the doppler shift and spectral spreading from a) CW1 tow at Site A; b) CW2 tow at Site B; and c) CW3 tow at Site B. For run CW1 the source was on *Bartlett*, operating at 350 Hz, and signals received on the *Alliance* towed array; for runs CW2 and CW3 the source was on *Alliance*, operating at 375 Hz, and signals received on the SACLANTCEN vertical array.

CW1 was taken in sea state 3, CW2 was taken in sea state 2, and CW3 in sea state 5. (The *Bartlett* log gives sea states of 2, 1.5 and 4, respectively). Apart from the main doppler shift of the signal due to the relative motion of the projector and receiving hydrophone, there are many features in these spectra that merit interpretation. Typically there is a dynamic range of 70 dB within which both regularly spaced single frequencies as well as spectral concentrations - usually centered around the zero-doppler-shifted transmission frequency, but also occasionally elsewhere - that make their appearance well below the level of the main arrival.

Note the asymmetric behaviour of the main peak. This is probably due to the relative velocity V_{rel} of the source and receiver, rather than sea-surface motion. If one assumes scatterers which are not moving, the scattering ranges from $-V_{rel}$ to $+V_{rel}$, where V_{rel} is the relative motion of the source and receiver. When towing the source directly away from the receiver, the direct arrival appears at a frequency corresponding to $-V_{rel}$ and the scattering occurs up to frequencies corresponding to $+V_{rel}$. Outside this band, the spreading appearing in these figures is due to additional sensor motions, sea surface motion, or widening due to the spectral window.

4.2. REVERBERATION

A great deal of reverberation data were taken during the trial, of which a sample is presented here.

Figure 19 shows the CBS time series on selected beams for a HFM pulse H1 during Run C1. Three types of reverberation are evident:

- (i) reverberation following the main blast, after 15-35 s;
- (ii) higher reverberation around 55 s from an extended feature (likely the bottom feature *Haig Frais*);
- (iii) a compact feature at about 75 s.

The latter feature is more evident in the matched-filtered output (Fig. 20a) where it appears as a spike some 30 dB above the noise. Kirsteins [17] has applied reverberation suppression techniques to this particular feature. It is not known what the feature is, but it persists for several hours; Fig. 20b shows the feature 90 minutes later, on another beam, at time 55 s. Due to poor navigational information on *Alliance* at this time, it is difficult to localize; but it is known that there are shipwrecks in the area.

Similar point-like scattering features are common at Site A, where spikes can easily rise 30 dB out of the noise in the matched filter output. Figure 21 illustrates such features on beams 57 and 65, at times of about 90 s and 93 s respectively. These are about 75 s after the pulse, or from a range of about 55 km. Small patches of high bottom reflectivity were noted on the NRL echo-sounder records in the area – a sample appears in Fig. 19 of Max *et al.* [1]. The correlation between the scattering features and locations of the patches should be investigated.

Figure 22 shows a polar plot of all 65 beam time series from a ping on Run C1. Beams are mapped into azimuth, and time is mapped into range; the received power is superposed on the bathymetry. The solid line shows the array heading – almost due west; the circle defines 60 s after the main arrival at the array. The data are the received CBS time series, before the matched filter was applied, so the compact feature of Fig. 20a is spread over 2.5 to 3 seconds, due to the 2.4 s pulse and multipath spreading by the shallow-water waveguide. Note also the left-right ambiguity in the diagram, due to the conical beams of the towed array.

Figure 23 shows the reverberation received on the vertical array for the SUS charge run at Site B (Run B2SUS). These data are quite different from the towed array data, since the geometry is bistatic, and there is no azimuthal discrimination.

Polygons at Sites A and C

Figures 24 and 25 show some reverberation polygons from Sites A and C, using the HFM pulses. A "stacking" procedure [18] has been used to eliminate the left-right ambiguity seen in Fig. 22. Due to the high sea state and ambient noise, no bathymetric features were resolvable in the data.

Synopsis

From at-sea monitoring the following impressions of reverberation were obtained:

- Site A was expected to show little feature scattering, but showed a lot;
- Site B was expected to show considerable structure, but showed little;
- Site C, with a thin sediment, was uncertain; it showed a lot of variability.

These impressions need to be confirmed and quantified. The feature scattering deserves particular attention to determine if it can be related to shipwrecks, as Site C might suggest, or patches of high bottom reflectivity, as observed on the NRL echo-sounder at Site A.

4.3. AMBIENT NOISE

The ambient noise was quite high during the experiment due to (i) high fishing activity and ship traffic in the area; (ii) fairly strong winds and high sea states for this time of year; and (iii) a noisy propeller bearing on *Alliance* which caused very high noise in certain headings with respect to the sea/swell.

The instantaneous ambient noise readings for various beams can be seen in Figs. 20, 21, and 23, by looking at the background before the main blast arrival. In Fig. 22 the periodic noise from the of the *Alliance* propeller shaft can be seen as arcs in the forward beams. Some of the arcs in Fig. 25 will also be due to noise from the propeller shaft. High noise level appears to come from bearings many degrees from the forward endfire direction; this is a consequence of mapping the beam angle to bearing and corresponds to bottom-bounce arrivals from the direction of the ship.

5 Summary

This report describes the joint SACLANTCEN / Naval Research Laboratory sea trial *Celtic Duet*. The purpose of the trial was to obtain monostatic and bistatic reverberation data, with supporting propagation and environmental measurements. This report includes reasonably-detailed descriptions of navigation tracks and environmental measurements, as well as a summary of the sea surface spectra analysis and seabed information for the area.

Though primarily an environmental report, a few selected acoustic results are presented. The CW propagation tows were very useful in determining data quality, and in checking bottom parameters for modelling. Spectral spreading and spatial coherence were also obtained from the CW data. Ambient noise during the trial was high due to fairly high winds, heavy shipping in the area, and a propeller on *Alliance* which became noisy during the trial. A substantial amount of reverberation data were collected; of particular interest, and deserving further investigation, are the scattering features observed at Sites A and C.

ACKNOWLEDGEMENTS: This sea trial depended on support and cooperation from many people and agencies, including the captains and crews of the ships *Alliance* and *Bartlett*, and the technical support from the SACLANTCEN Ocean Engineering Department, Electrical Engineering Department, Computer Department, and Ship Management Department. R.H. Clarke was partially supported by the UK Ministry of Defence and SACLANTCEN; students at Imperial College provided some post-cruise analysis of the waverider and CW data. The Seabed Acoustics Group at SACLANTCEN provided additional support through a follow-on sea trial; M. Max in particular provided pre-cruise advice on site selection and post-cruise analysis of the bottom properties. The cooperation with NRL was superb: Bruce Pasewark was scientist-in-charge for NRL; Steve Wolf and Roger Gauss provided additional guidance on experiment design and execution. NRL provided a PC waveform generator for *Alliance*; their personnel on *Alliance*, Jon Berkson and Matt Healy, were an integral part of our team and made significant contributions, as did John Preston, SACLANTCEN representative aboard the *Bartlett*..

References

[1] Max, M.D., Michelozzi, E., Turgutcan, F. and Tonarelli, B. Geoenvironmental characterization of selected shallow-water sites on the western European continental shelf (SWAP), SACLANTCEN SM-288. La Spezia, Italy, SACLANT Undersea Research Centre, 1995.

[2] Max, M.D. Personal communication, 1992.

[3] Ellis, D.D. and Chapman, D.M.F. Modelling of shear-wave related acoustic propagation on the UK Continental Shelf, DREA Technical Memorandum 84/P. Dartmouth, NS, Canada, Defence Research Establishment Atlantic, August 1984.

[4] Ellis, D.D. and Chapman, D.M.F. A simple shallow water propagation model, including shear wave effects, Journal of the Acoustical Society of America, 78, 1985: 2087–2095.

[5] Buckingham, M. and Jones, S.A.S. A new shallow-ocean technique for determining the critical angle of the seabed from the vertical directionality of the ambient noise in the water column, Journal of the Acoustical Society of America, 81, 1987: 938–946.

[6] Caiti, A. and Max, M. D. In-situ acoustic properties of chalk seafloor. In: L. Bjorno, editor. Proceedings of the Second European Conference on Underwater Acoustics, Copenhagen, Denmark, 4-8 July, 1994. Luxembourg, European Commission, 1994: Vol. 2, pp. 949-954.

[7] Hutchens, R.W., McKeown, D.L. and King, L.H. A deep tow high resolution system for continental shelf mapping, Geoscience Canada, 32, 1976: 95–100.

[8] Jones, E.A. The SACLANTCEN Technical Support Division, SACLANTCEN Special Report M-105. La Spezia, Italy, SACLANT Undersea Research Centre, 1989.

[9] Wadhera, K. Display, Processing and Interpretation of Ocean Surface Height Measurements, Final-Year Degree Project Report, Department of Electrical and Electronic Engineering, Imperial College, University of London, UK, June 1994.

[10] Brekhovskikh, L. and Lysanov, Y. Fundamentals of Ocean Acoustics. Berlin, Springer, 1982: p.19.

[11] Kinsman, B. Wind Waves, Prentice-Hall, 1965.

[12] Pierson, W.J. and Moskowitz, L. A proposed spectral form of fully developed wind seas based on the similarity theory of S. A. Kitaigorodskii, Journal of Geophysical Research, 18, 1964: 5181-5190.

[13] MATLAB Reference Guide. Natick, MA, USA, The MathWorks, Inc., 1992.

[14] Porter, M. The KRAKEN normal mode program, SACLANTCEN SM-245. La Spezia, Italy, SACLANT Undersea Research Centre, 1991.

[15] Schmidt H. SAFARI: Seismo-acoustic fast field algorithm for range-independent environments - User's guide, SACLANTCEN SR-113. La Spezia, Italy, SACLANT Undersea Research Centre, 1988.

[16] Wang, Q. and Zhang, R. Sound spatial correlation in shallow water, Journal of the Acoustical Society of America, 92, 1992: 932–938.

[17] Kirsteins, I. P. Model-aided data adaptive suppression of reverberation. In: R. Weatherburn and G. Murdock, editors, Low Frequency Active Sonar. SACLANTCEN Conference Proceedings CP-42, August 1993: Vol. 1. Paper C/11.

[18] Preston, J., Akal, T. and Berkson, J. Analysis of backscattering data in the Tyrrhenian Sea, Journal of the Acoustical Society of America, 87, 1991: 119-134.

[19] Harris, F. J. Multirate FIR filters for interpolating and desampling. In Handbook of Digital Signal Processing Engineering Applications, D. F. Elliott (ed.), Academic Press, San Diego, CA, USA, 1987, Chapter 3.

[20] Vaidyanathan, P.P. Design and implementation of digital FIR filters. In Handbook of Digital Signal Processing Engineering Applications, D. F. Elliott (ed.), Academic Press, San Diego, CA, USA, 1987, Chapter 2.

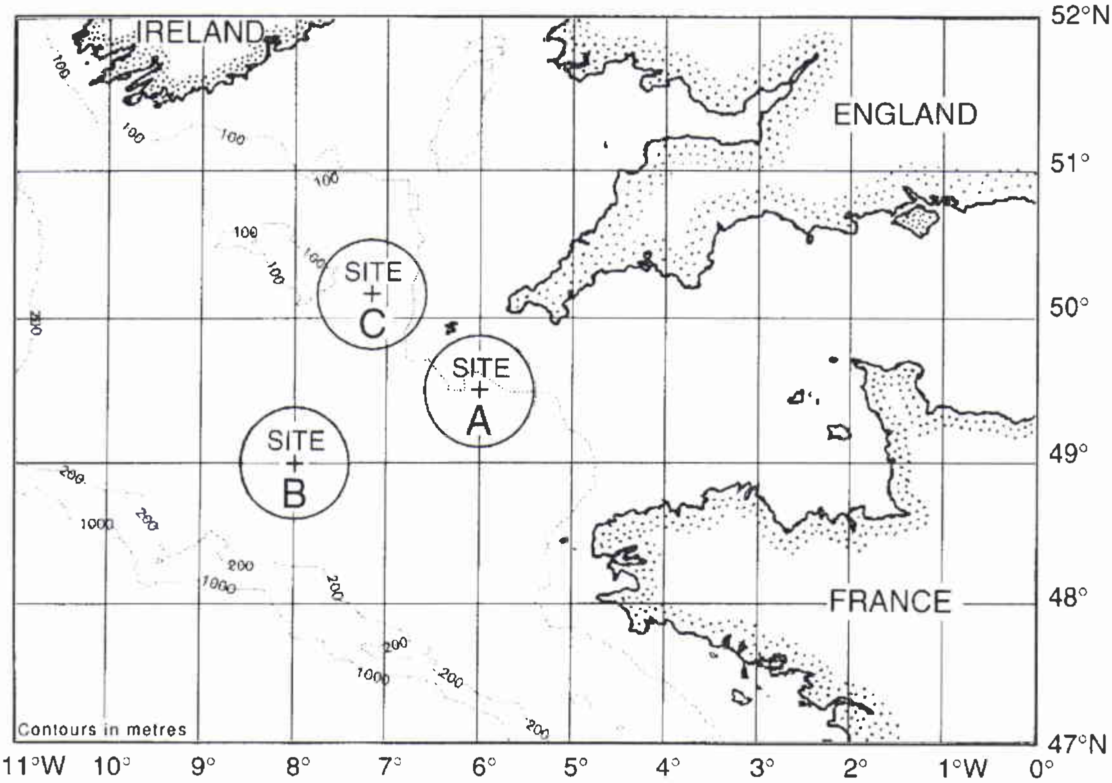

Figure 1 *The three sites of the Celtic Duet experiments.*

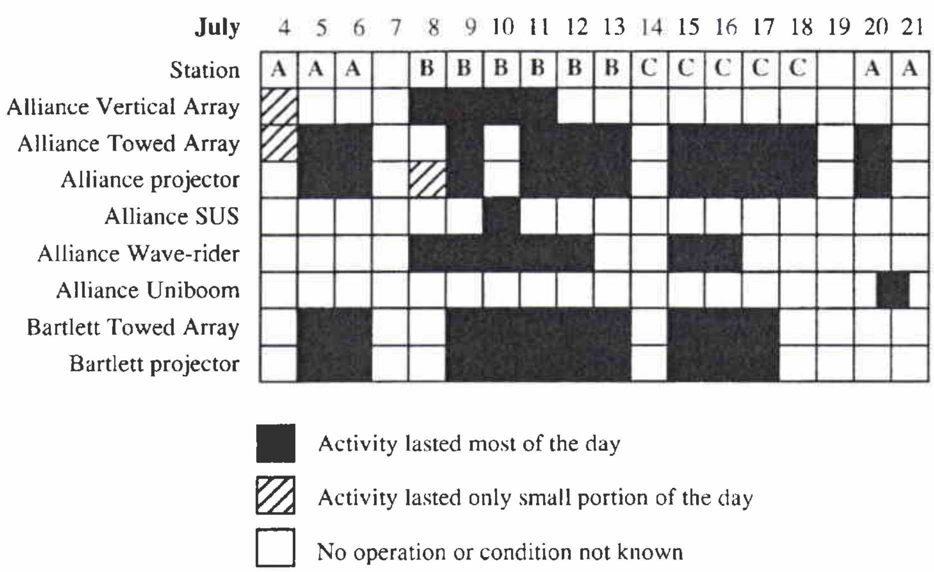

Figure 2 *Schematic of the main hardware deployments during the trial Celtic Duet.*

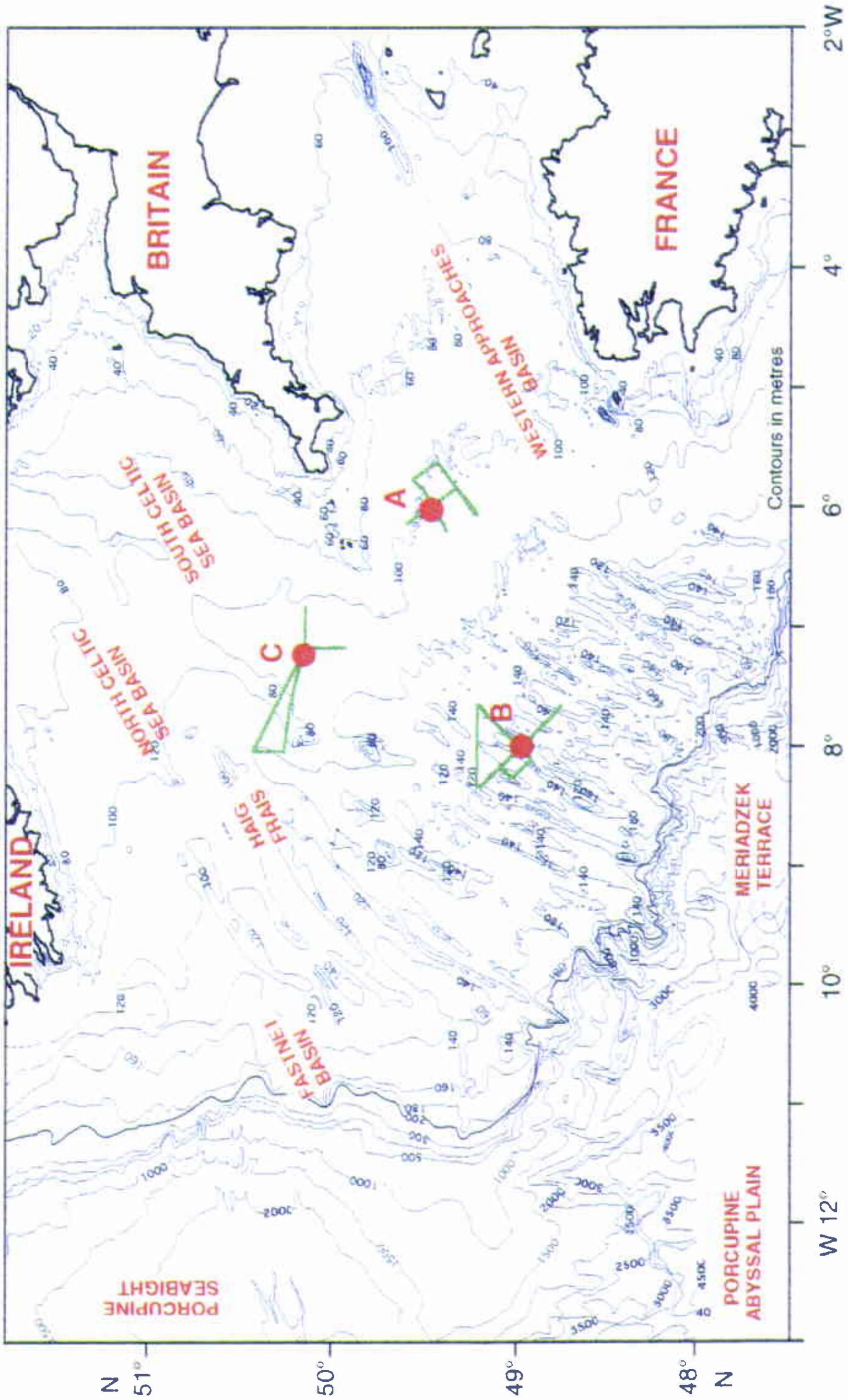

Figure 3 *Map of bathymetry showing the three experiment sites (red dots) where the Uniboom system was deployed (tracks are bold green lines) during Celtic Duet and the follow-on trial by the Seabed Acoustics Group; from Max et al. [1].*

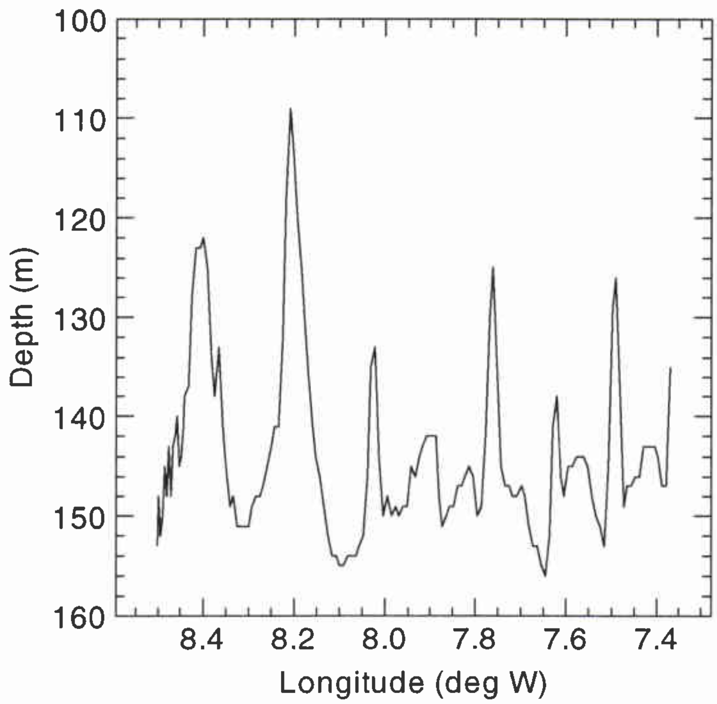

Figure 4 *Detailed bottom bathymetry from echo sounder along a track perpendicular to the ridges of the sand waves at Site B.*

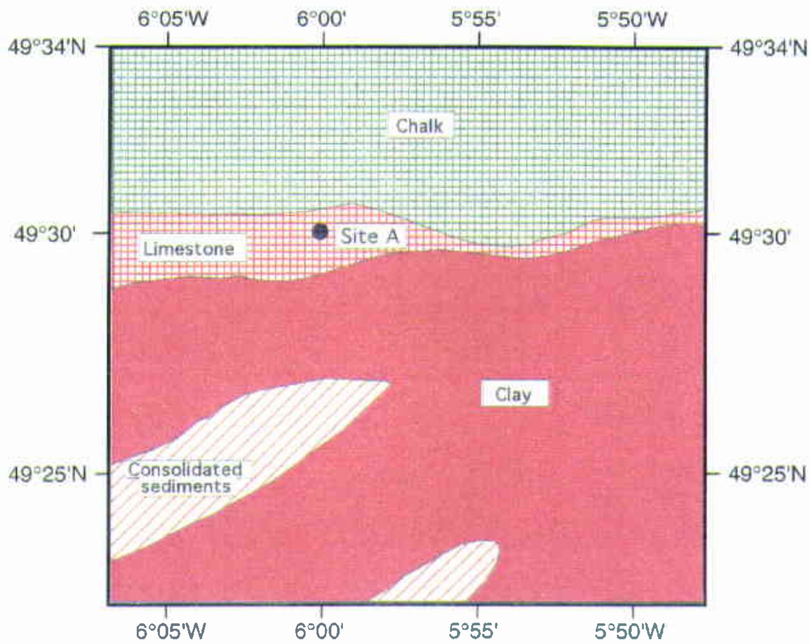

Figure 5 *Map of sediments near Site A, showing that this position was in a boundary zone; (from Max et al. [1]).*

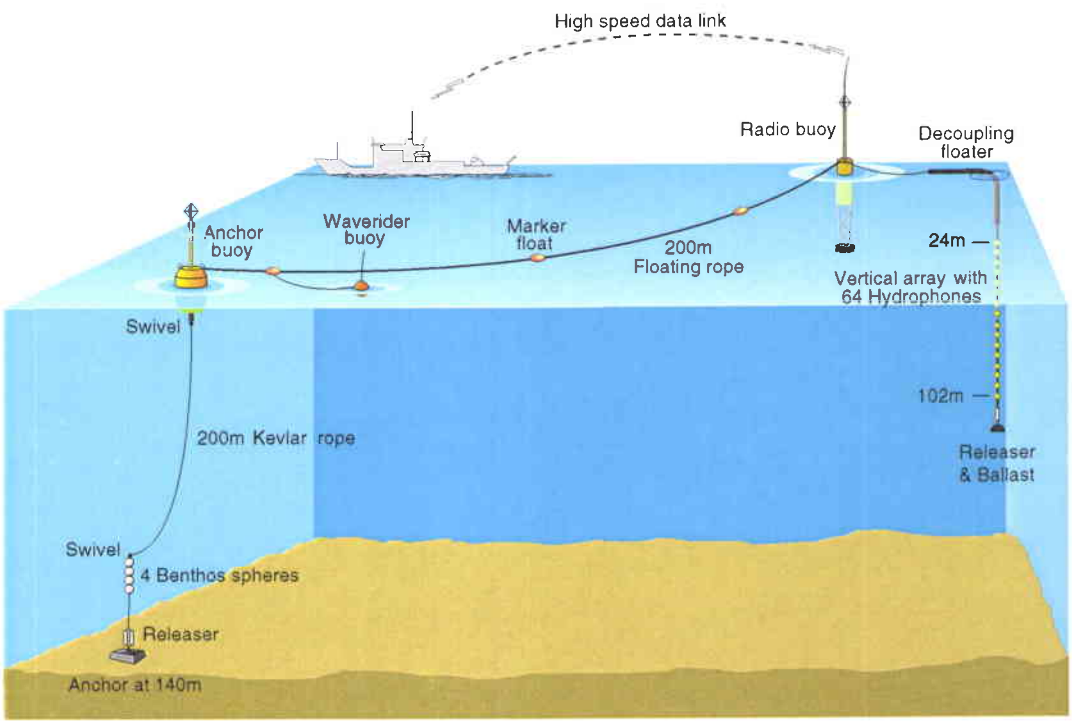

Figure 6 *Typical deployment of vertical array and waverider buoy at Site B.*

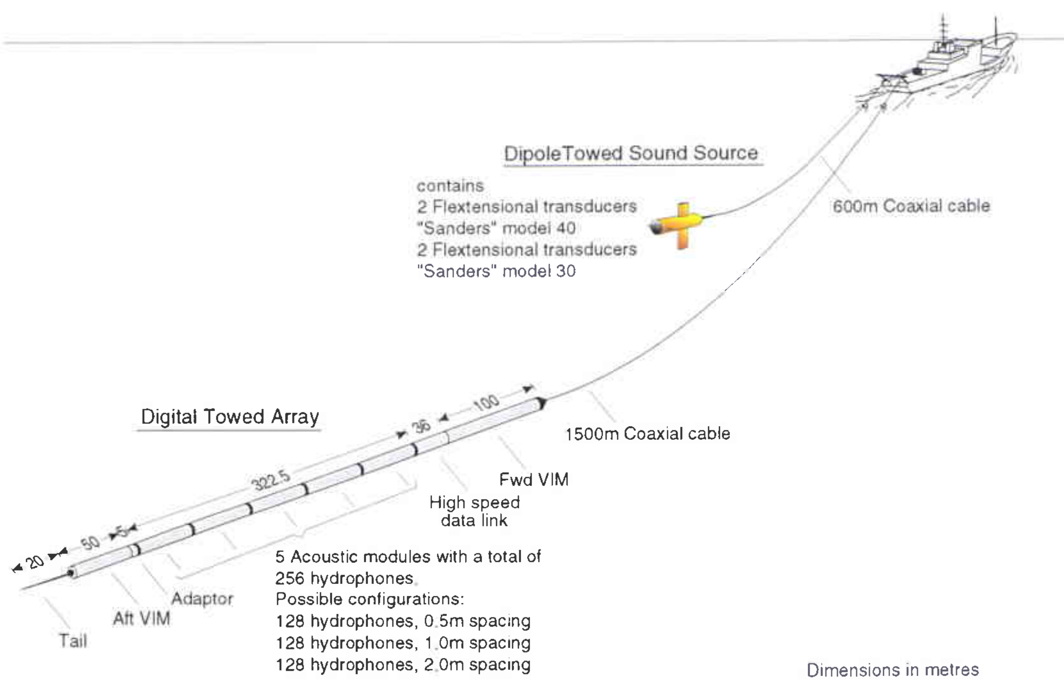

Figure 7 *Configuration of the towed array and sound source during the Celtic Duet sea trial.*

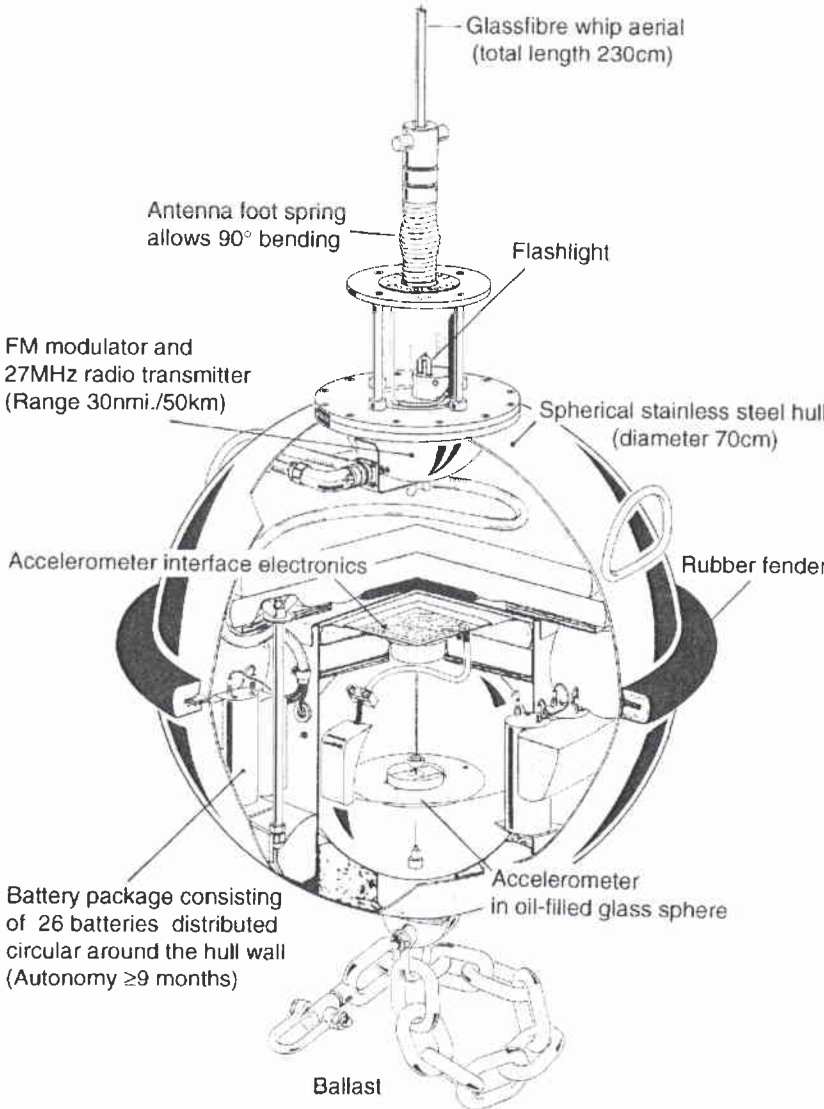

Figure 8 *Diagram of the Waverider® buoy.*
®Registered trademark by DATAWELL, Haarlem, The Netherlands

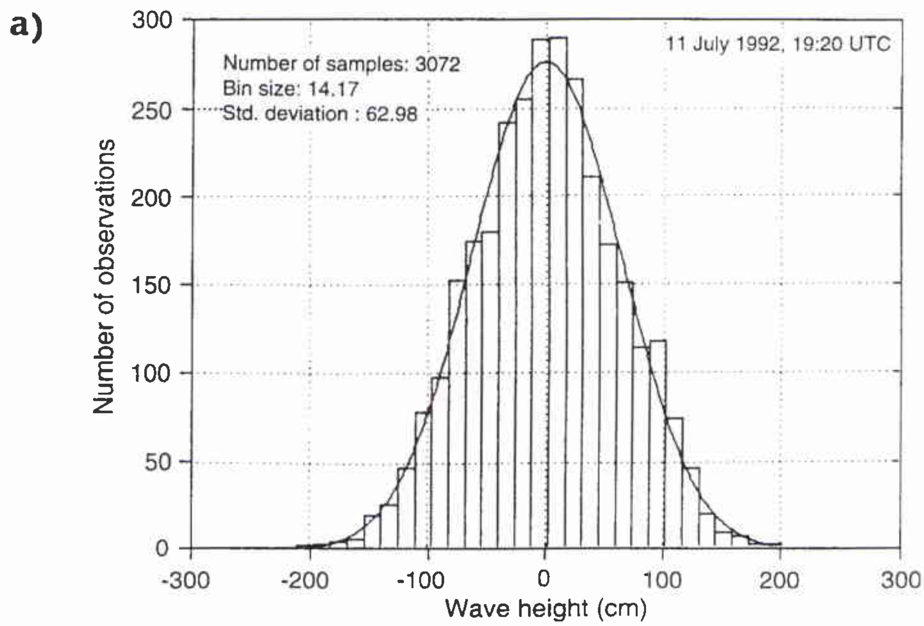

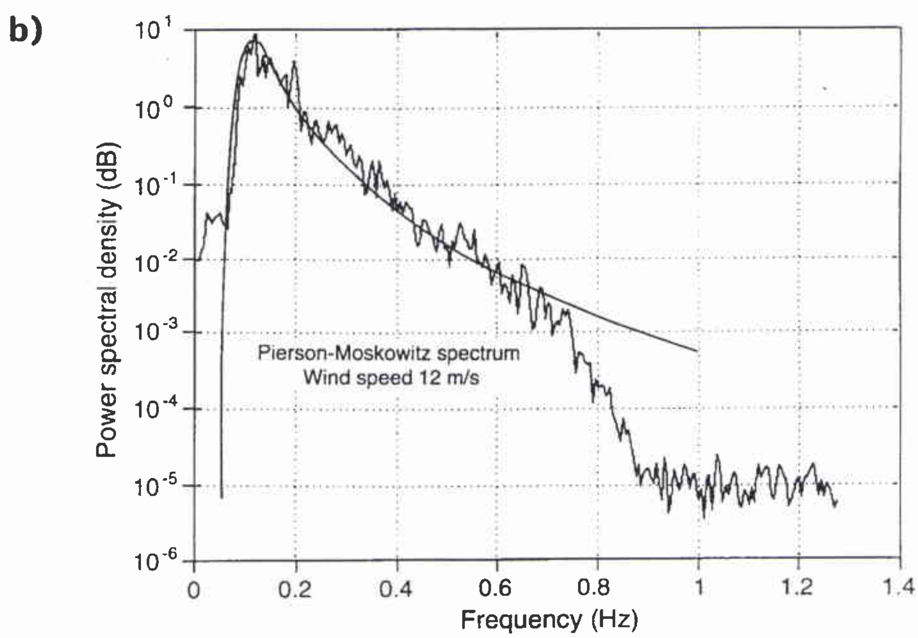

Figure 9 (a) *Histogram of sea-surface height measurements from waverider buoy (the solid line is a fit to a Gaussian p.d.f. of zero mean);* (b) *power spectral density of sea-surface height measurements compared with the Pierson-Moskowitz spectrum.*

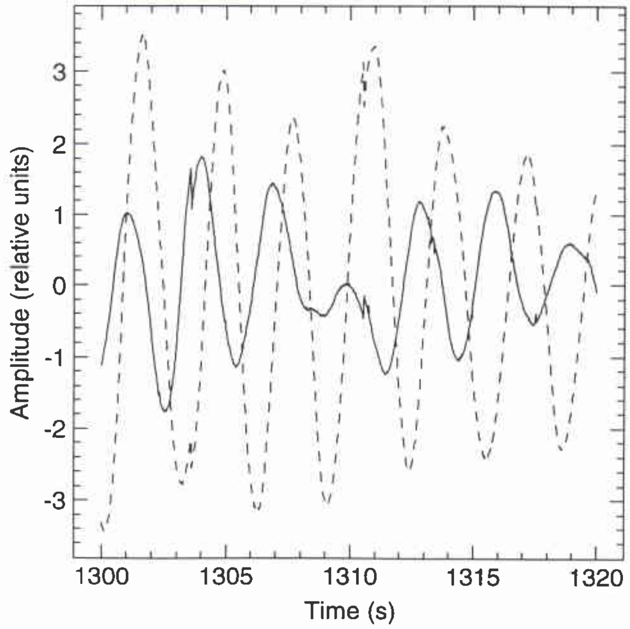

Figure 10 *Complex-band-shifted time series of CW tow from post-cruise playback; the real and imaginary components are shown by the solid and dotted lines respectively. Note the phase jumps at certain times.*

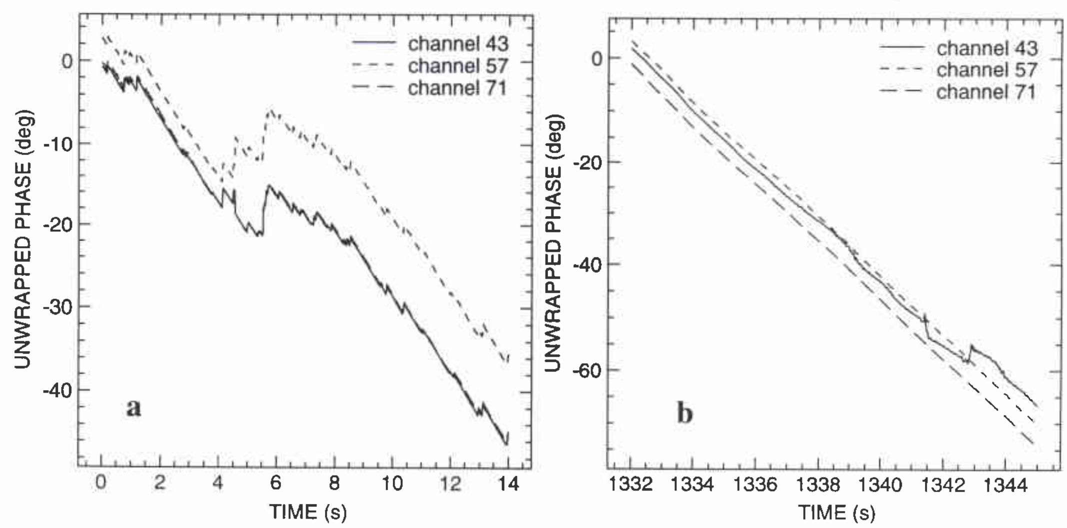

Figure 11 (a) *Unwrapped phase from 3 channels, showing jumps due to poor playback;* (b) *unwrapped phase from a good section of the playback; the jump near 1342 s on channel 43 is probably a real effect.*

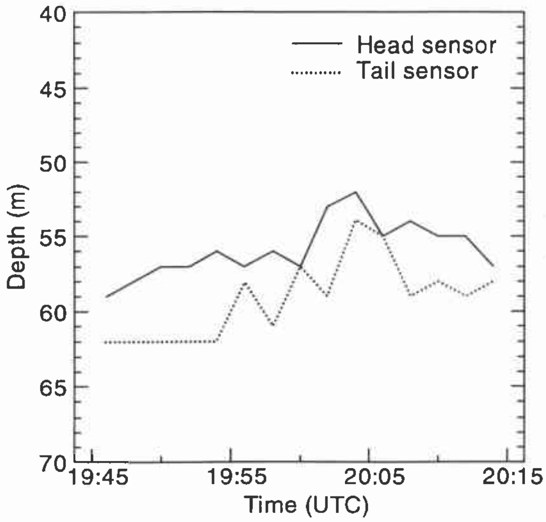

Figure 12 *Variation of two depth sensors on towed array during tow CW1.*

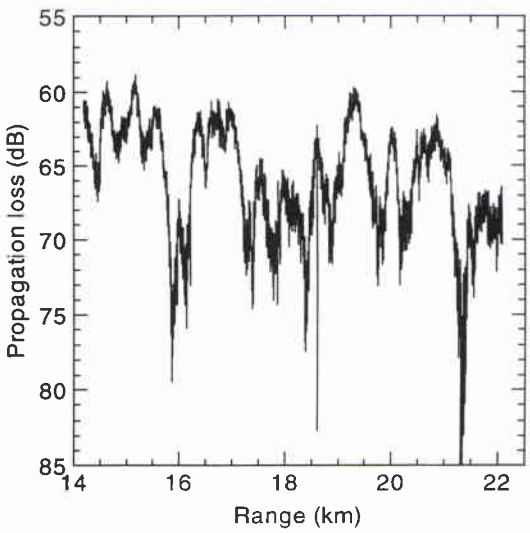

Figure 13 *Measured transmission loss versus range from CW tow at Site A.*

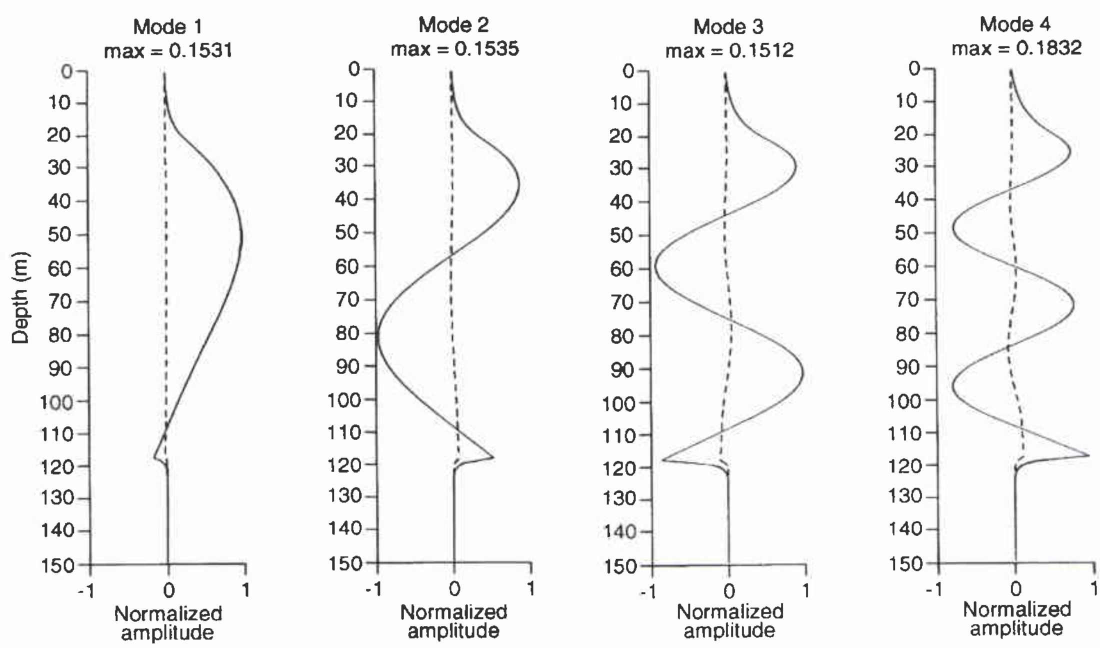

Figure 14 *Real (solid line) and imaginary (dashed line) components of normal mode functions from KRAKENC.*

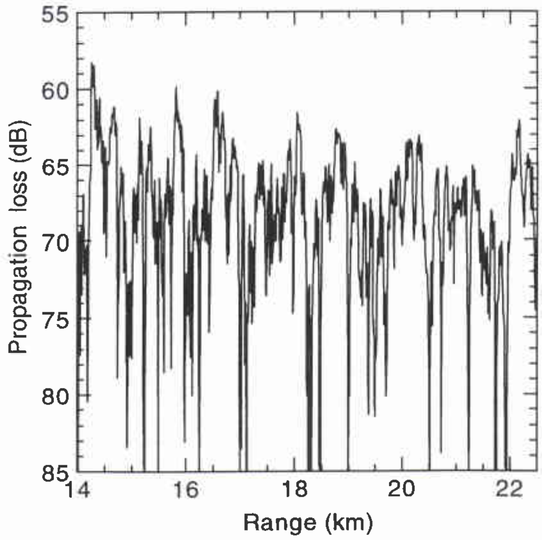

Figure 15 *Calculated transmission loss versus range from SAFARI for Site A using the acoustic model of Table 8. The overall levels are in good agreement with the values in Fig.13, but the detailed structure is different.*

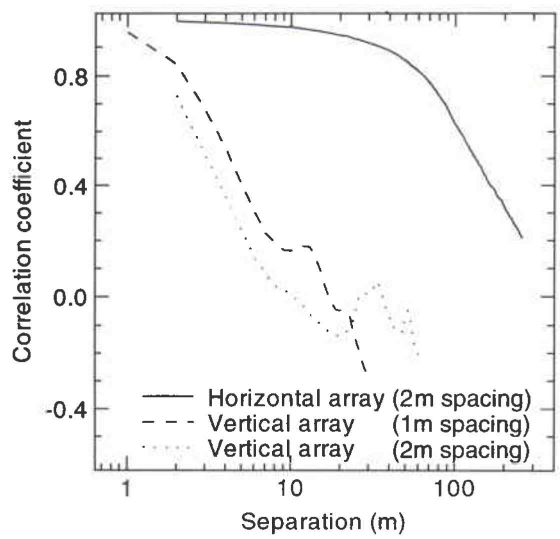

Figure 16 *Comparison of coherence between hydrophones of horizontal array (SiteA) and vertical array (Site B).*

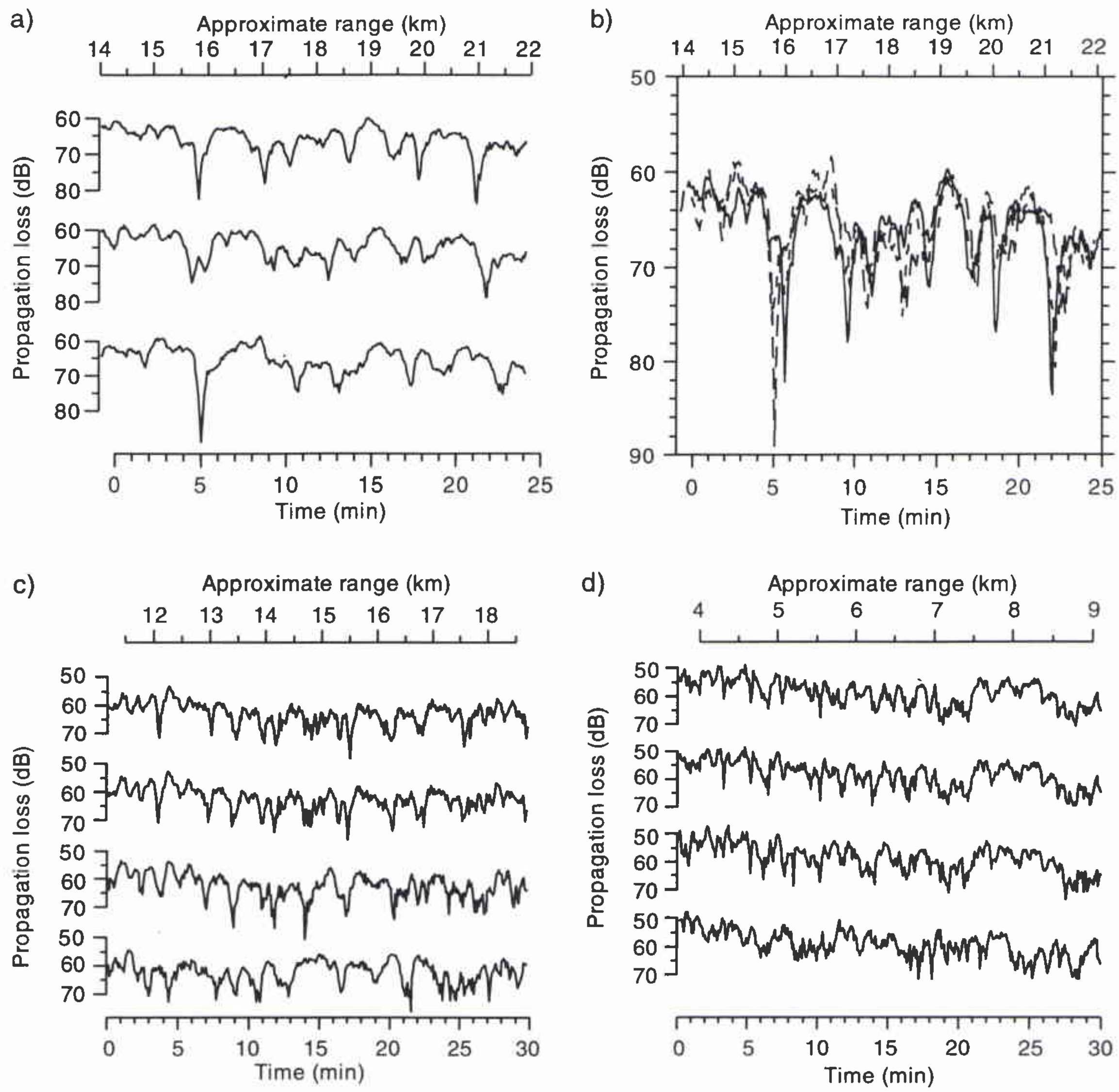

Figure 17 *Propagation loss vs range for:*

a) *run CW1: first (upper curve), middle (middle curve) and end hydrophones (lower curve) of the towed array ; (128 m separation between hydrophones).*

b) *same as a), but with a 24 s (~128 m) delay applied to the middle hydrophone (short dashed line), and a 48 s delay applied to the end hydrophone (long dashed line); curves have no vertical offset.*

c) *run CW2: 4 hydrophones of the vertical array at separations of 1, 4, and 10 m in depth.*

d) *run CW3: 4 hydrophones of the vertical array at separations of 1, 4, and 10 m in depth.*

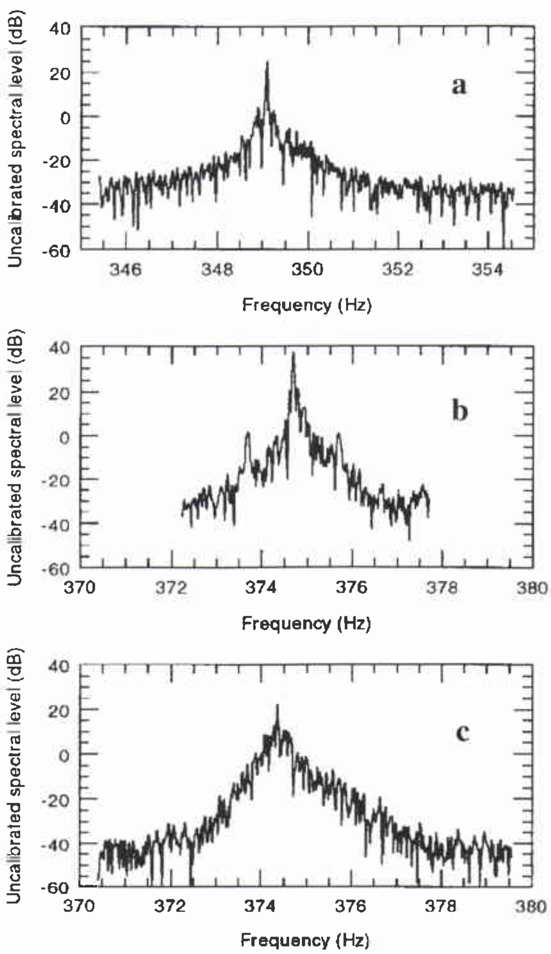

Figure 18 *Spectral spreading from* (a) *CW1 tow at Site A,* (b) *CW2 tow at Site B,* (c) *CW3 tow at Site B.*

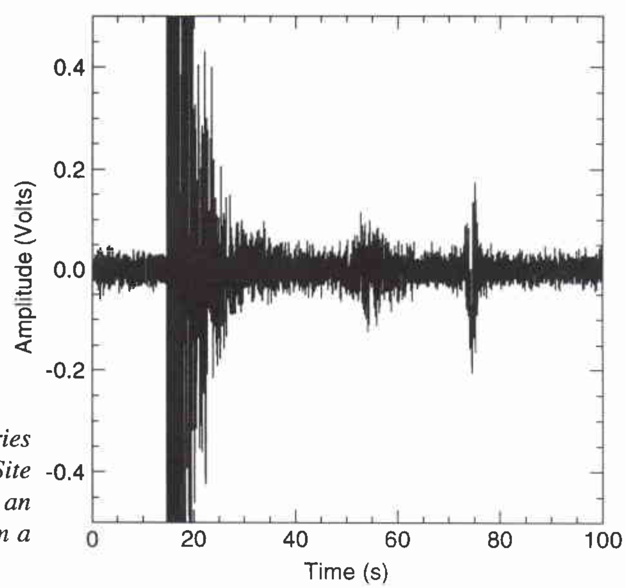

Figure 19 *Real component of CBS time series showing three types of reverberation at Site C:* (i) *after main blast (15-35 s),* (ii) *from an extended feature at 50-60 s, and* (iii) *from a point-like feature near 75 s.*

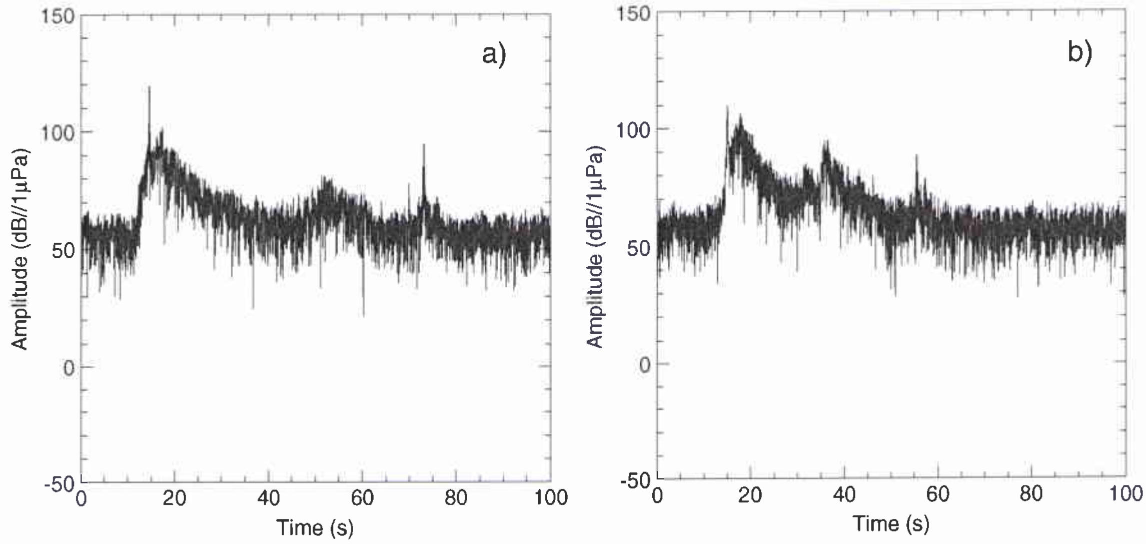

Figure 20 (a) *Matched filter output from Fig. 19; note in particular the compact feature at 74 s.* (b) *The compact feature appears at 55 s, stronger on another beam, 90 minutes later.*

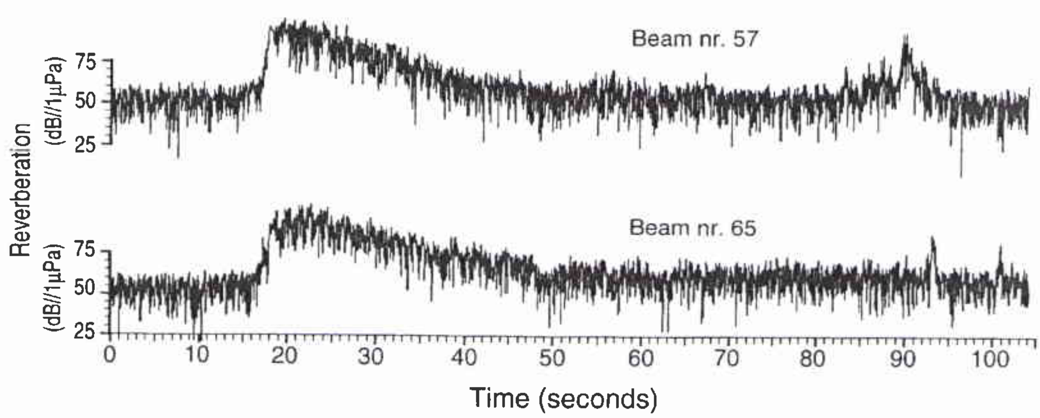

Figure 21 *Matched filter output of reverberation at Site A, showing features at about 90 s on beams 57 and 65.*

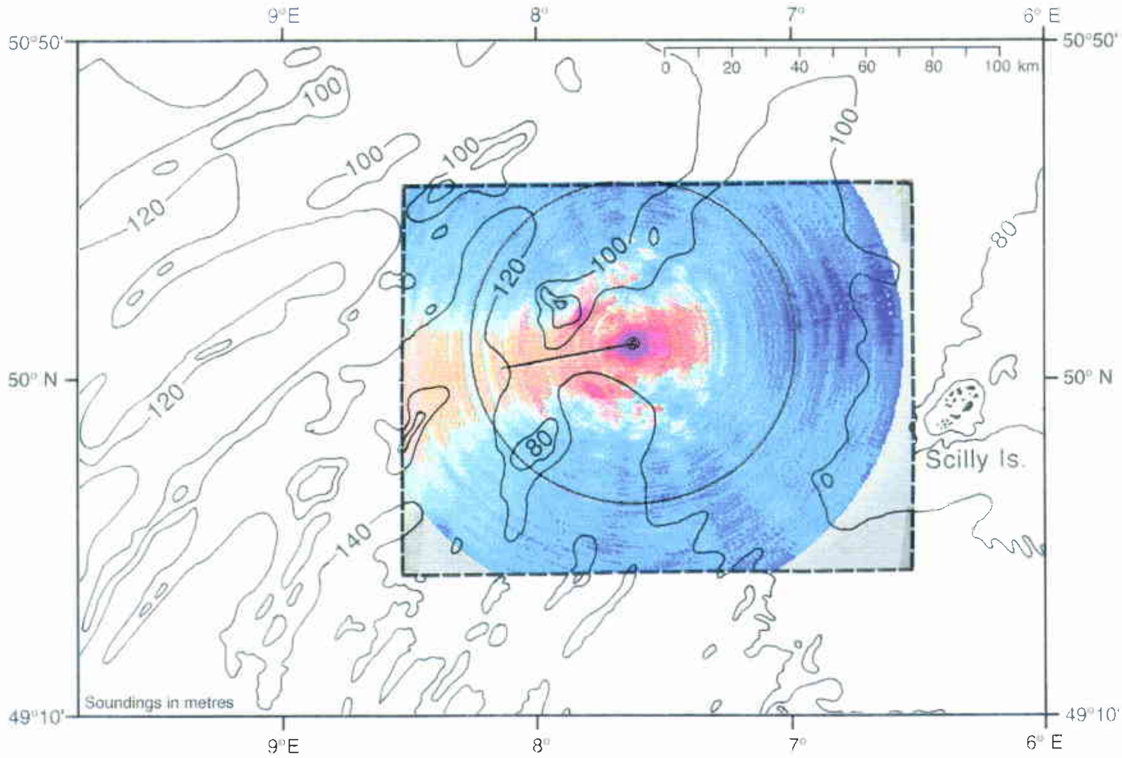

Figure 22 *Polar plot of all beams for Site C; the bathymetry is superimposed. Note the strong ship noise in the forward beams.*

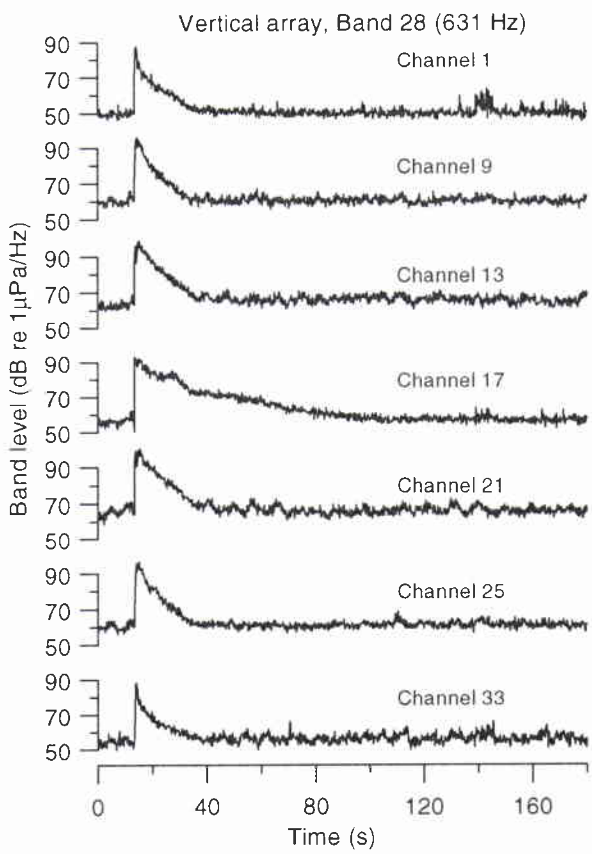

Figure 23 *Tenth-decade output of reverberation from run B2SUS, received on selected beams of the vertical array.*

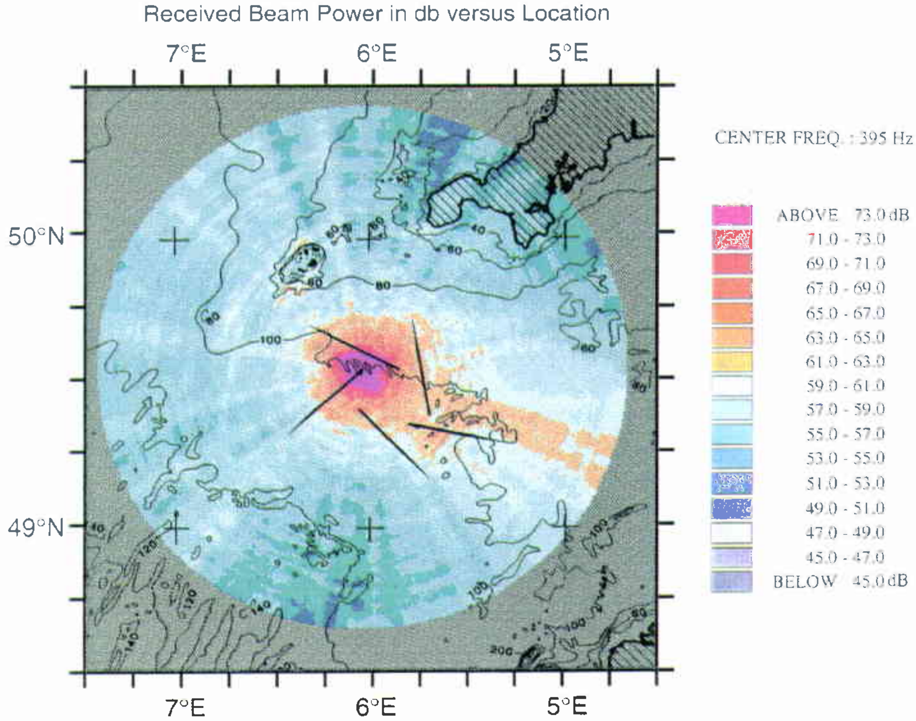

Figure 24 *Reverberation polygon for Site A at 395 Hz. The bathymetry is superimposed.*

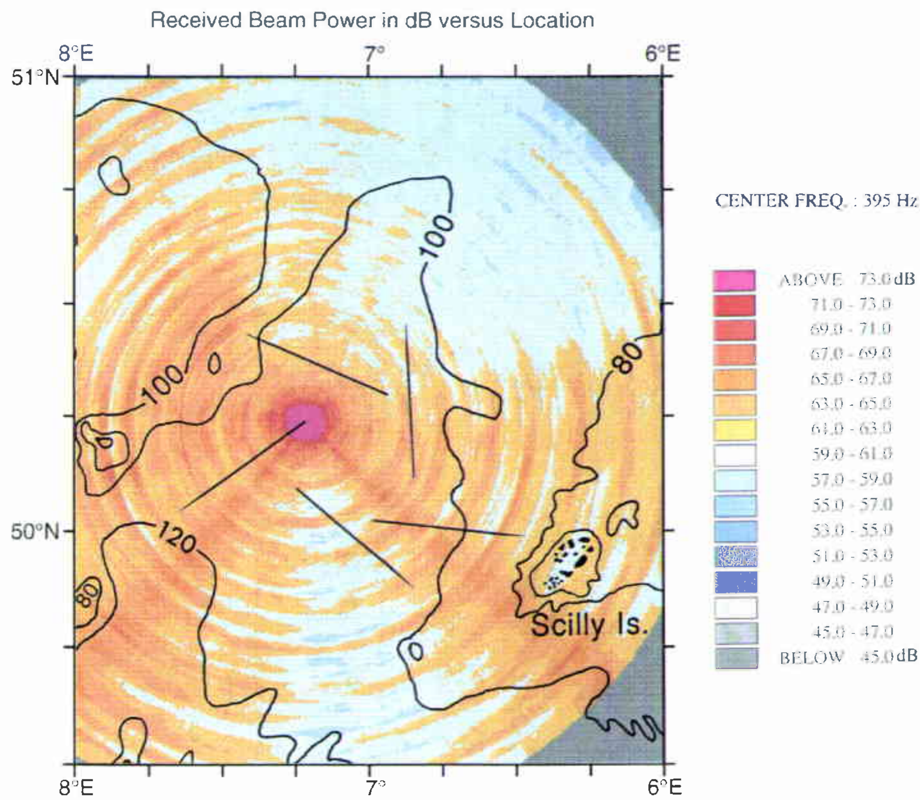

Figure 25 *Reverberation polygon for Site C at 395 Hz. The bathymetry is superimposed.*

intentionally blank page

Appendix A
Navigation Tracks

The navigation tracks for the various experiments are shown in Figs. A-1 to A-21; refer to Table 1 for the *Alliance* run identifiers. Brief descriptions of the experiments are given in Section 2.1. Additional environmental information is given in Section 2, and Appendices B and C. The following conventions apply to all figures:

1. The square indicates the initial position of *Alliance* for the experiment;

2. The succession of small black circles is the *Alliance* track (there is a data point approximately every two minutes, therefore the successive circles usually show as a continuous line);

3. The triangle indicates the initial position of *Bartlett* for the experiment;

4. The succession of black dots is the *Bartlett* track (the dot size is smaller for the *Bartlett* track than for the *Alliance* track; also the navigation data for the *Bartlett* are more sparse, one point every five minutes);

5. The lozenge indicates the position of the most recent deployment of the SACLANTCEN's vertical array;

6. The arrows indicate *Alliance* and *Bartlett*'s directions along the tracks.

Note that the *Alliance* GPS was not working well during the cruise, particularly at Site C, so there are occasional jumps in the tracks.

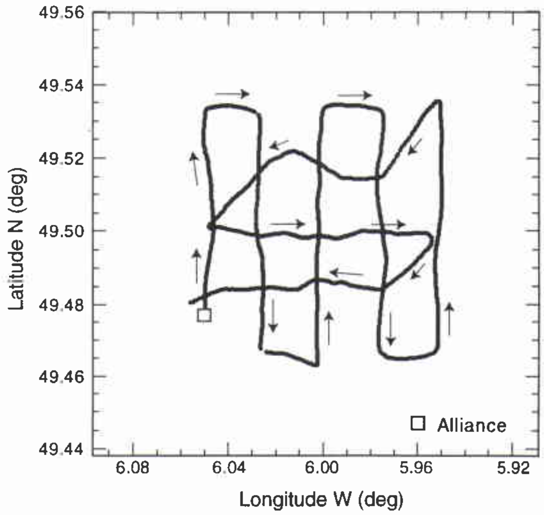

Figure A-1 *Navigation track for Run BATHY1*

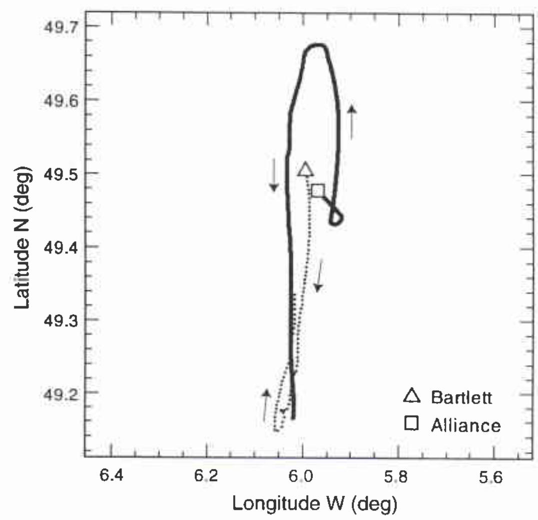

Figure A-2 *Navigation track for Run A1*

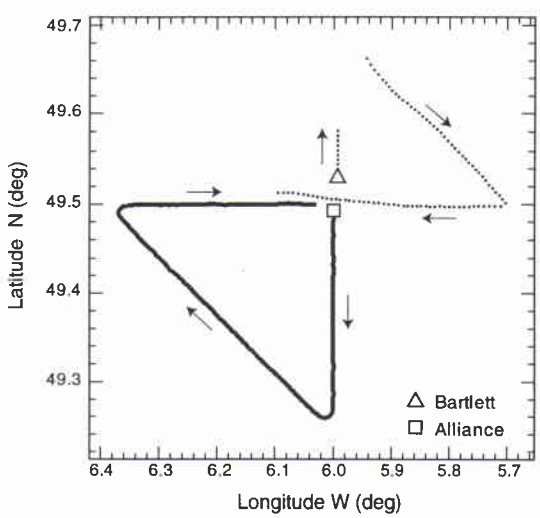

Figure A-3 *Navigation track for Run A2*

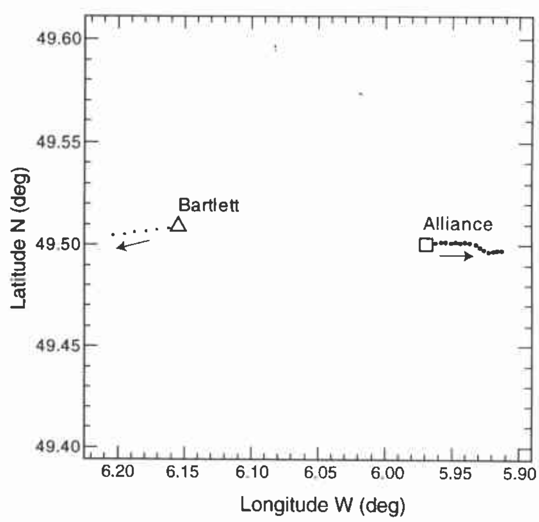

Figure A-4 *Navigation track for Run CW1*

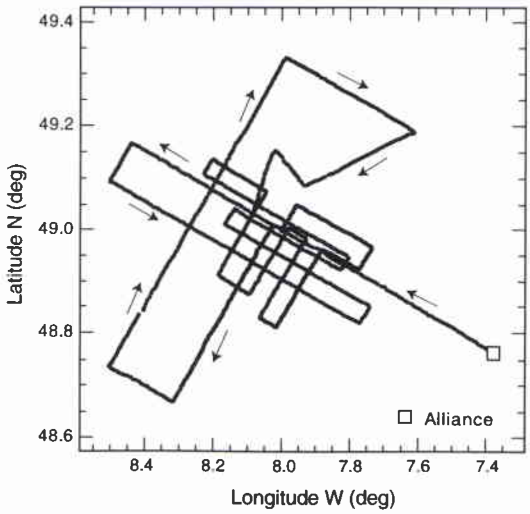

Figure A-5 *Navigation track for Run BATHY2*

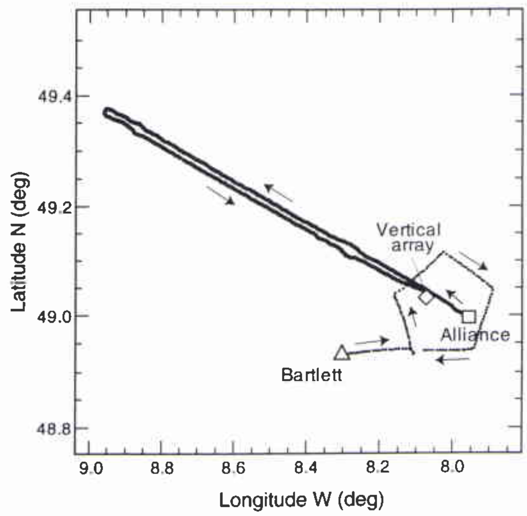

Figure A-6 *Navigation track for Run TLB*

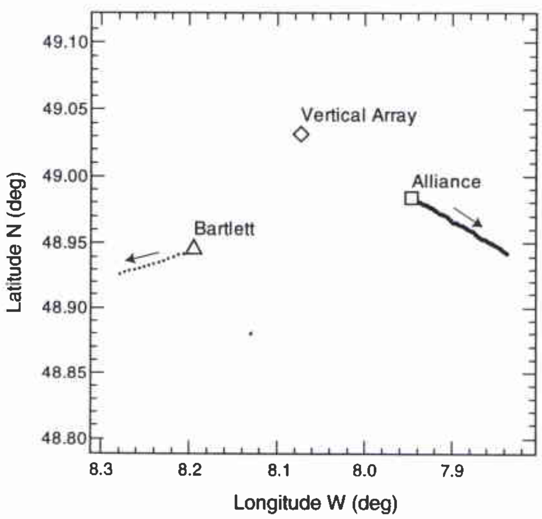

Figure A-7 *Navigation track for Run CW2*

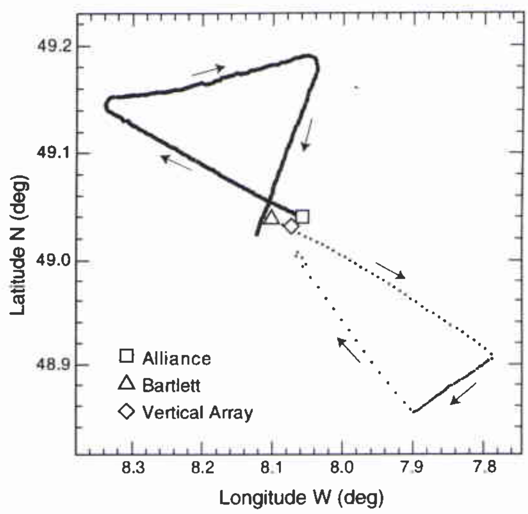

Figure A-8 *Navigation track for Run B1*

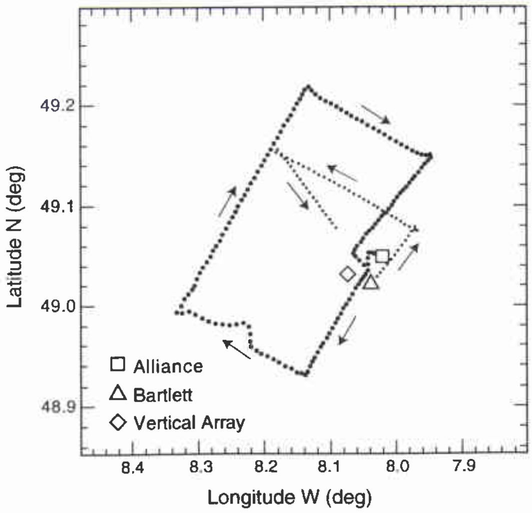

Figure A-9 *Navigation track for Run B2SUS*

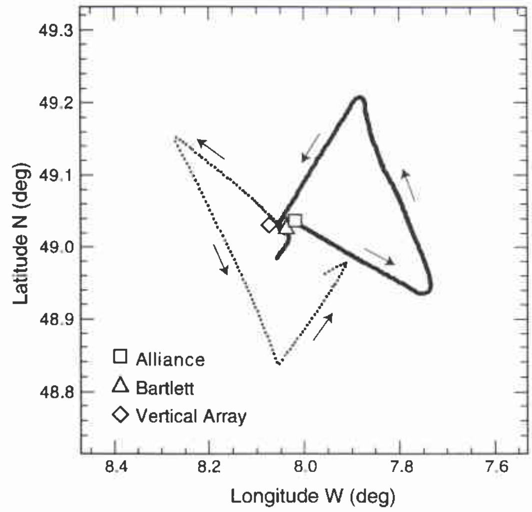

Figure A-10 *Navigation track for Run B2*

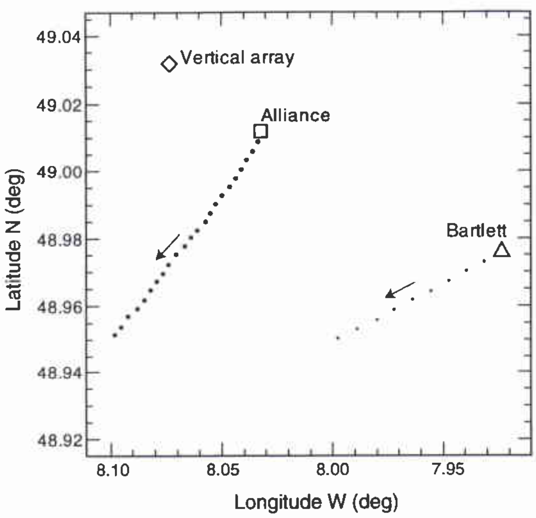

Figure A-11 *Navigation track for Run CW3*

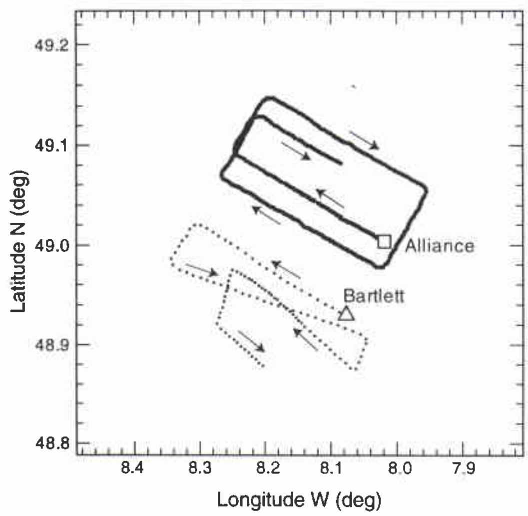

Figure A-12 *Navigation track for Run B3*

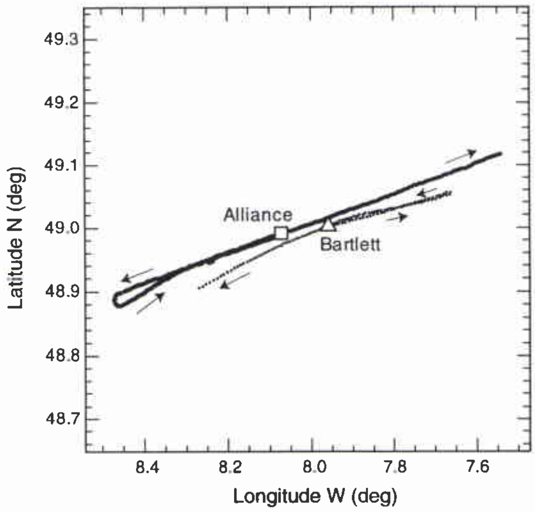

Figure A-13 *Navigation track for Run B4*

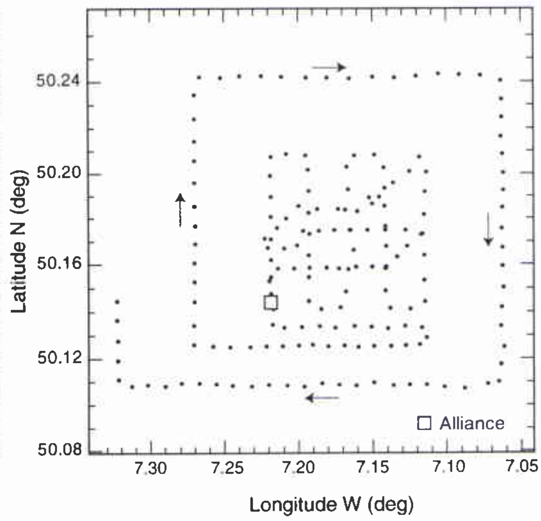

Figure A-14 *Navigation track for Run BATHY3*

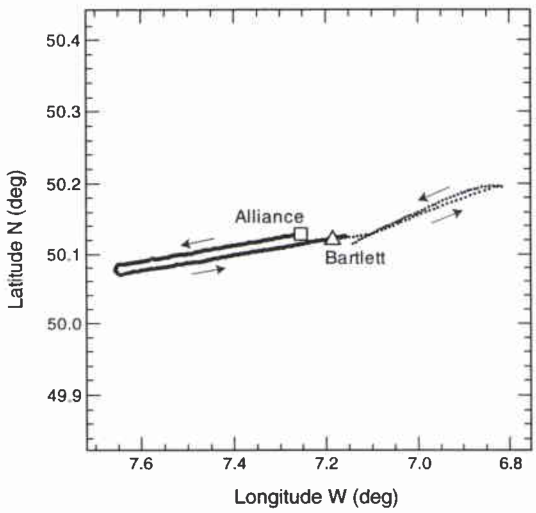

Figure A-15 *Navigation track for Run C1*

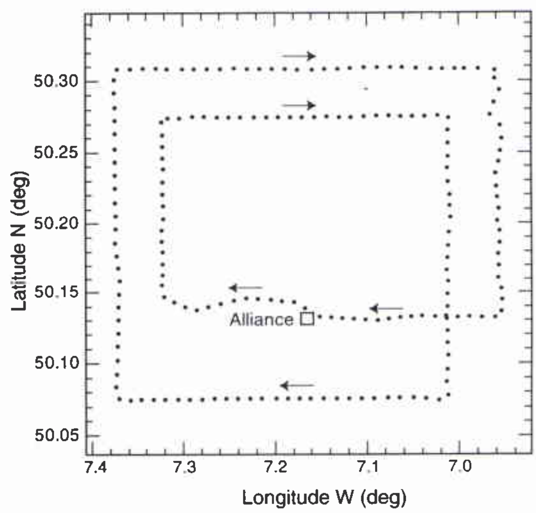

Figure A-16 *Navigation track for Run BATHY4*

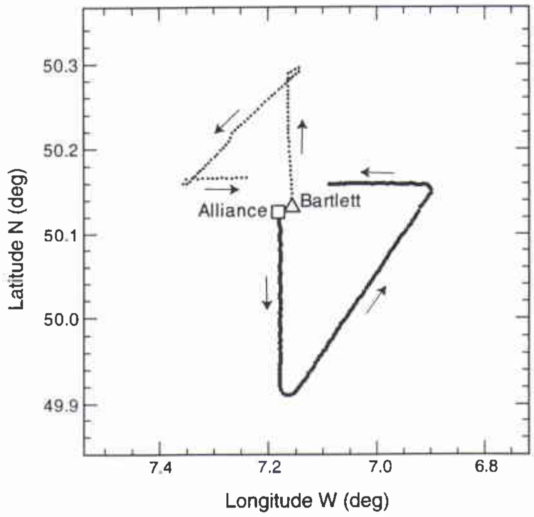

Figure A-17 *Navigation track for Run C2*

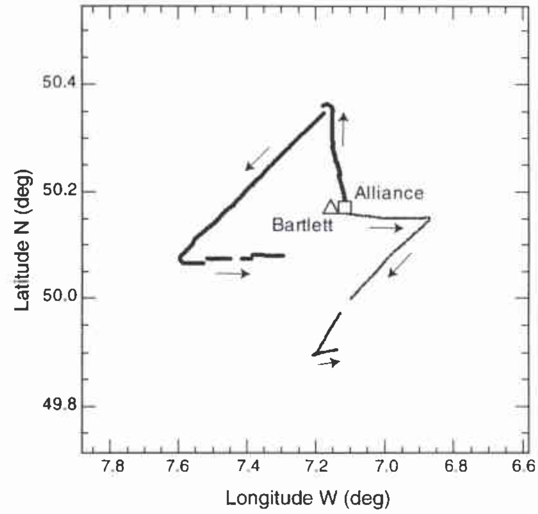

Figure A-18 *Navigation track for Run C3*

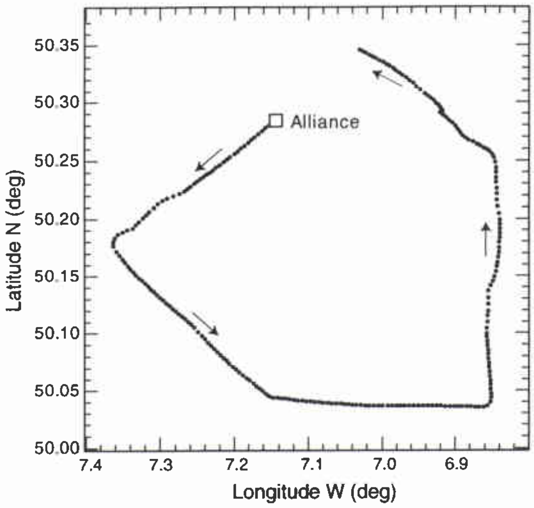

Figure A-19 *Navigation track for Run Polygl*

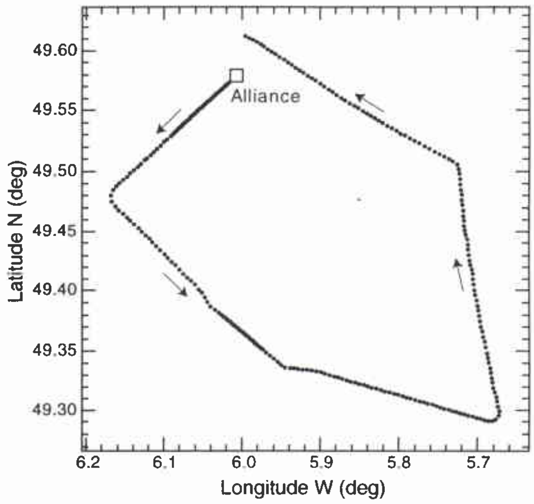

Figure A-20 *Navigation track for Run POLYG2*

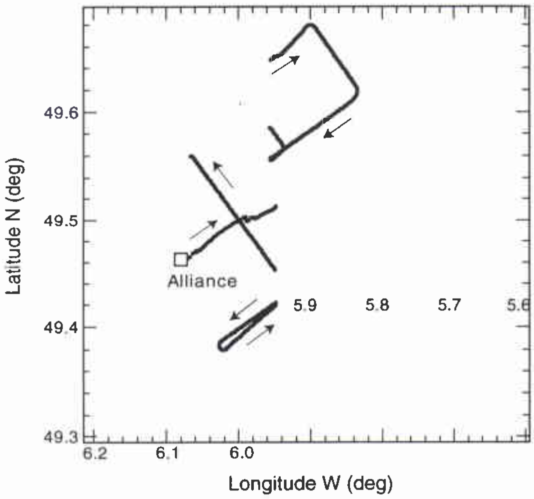

Figure A-21
Navigation track for Run UNIBOOM

Appendix B
Environmental Information

Environmental information from both *Alliance* and *Bartlett* for the various experiments has been collected (20 figures for *Alliance* and 14 figures for *Bartlett*); the labels refer to the *Alliance* run identifiers listed in Table 1.

Alliance and *Bartlett* data are grouped face to face for each experiment; the blank pages 67, 85 and 89 signify that no data from *Bartlett* is available for this experiment because *Bartlett* performed independent work. The same applies for runs *POLYG1*, *POLYG2* and *UNIBOOM* (pages 94-96).

Brief descriptions of the experiments are given in Section 2.1. Each figure has 6 graphs as a function of time: (i) water depth, (ii) sea state, (iii) wind speed, (iv) wind direction, (v) ship speed, and (vi) ship heading. The wind direction and ship direction (heading) units "(°T)" should be read as "degrees true".

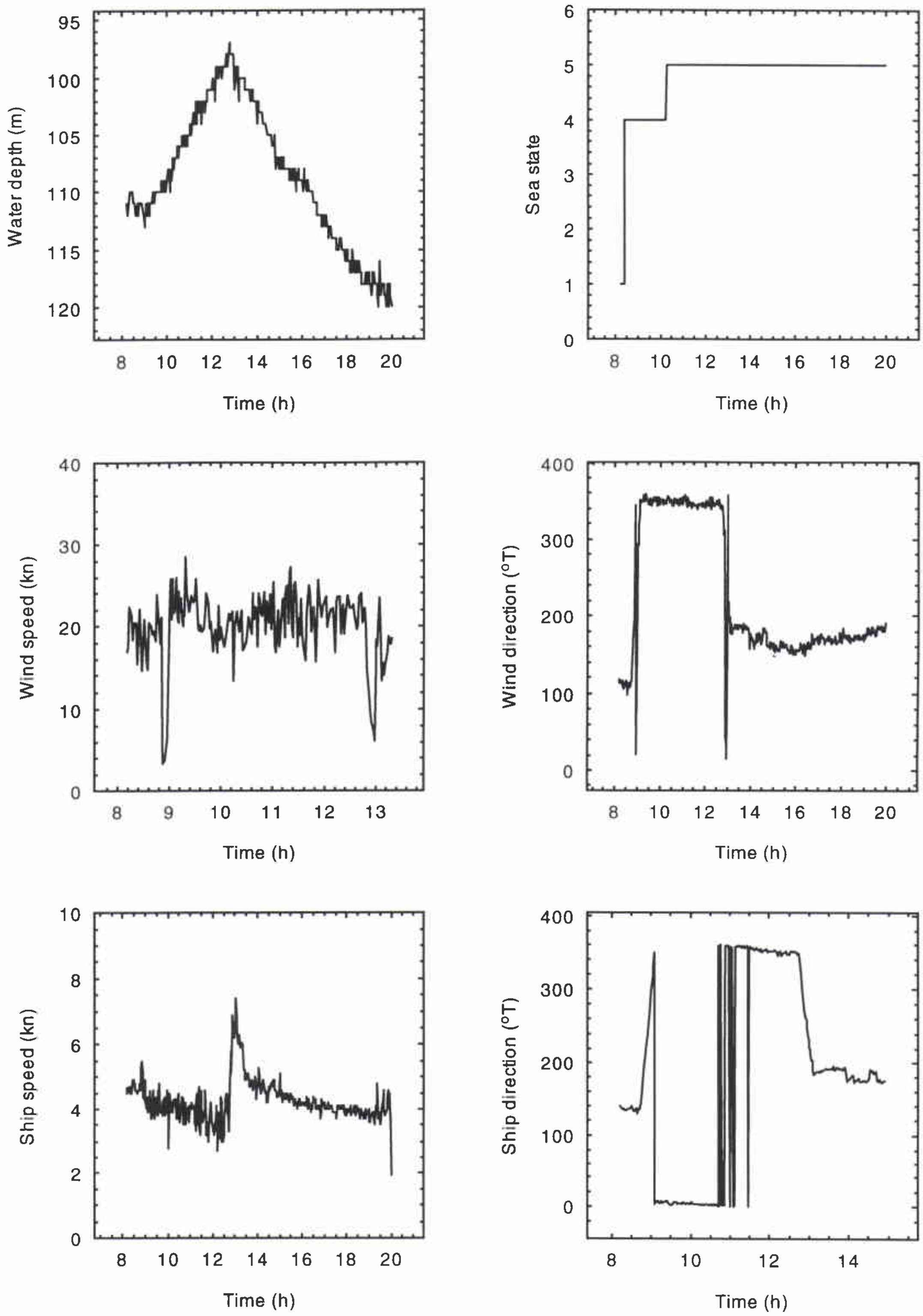

Figure B-1 *Environmental information for Alliance Run A1.***Figure**

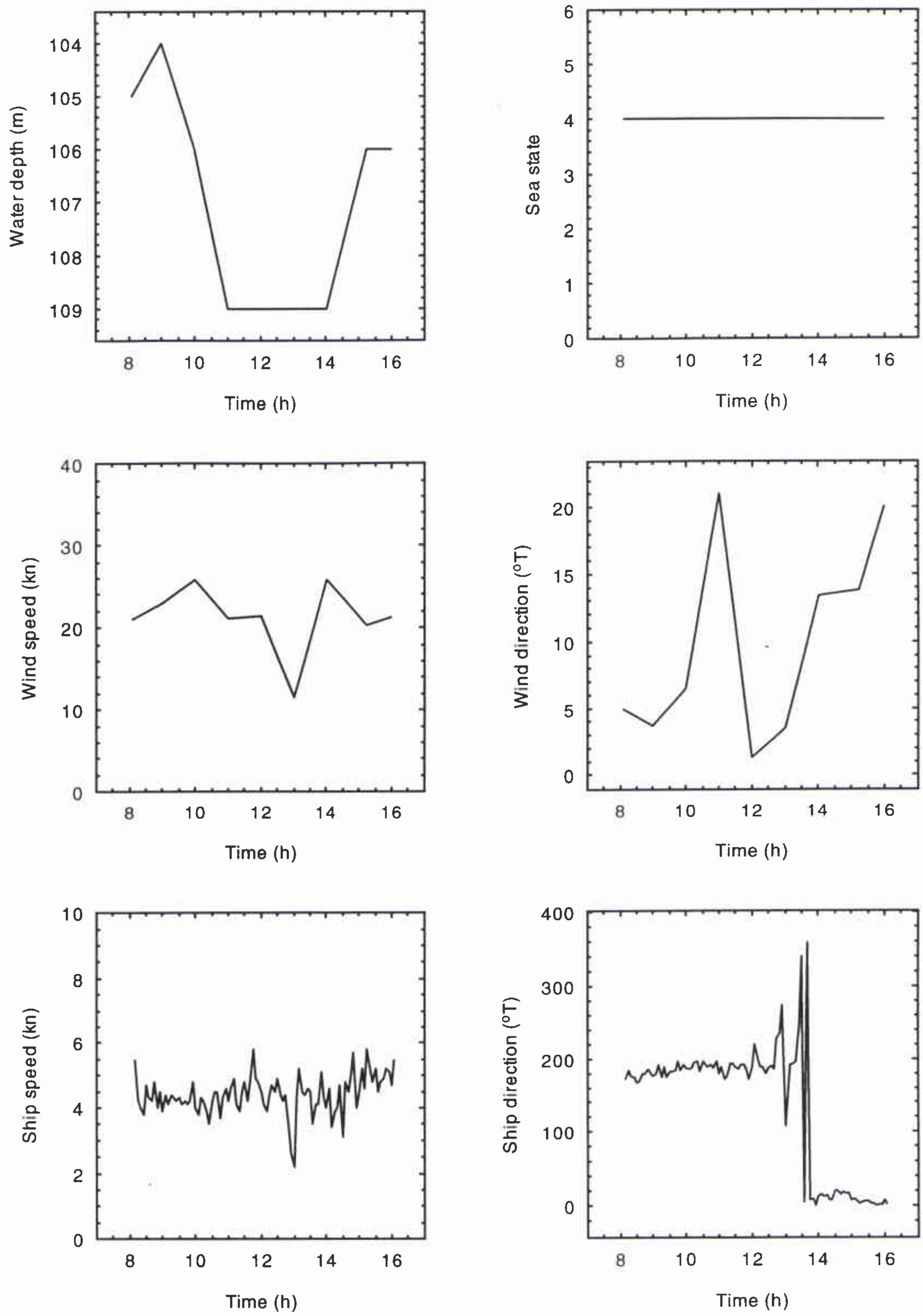

B-2 *Environmental information from Bartlett for Alliance Run A1.*

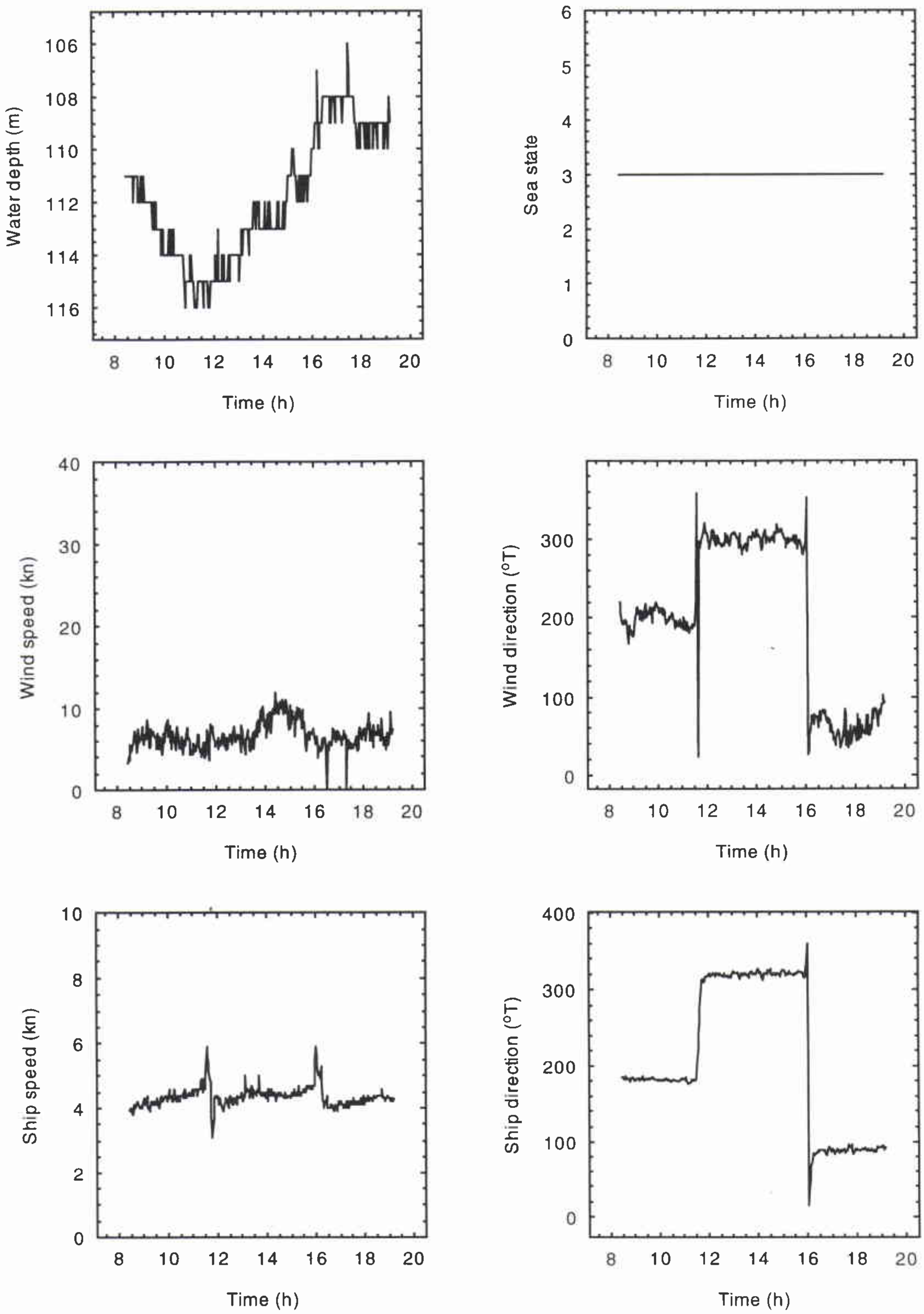

Figure B-3 *Environmental information for Alliance Run A2.*

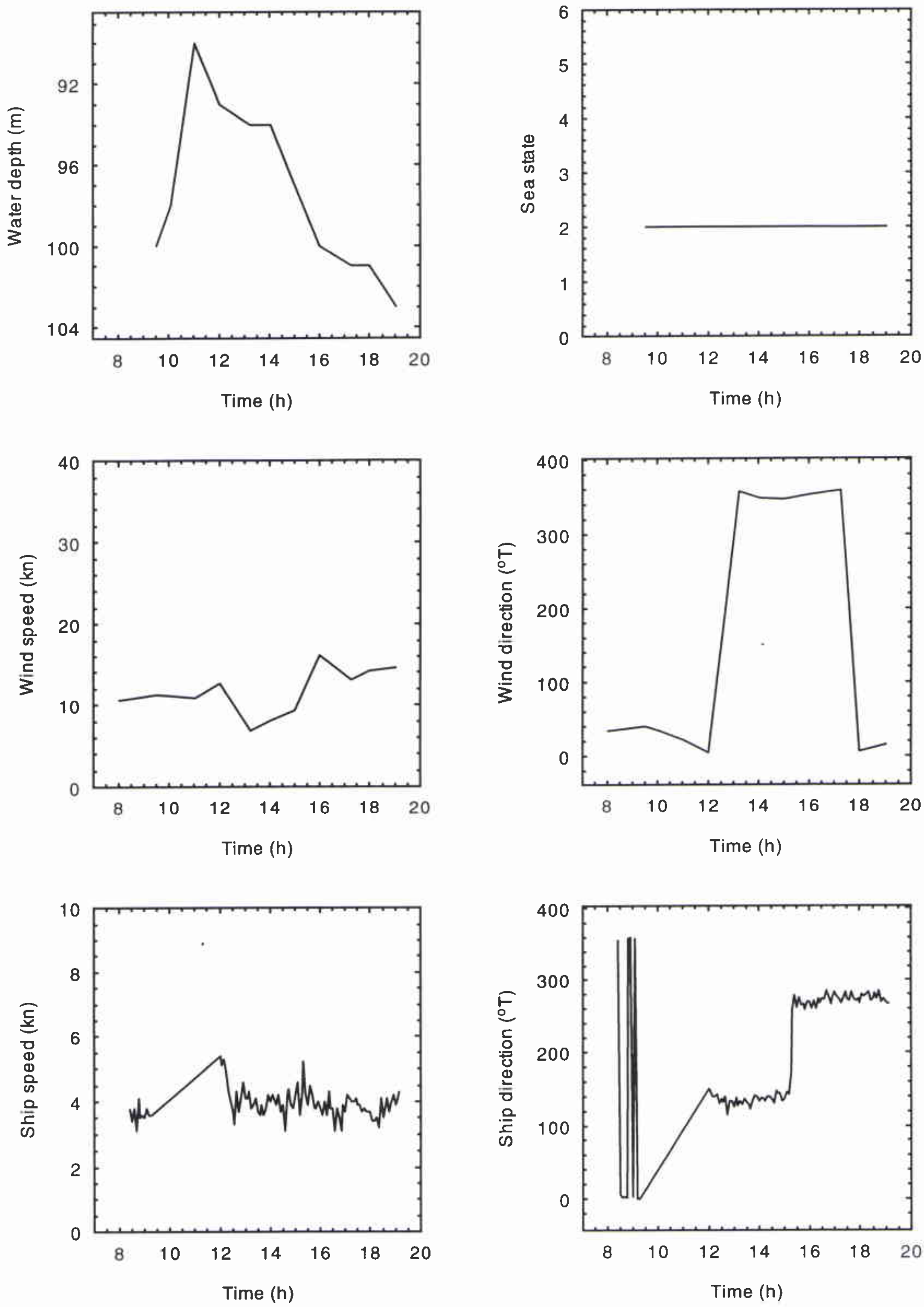

Figure B-4 *Environmental information from Bartlett for Alliance Run A2.*

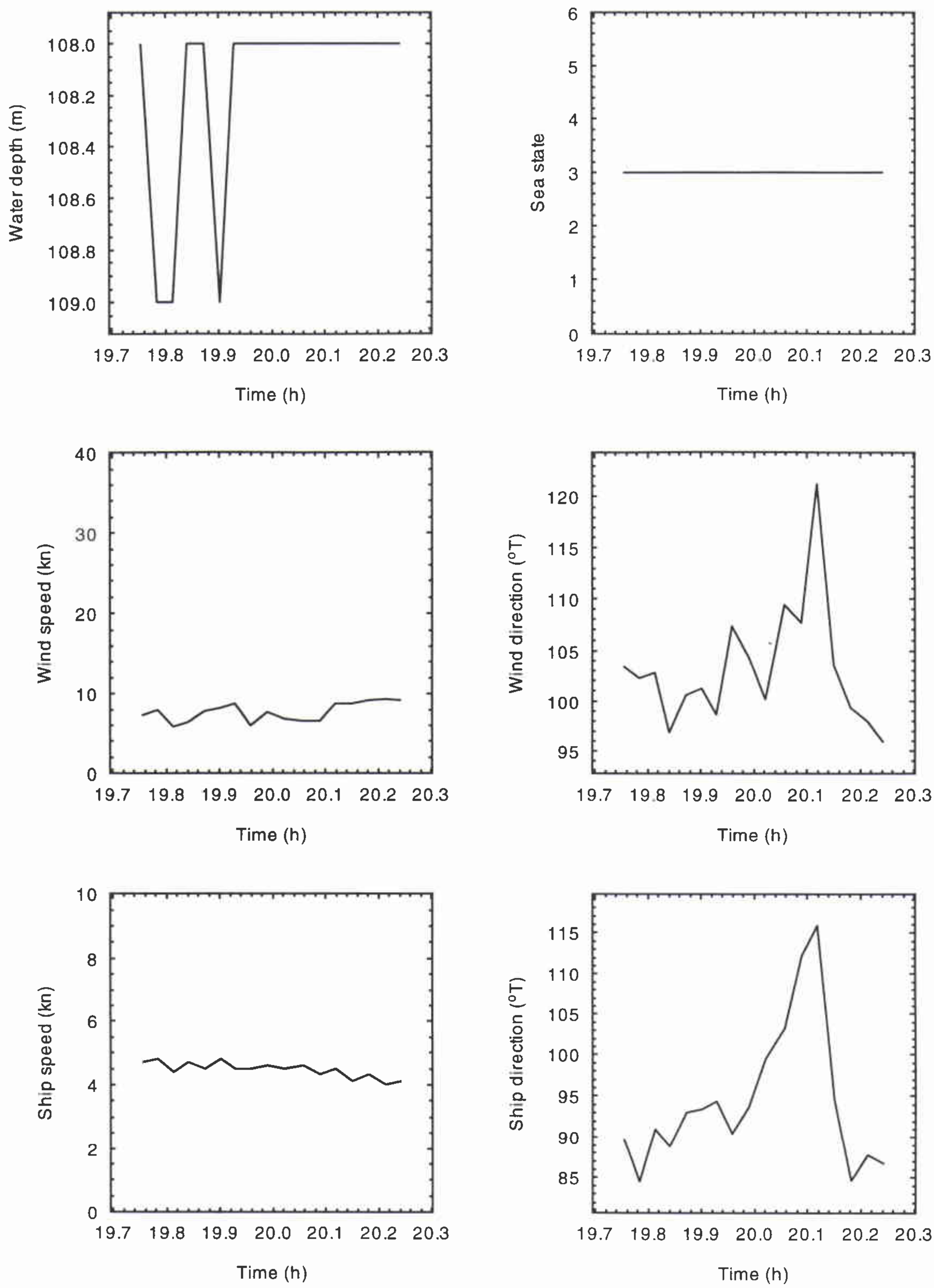

Figure B-5 *Environmental information for Alliance Run CW1.*

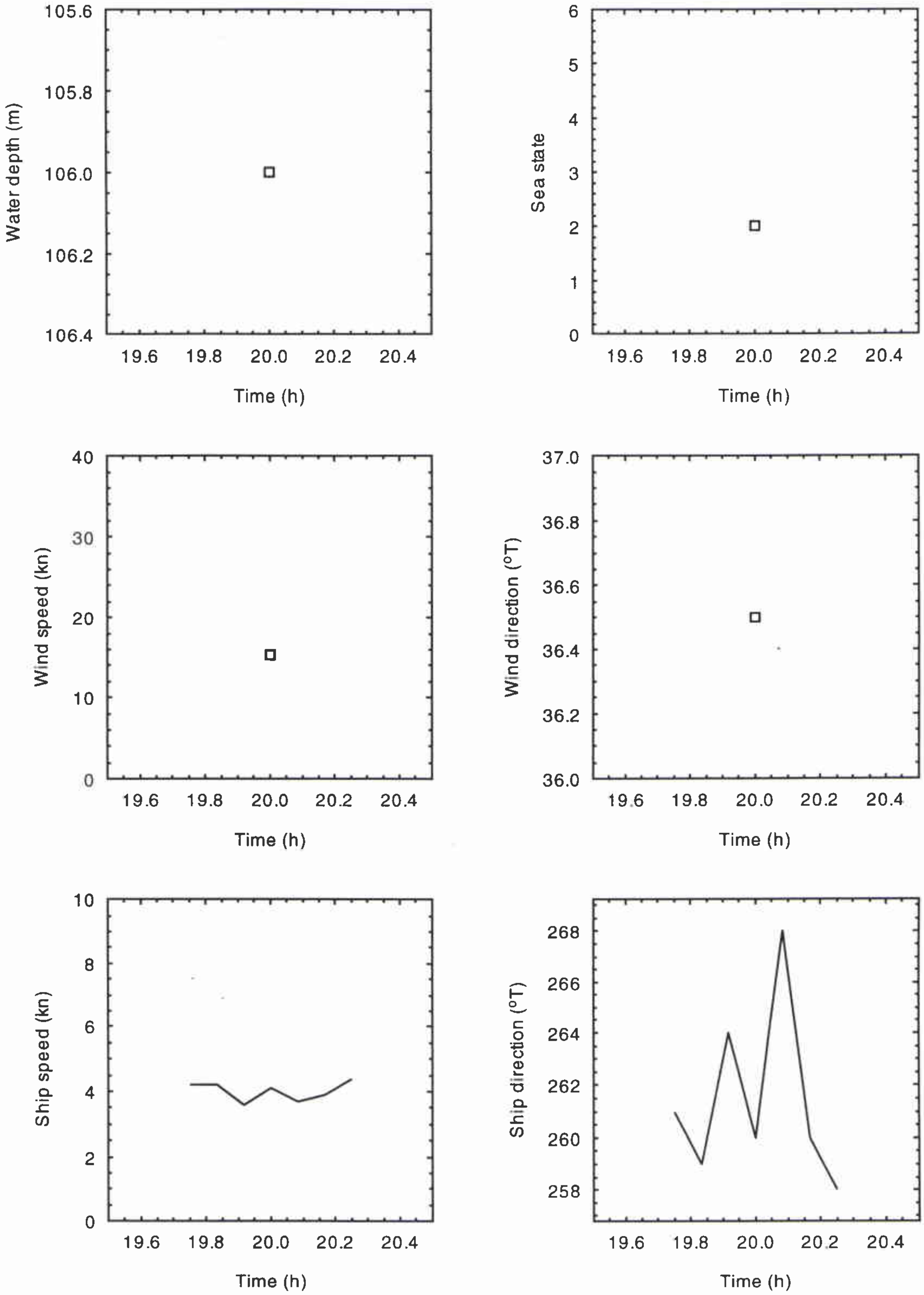

Figure B-6 *Environmental information from Bartlett for Alliance Run CW1.*

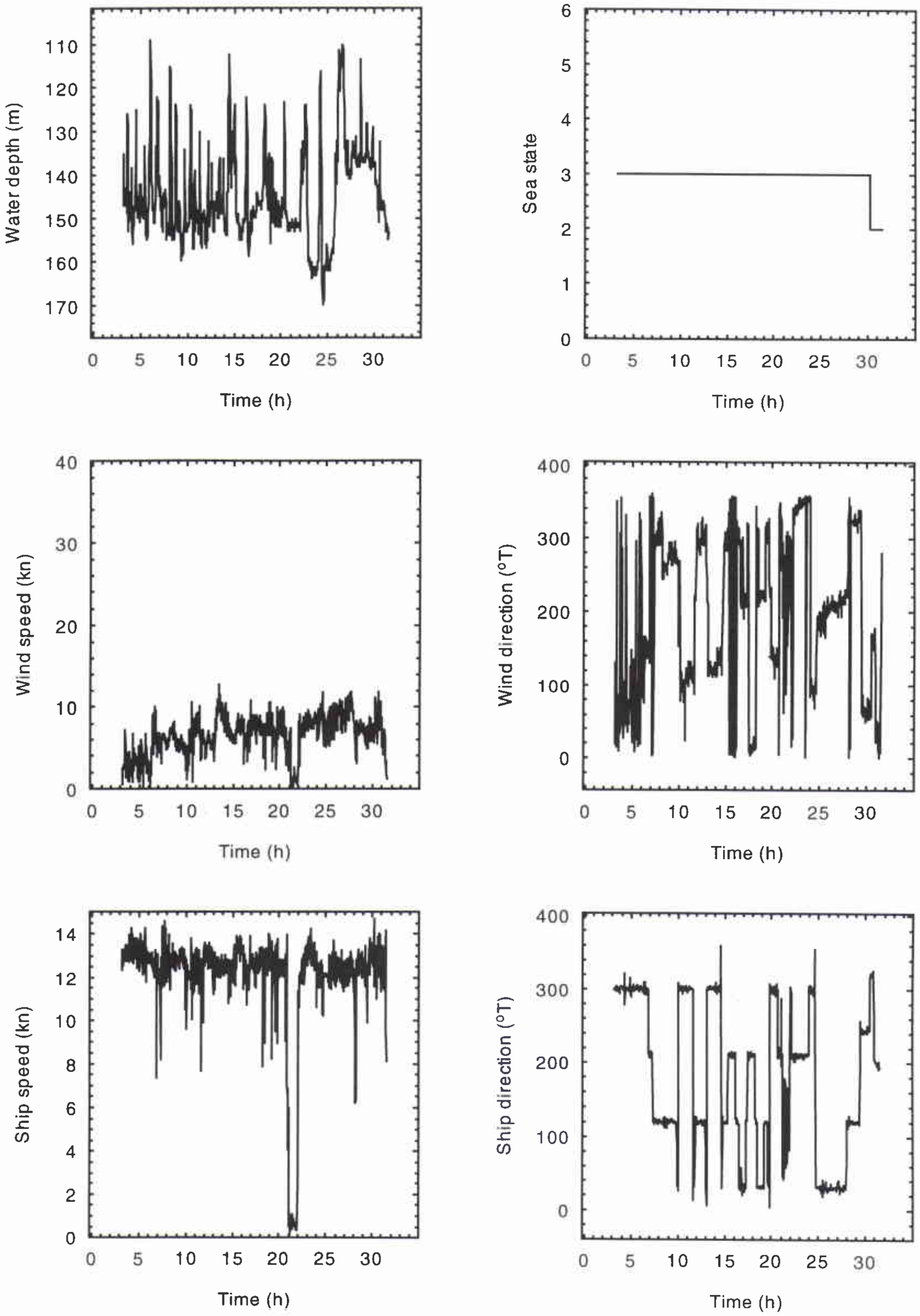

Figure B-7 *Environmental information for Alliance Run BATHY2.*

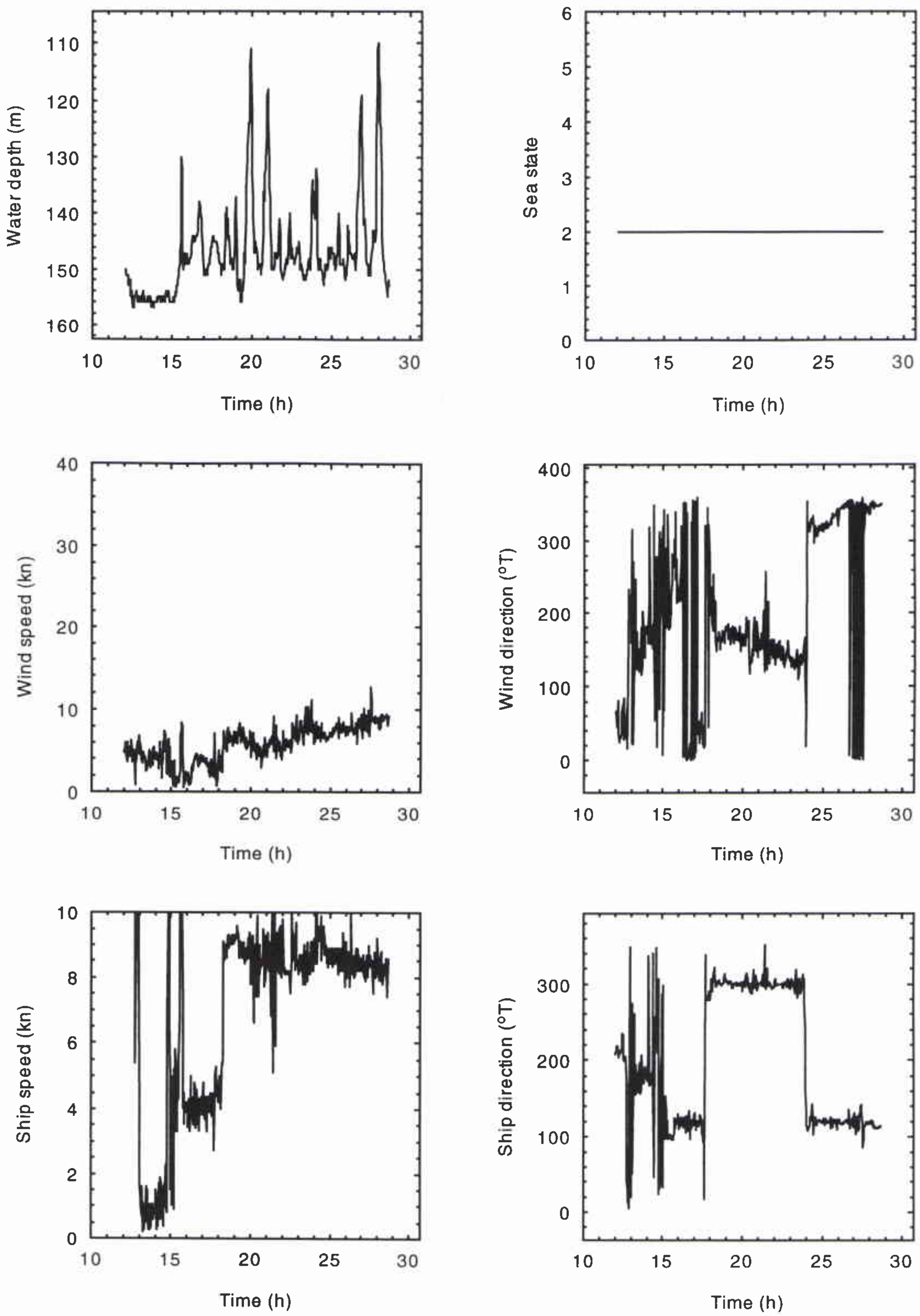

Figure B-8 *Environmental information for Alliance Run TLB.*

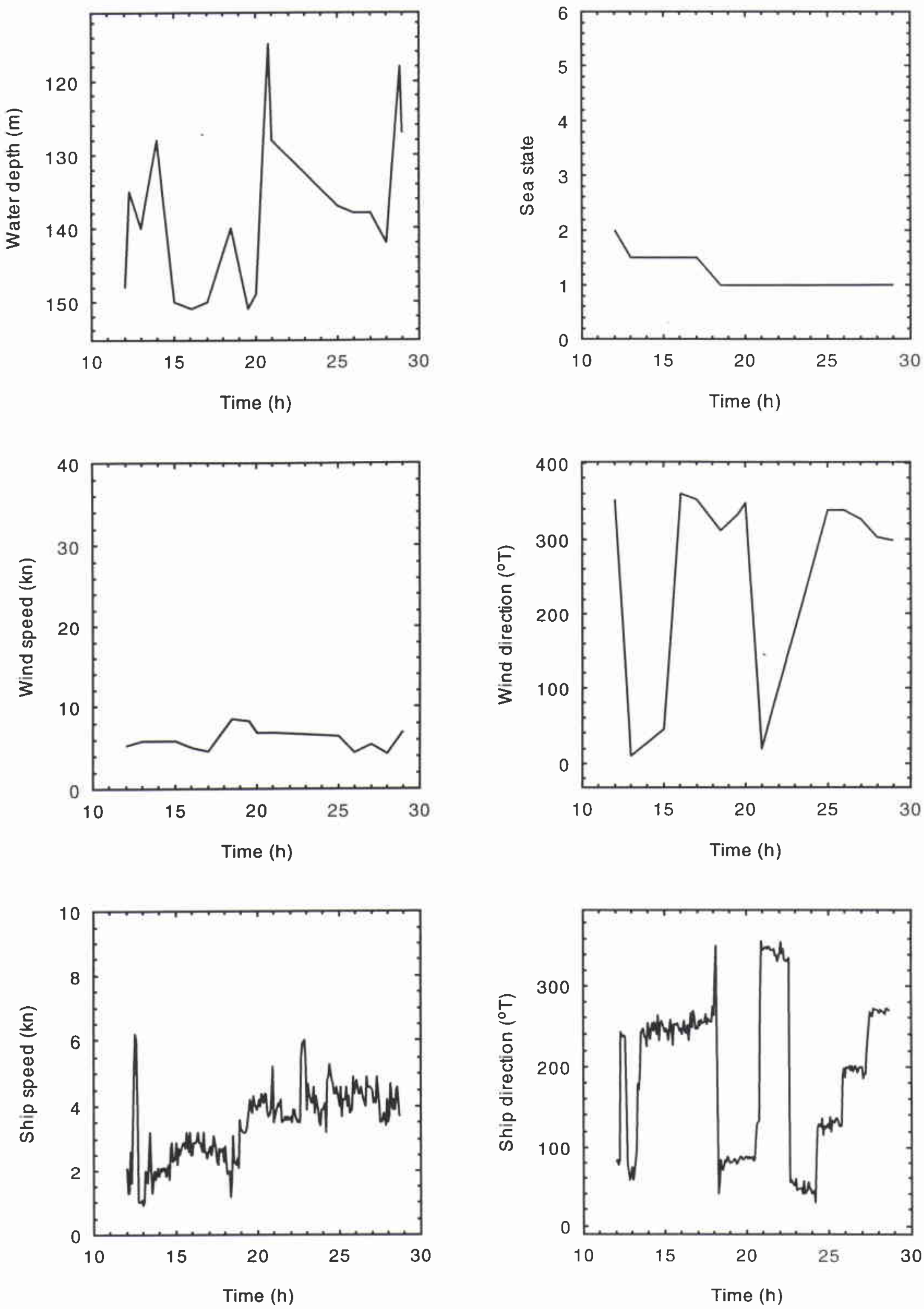

Figure B-9 *Environmental information from Bartlett for Alliance Run TLB.*

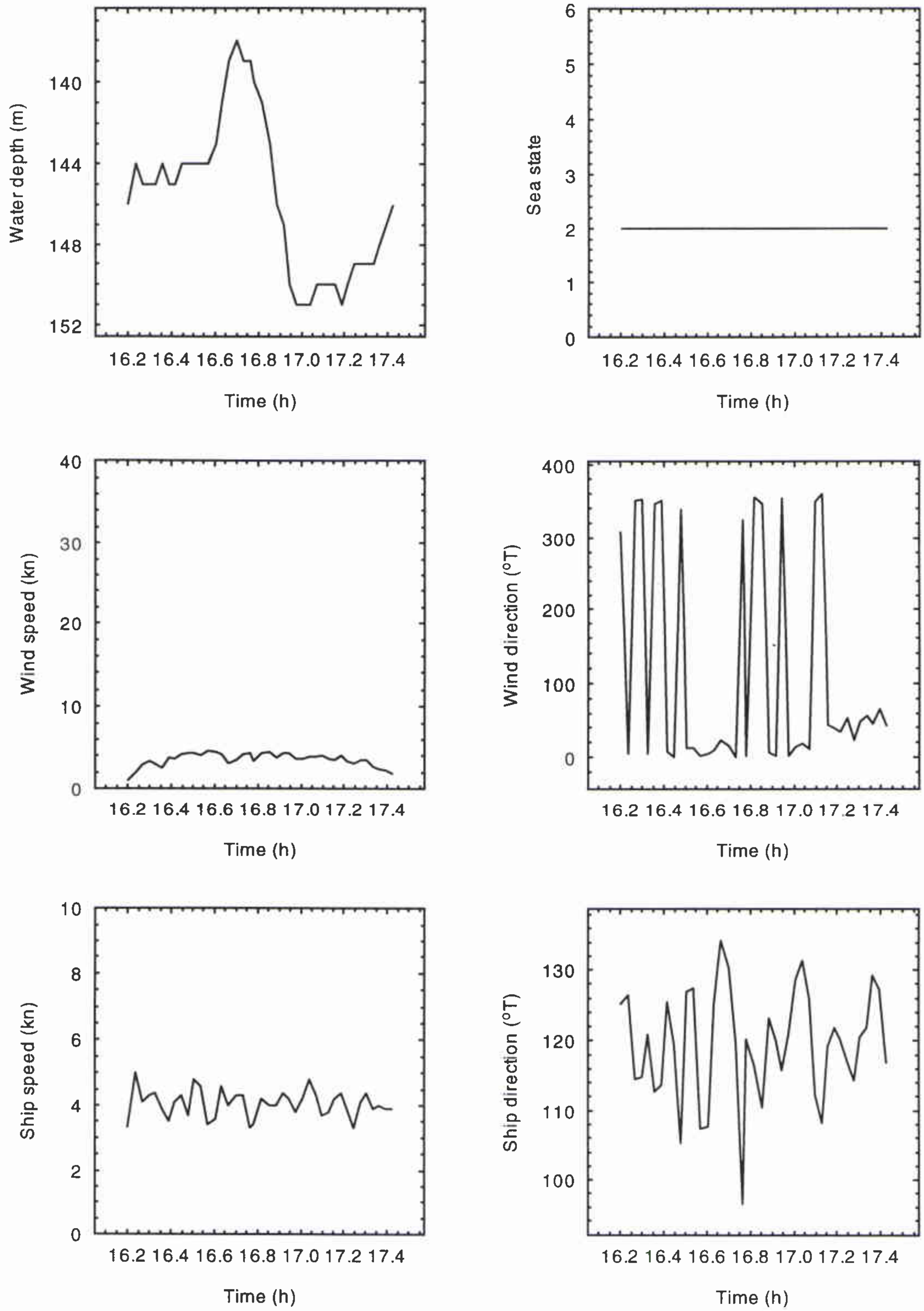

Figure B-10 *Environmental information for Alliance Run CW2.*

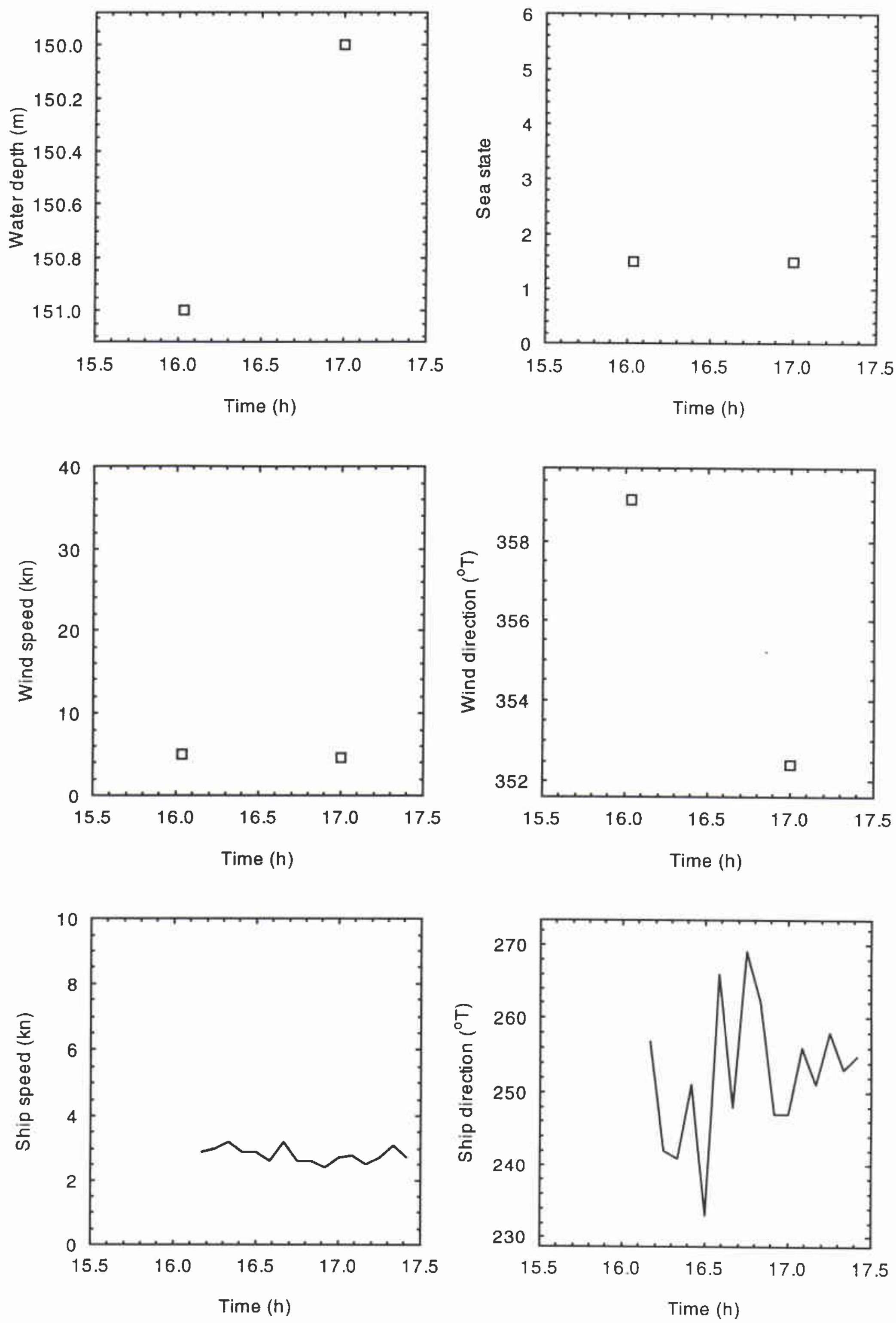

Figure B-11 *Environmental information from Bartlett for Alliance Run CW2.*

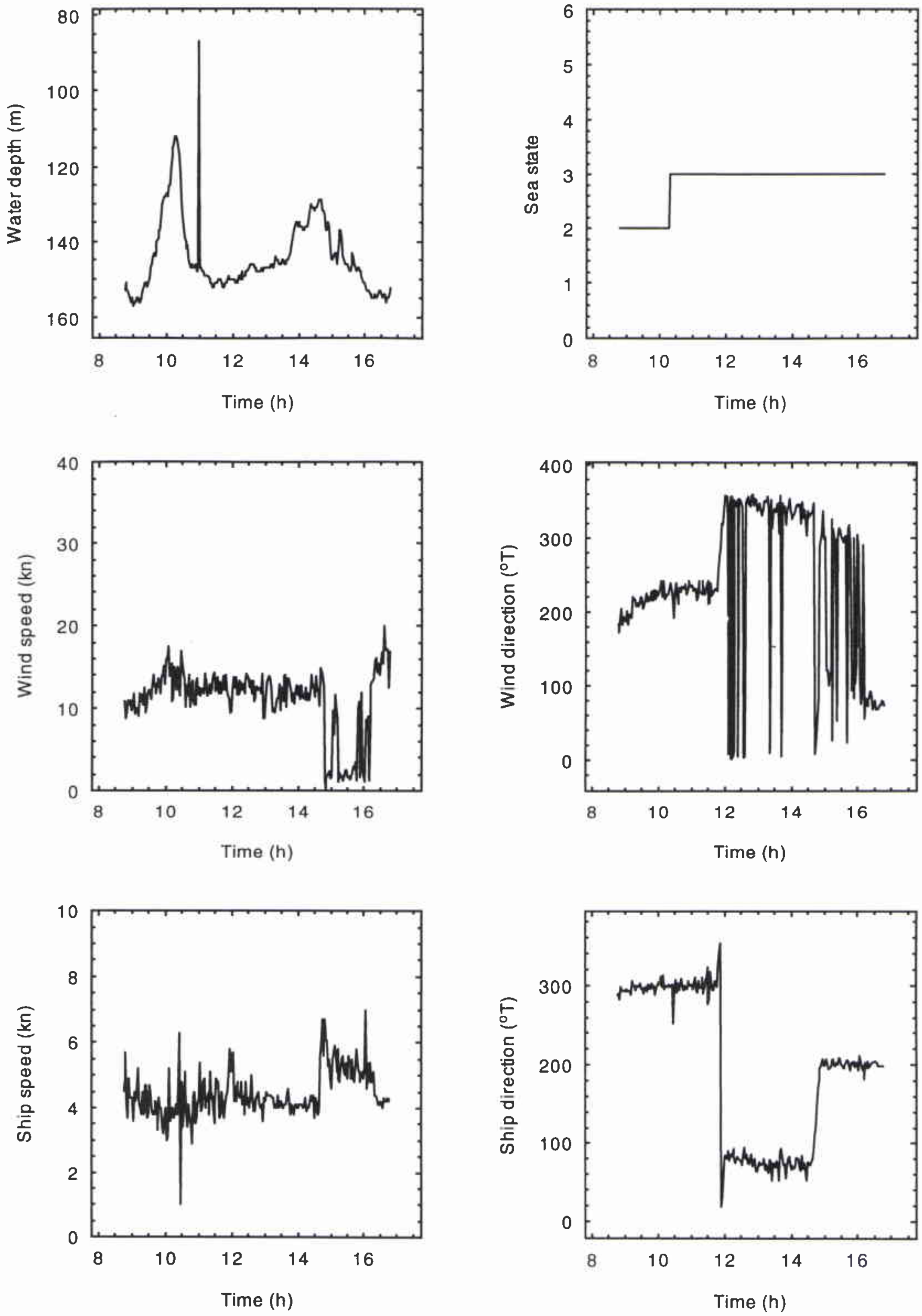

Figure B-12 *Environmental information for Alliance Run B1.*

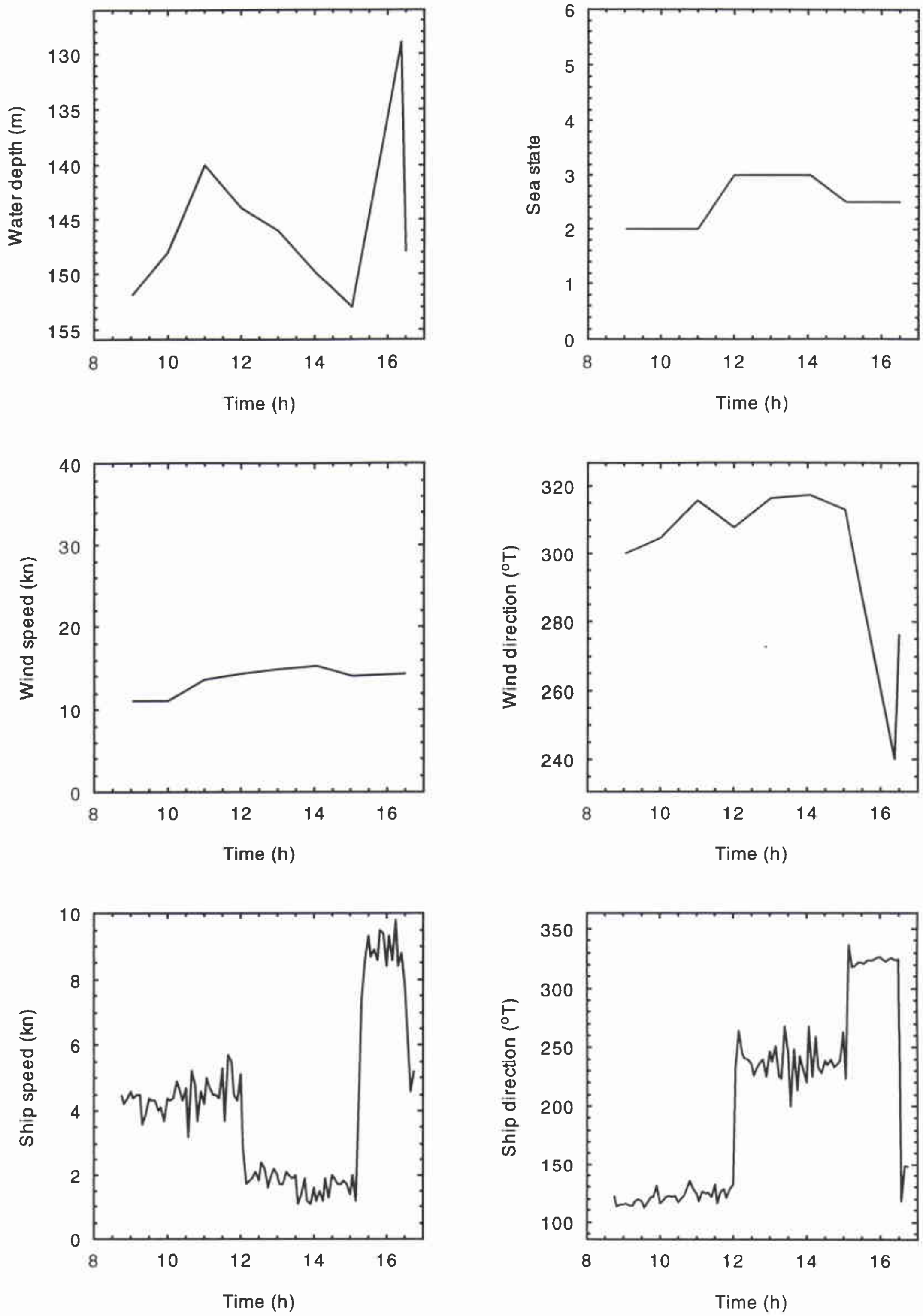

Figure B-13 *Environmental information from Bartlett for Alliance Run B1.*

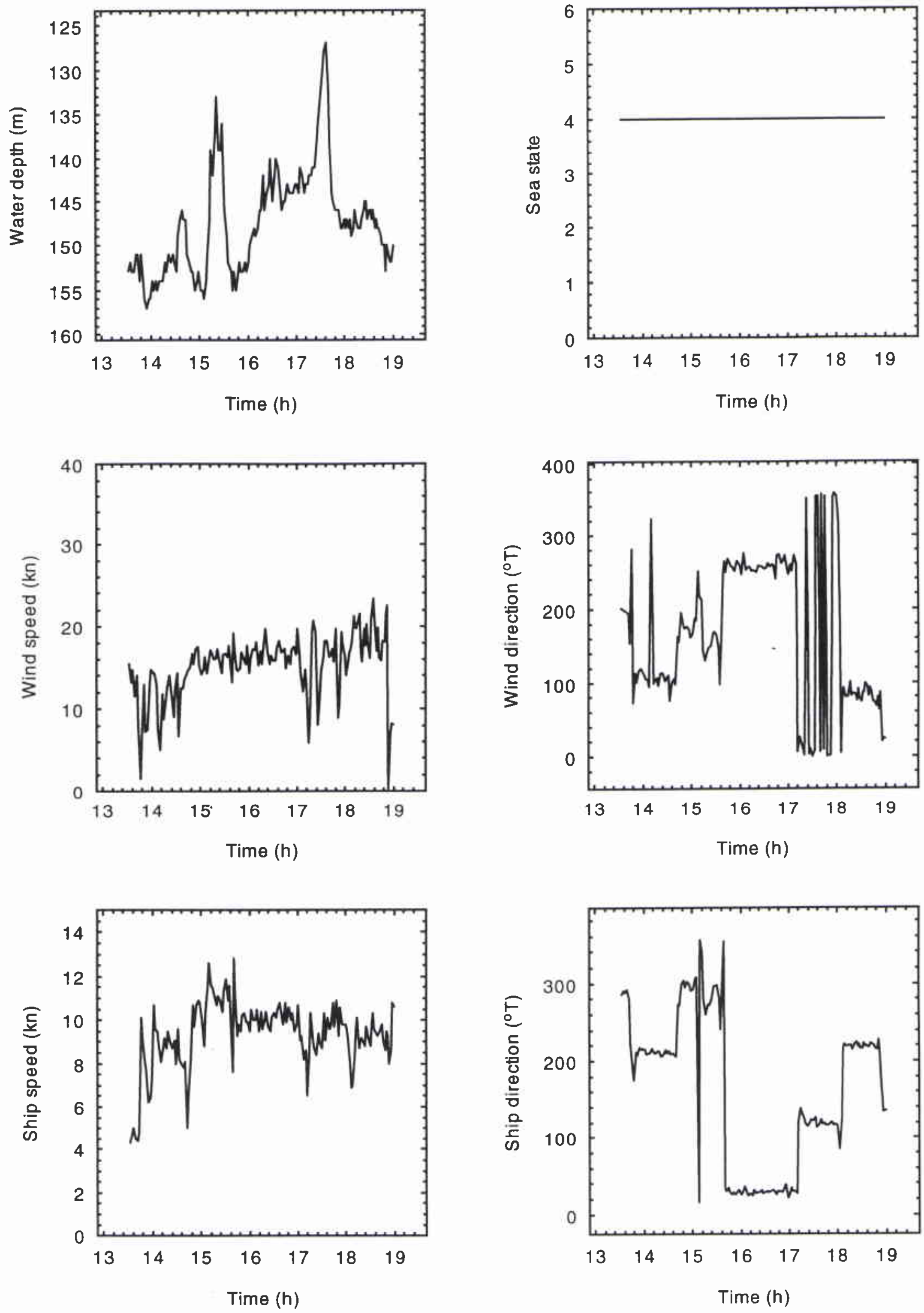

Figure B-14 *Environmental information for Alliance Run B2SUS.*

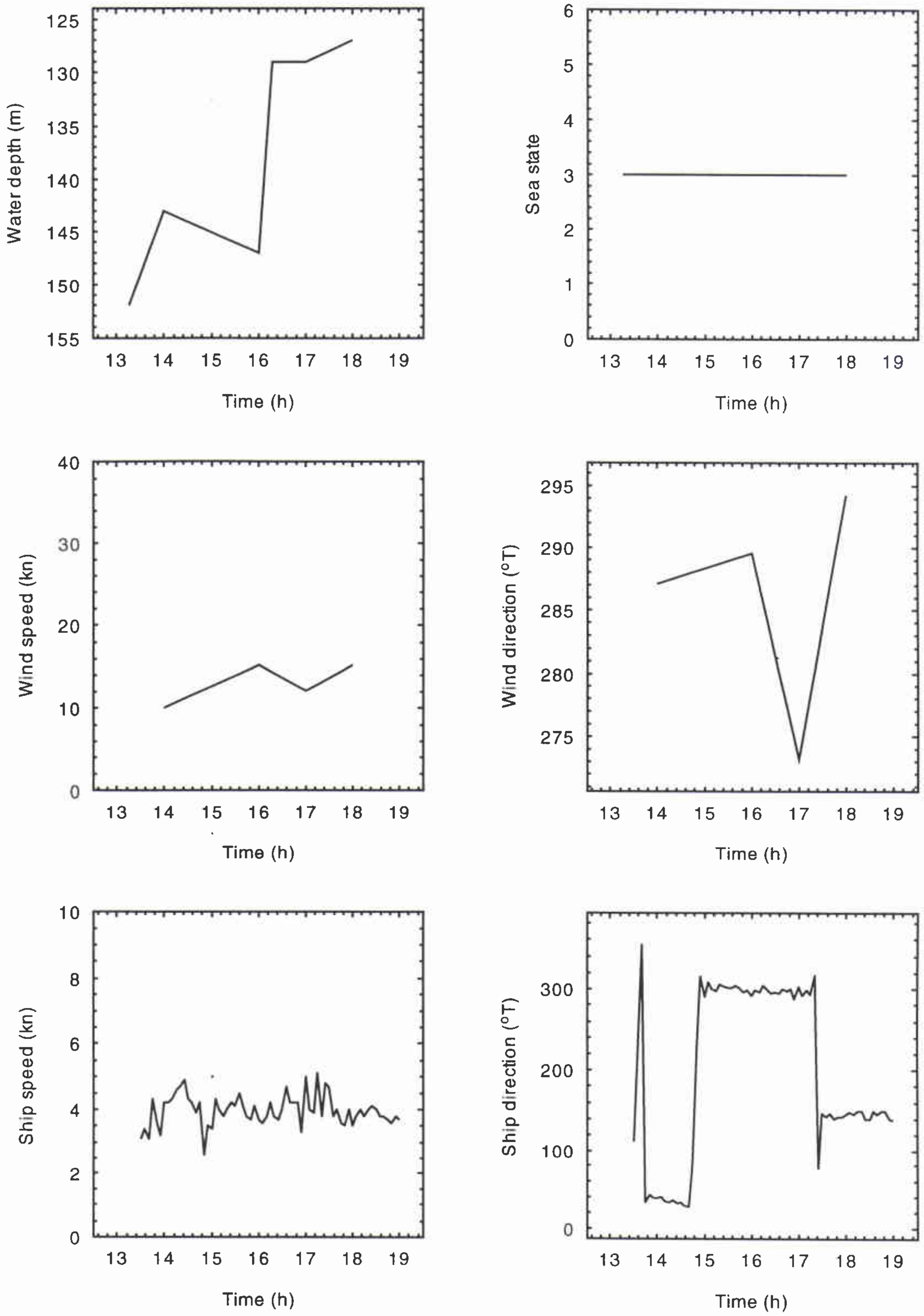

Figure B-15 *Environmental information from Bartlett for Alliance Run B2SUS.*

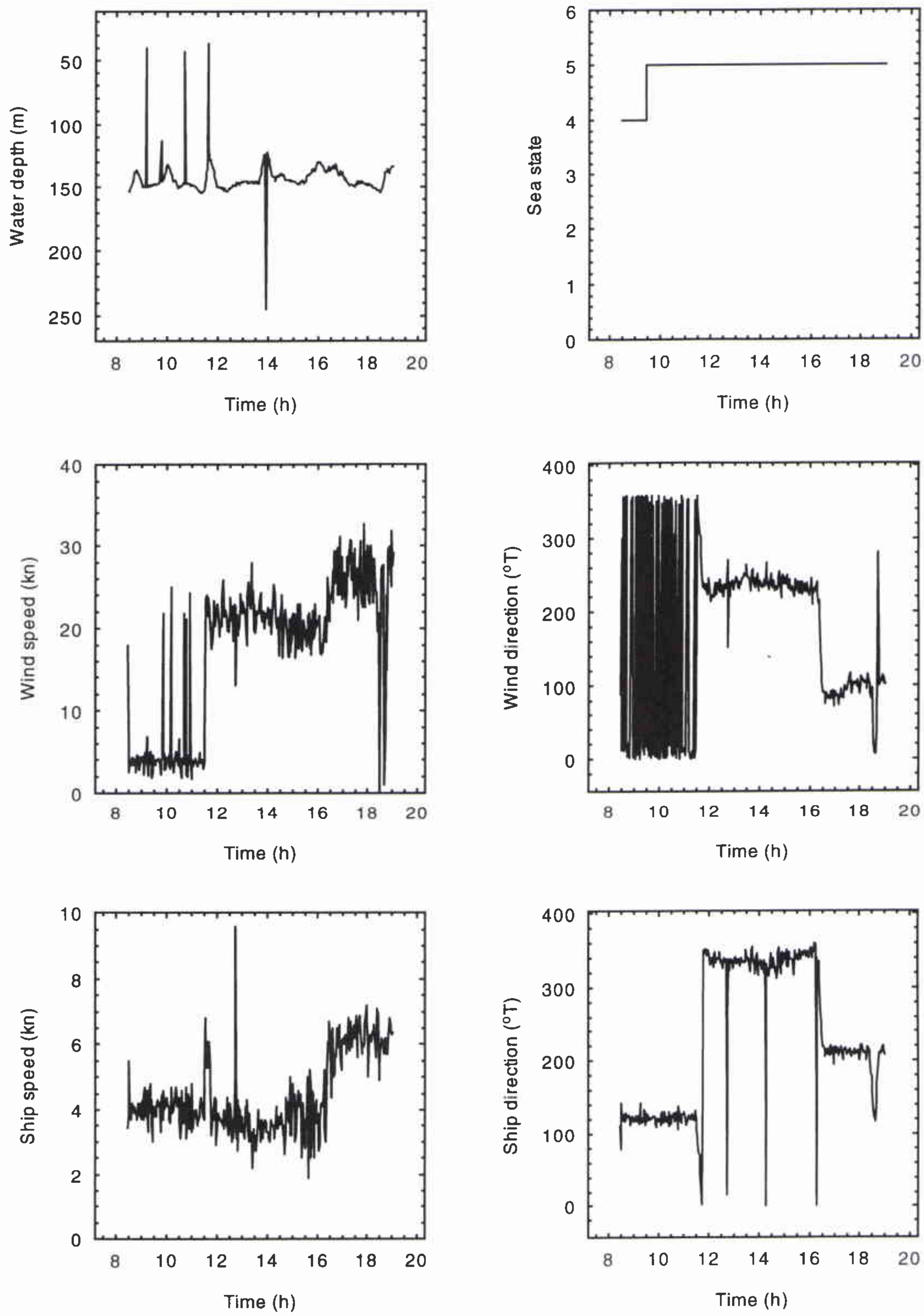

Figure B-16 *Environmental information for Alliance Run B2.*

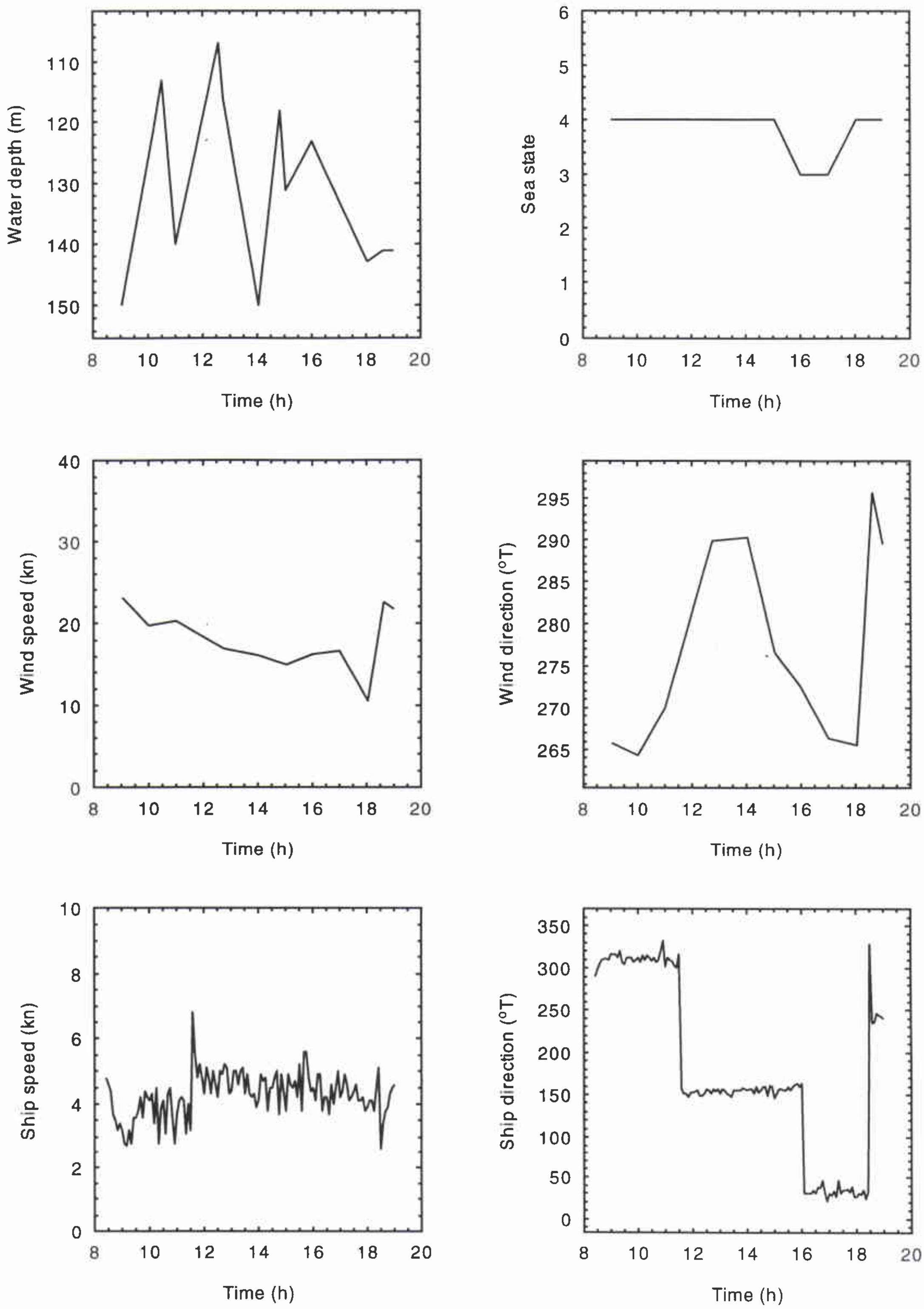

Figure B-17 *Environmental information from Bartlett for Alliance Run B2.*

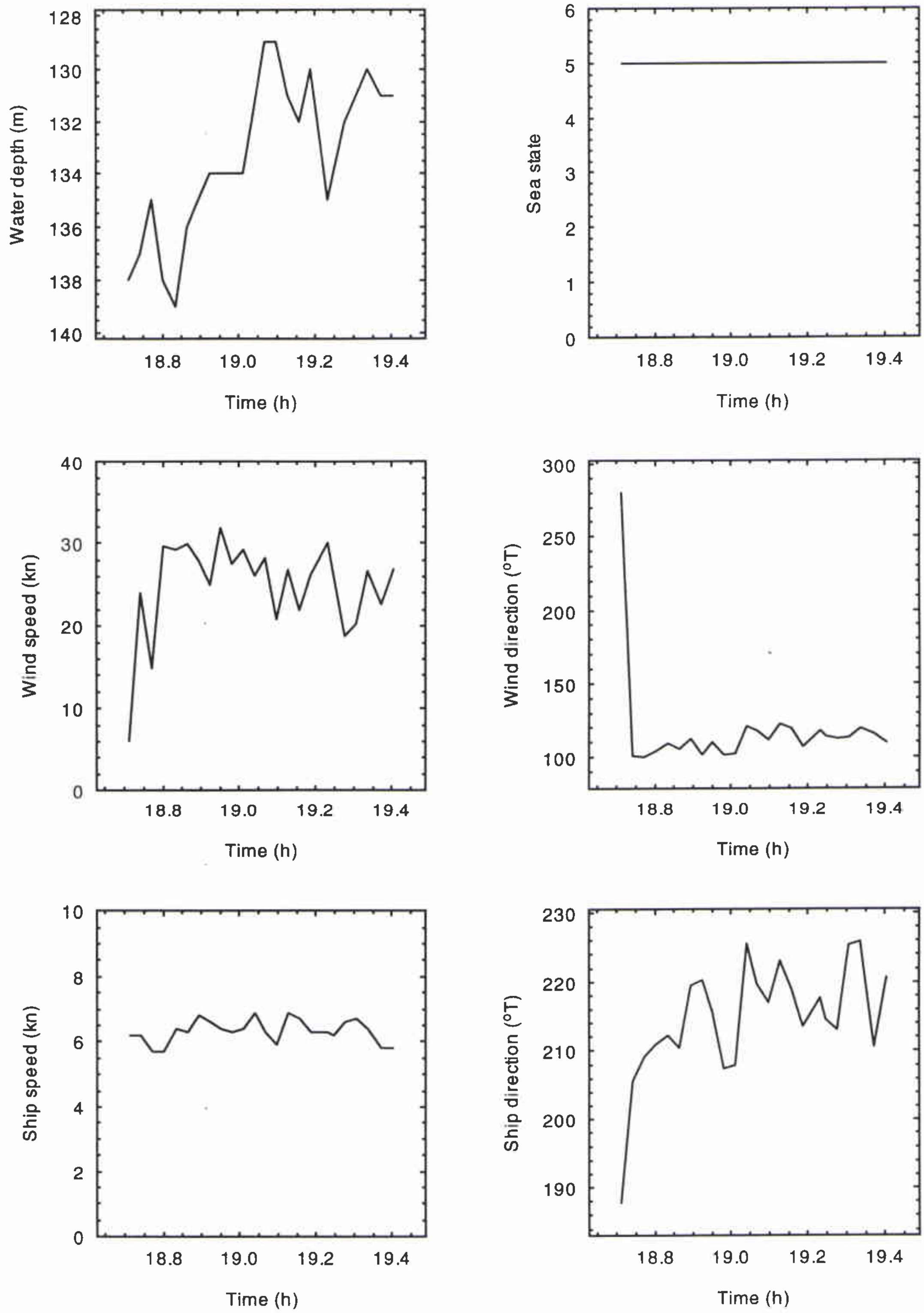

Figure B-18 *Environmental information for Alliance Run CW3.*

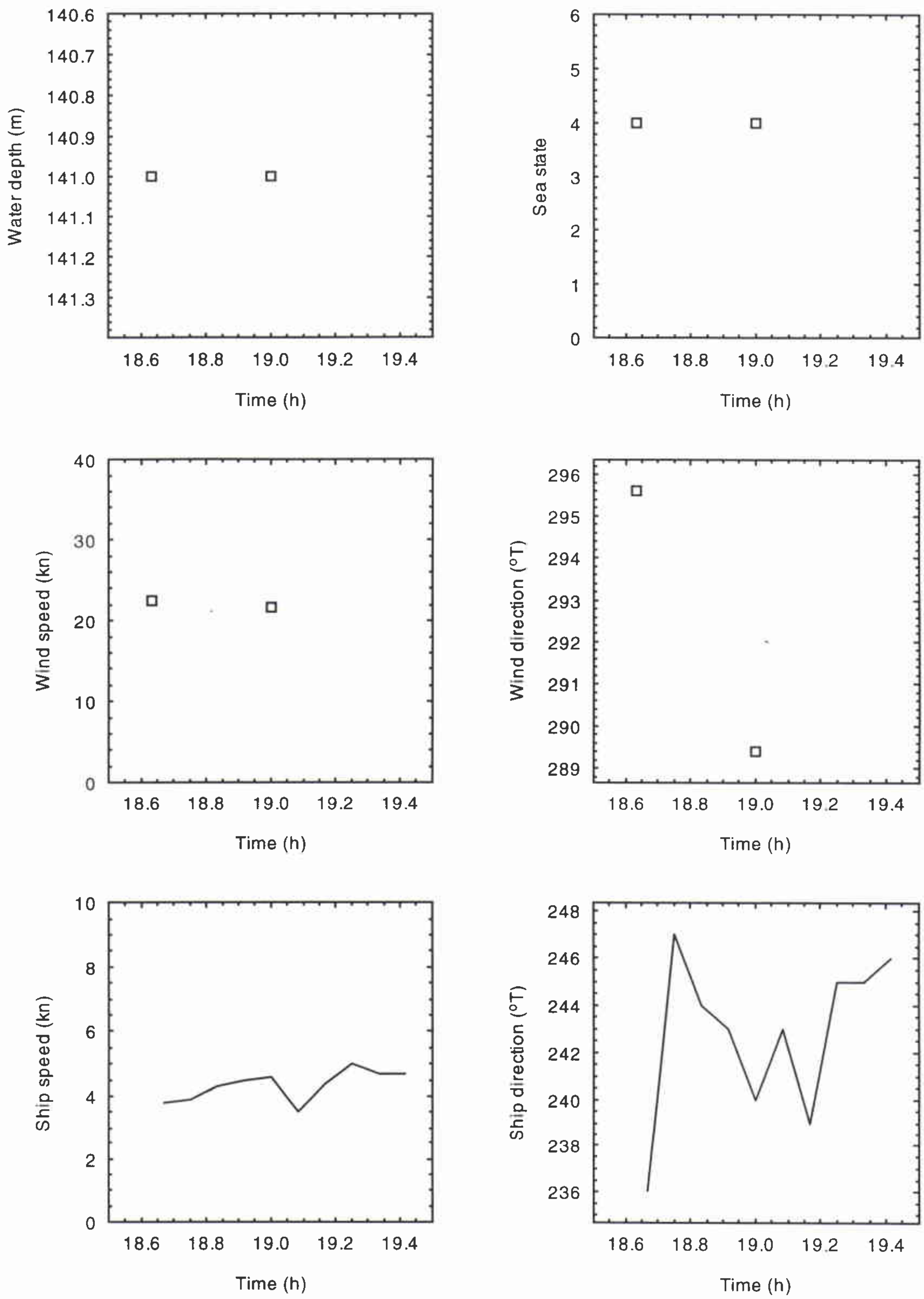

Figure B-19 *Environmental information from Bartlett for Alliance Run CW3.*

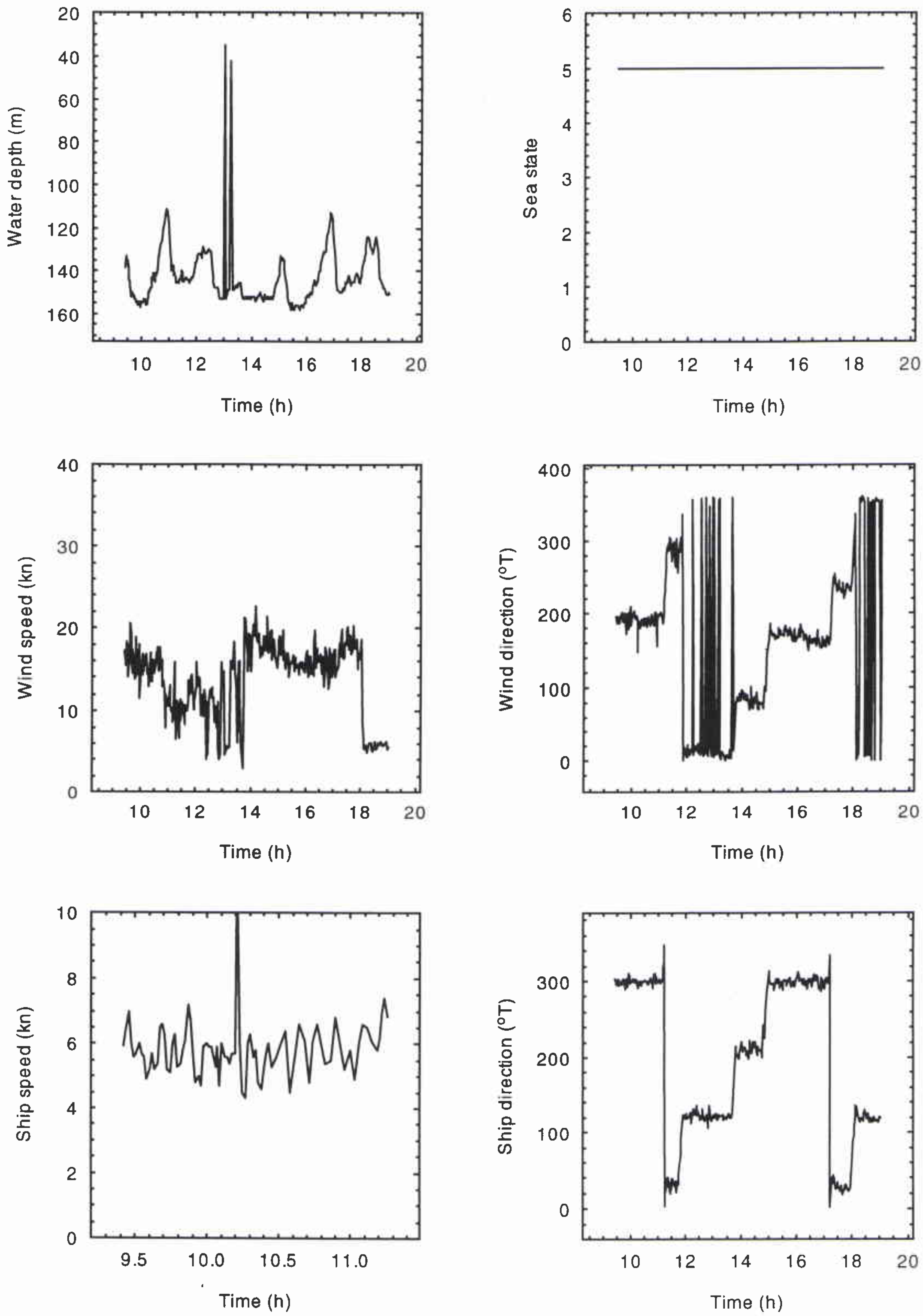

Figure B-20 *Environmental information for Alliance Run B3.*

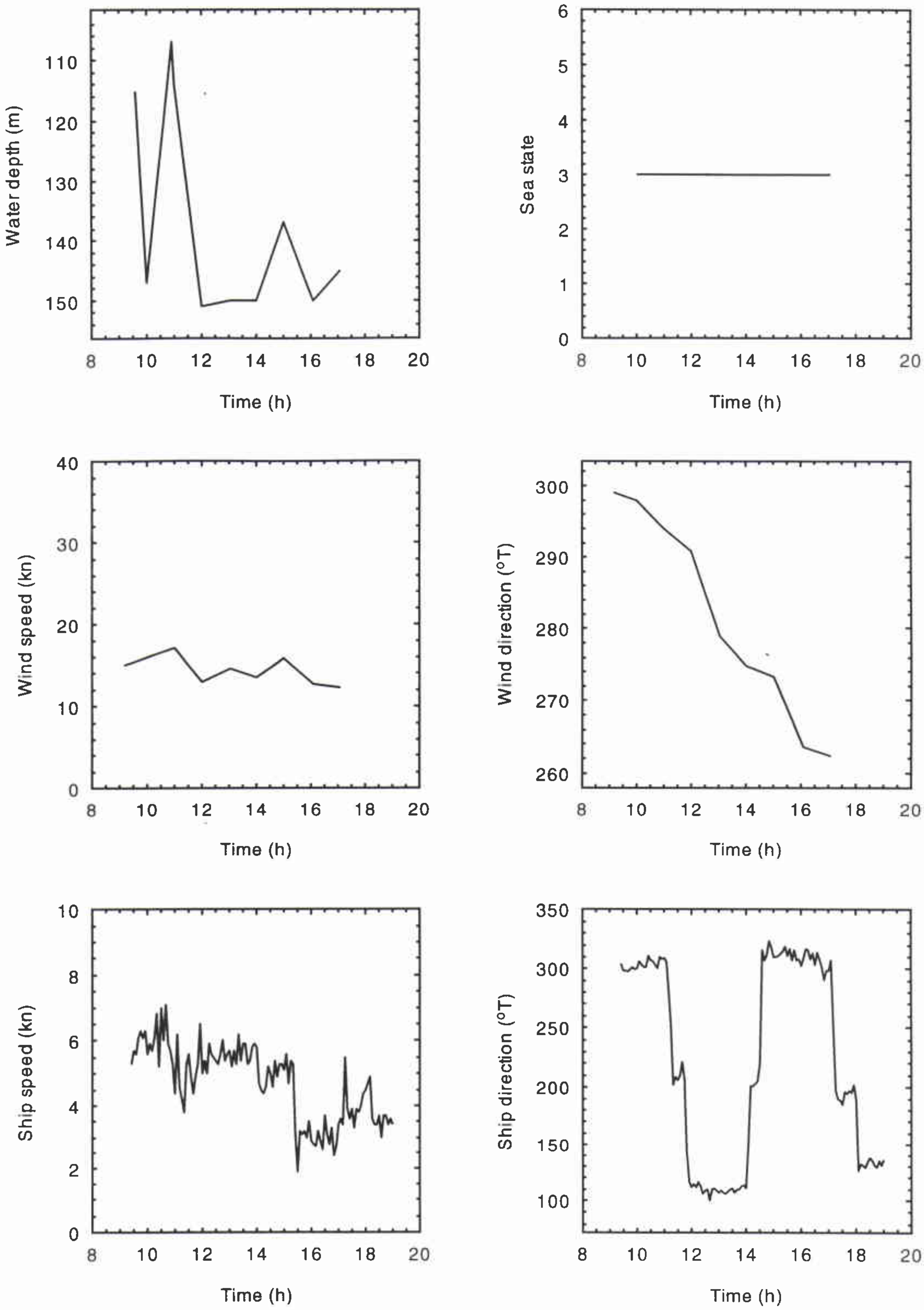

Figure B-21 *Environmental information from Bartlett for Alliance Run B3.*

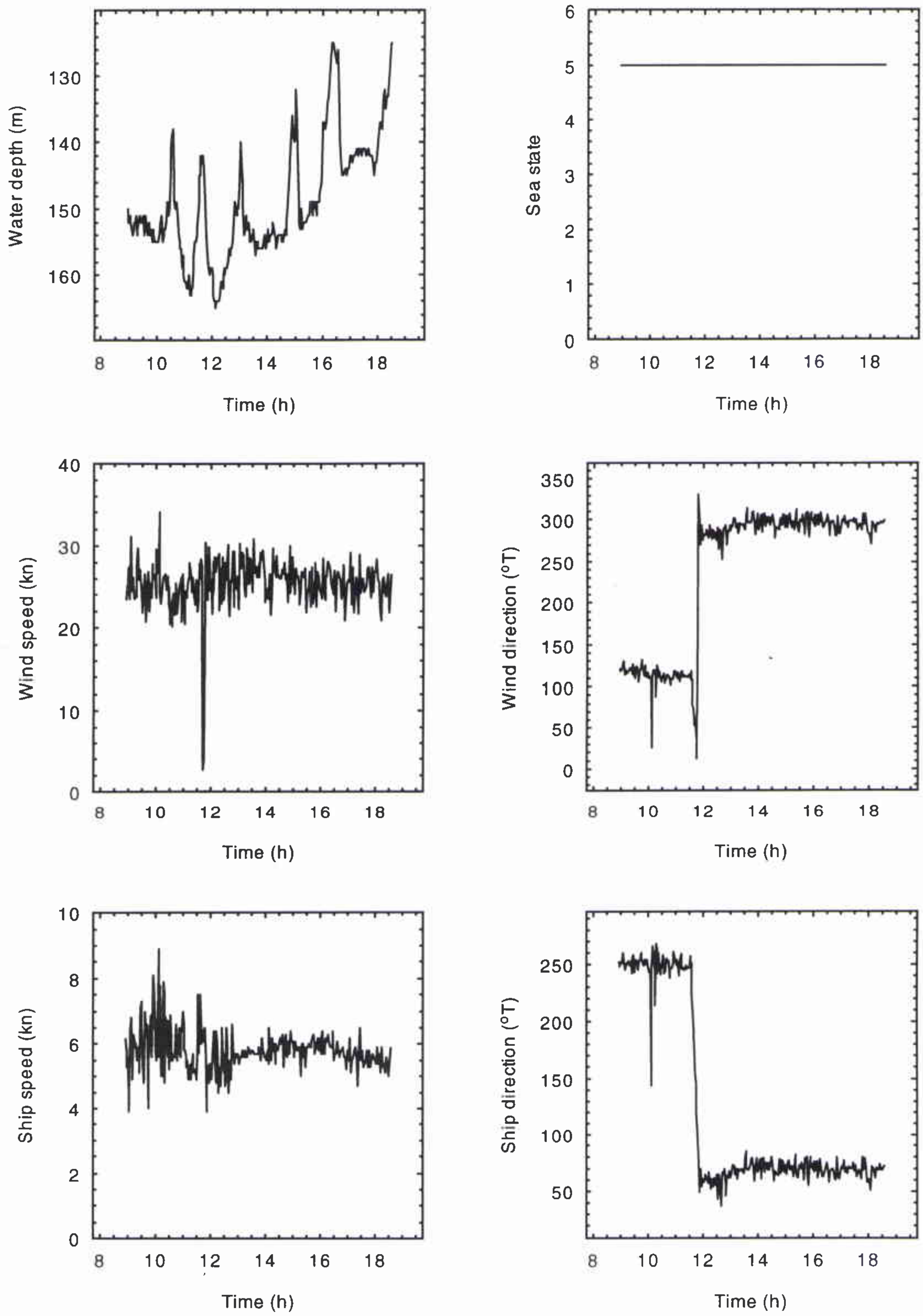

Figure B-22 *Environmental information for Alliance Run B4.*

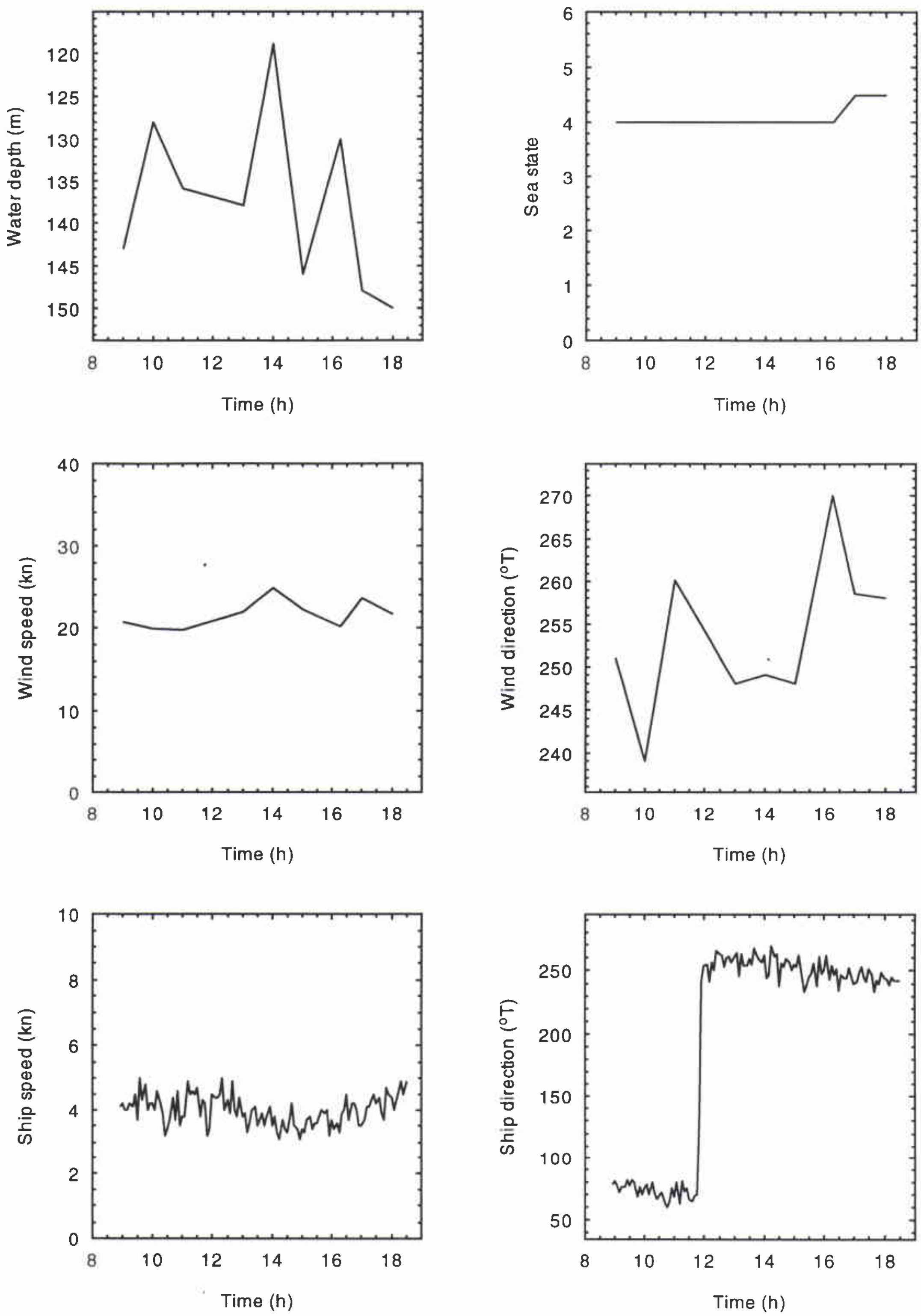

Figure B-23 *Environmental information from Bartlett for Alliance Run B4.*

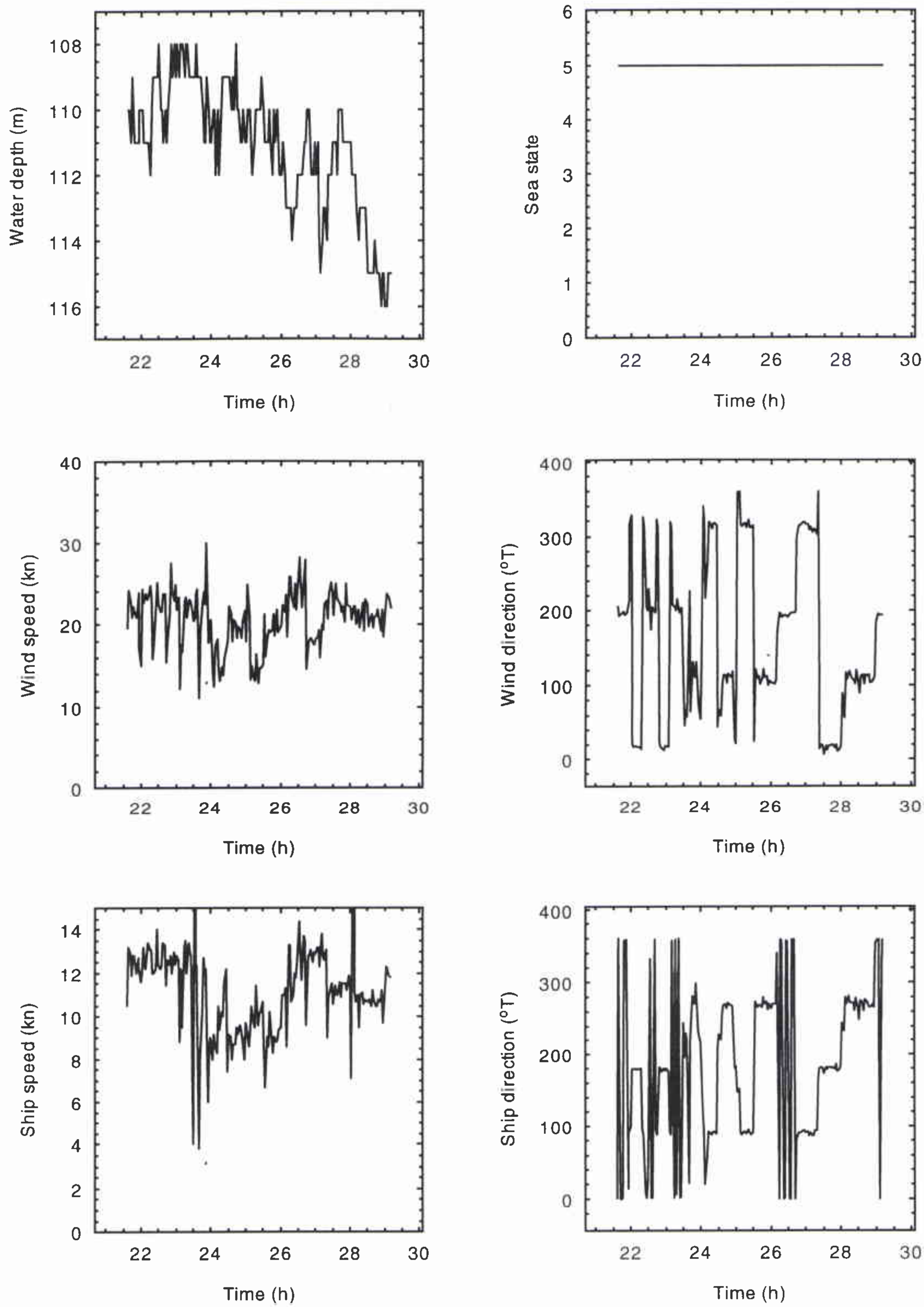

Figure B-24 *Environmental information for Alliance Run BATHY3.*

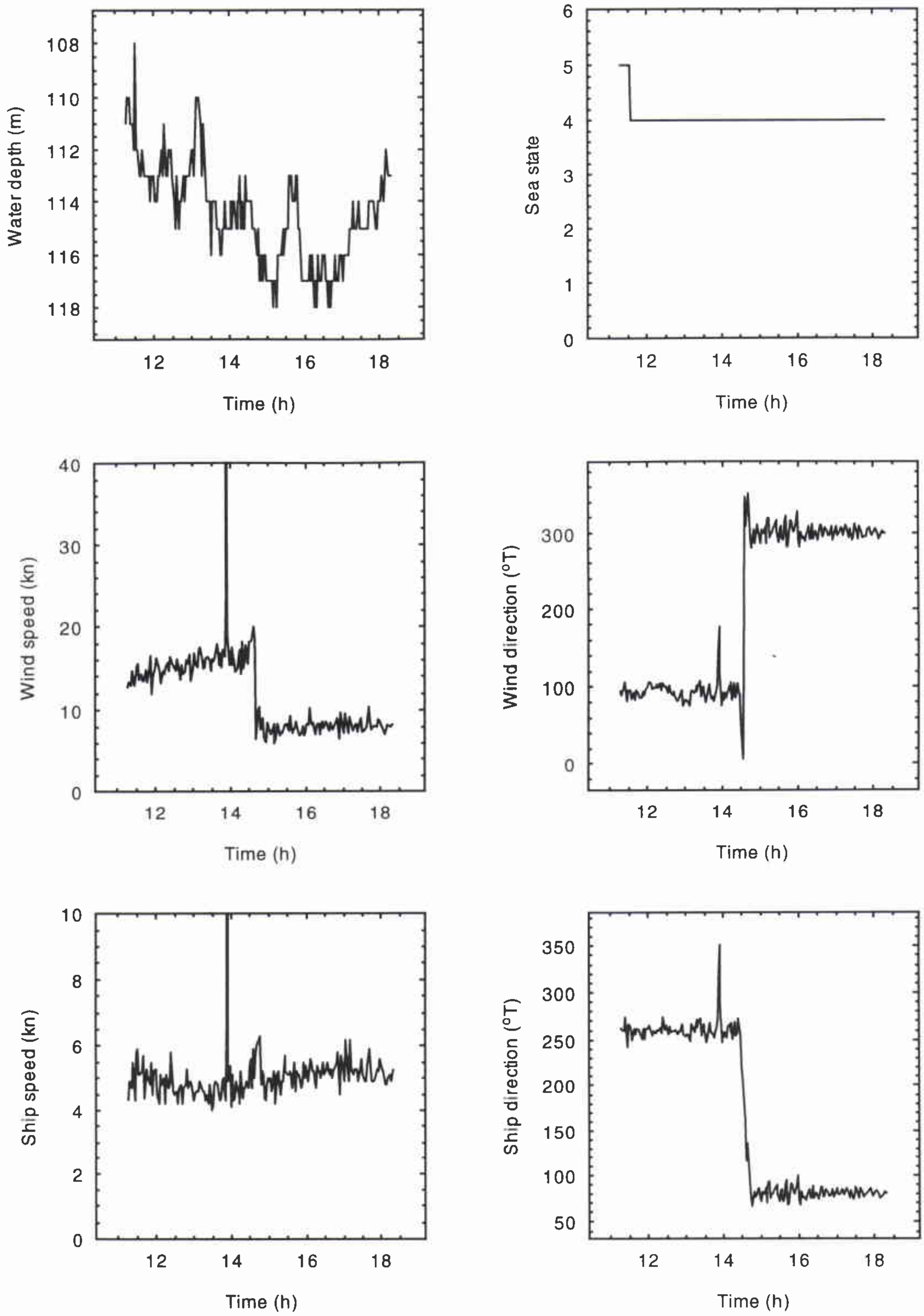

Figure B-25 *Environmental information for Alliance Run C1.*

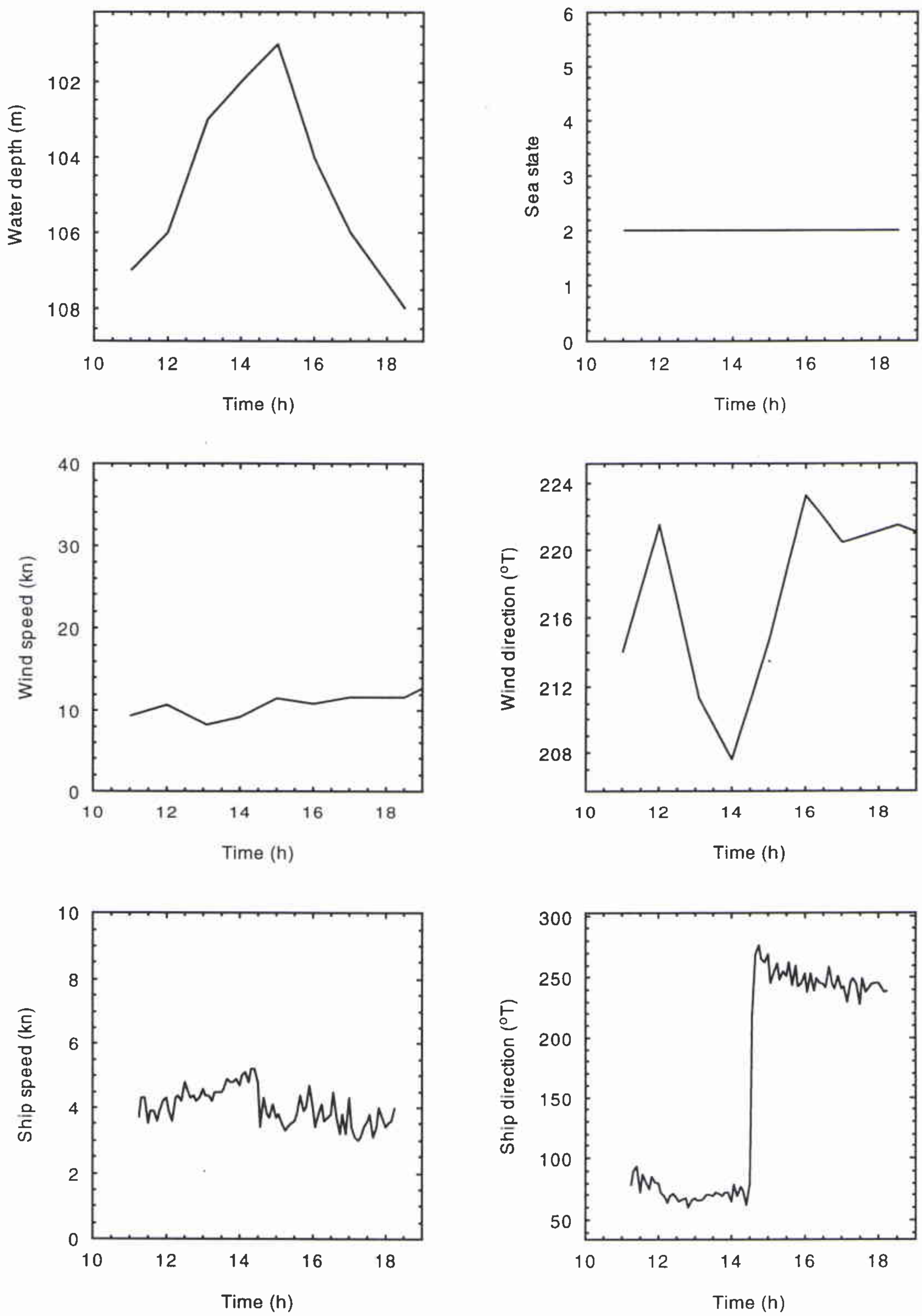

Figure B-26 *Environmental information from Bartlett for Alliance Run C1.*

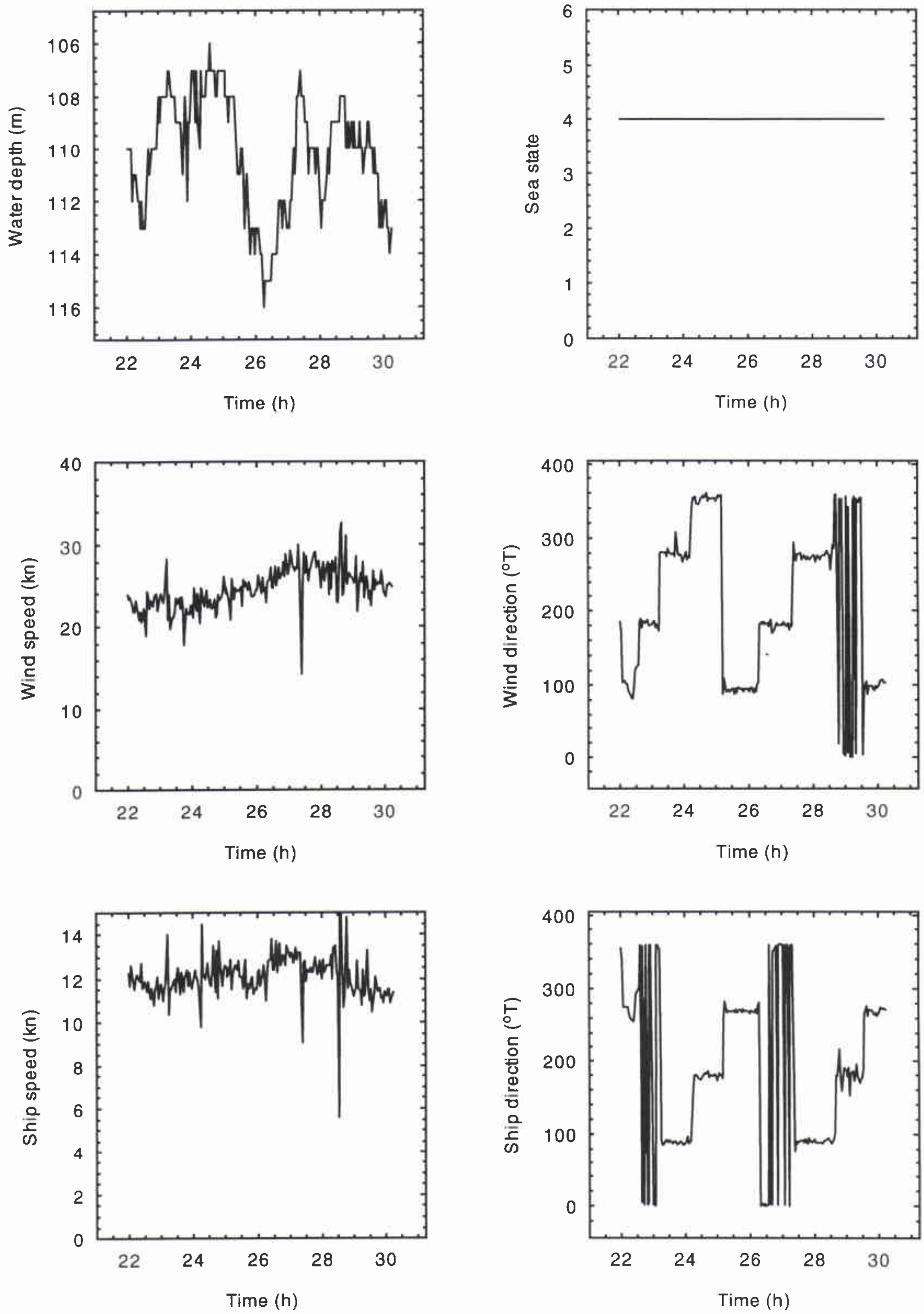

Figure B-27 *Environmental information for Alliance Run BATHY4.*

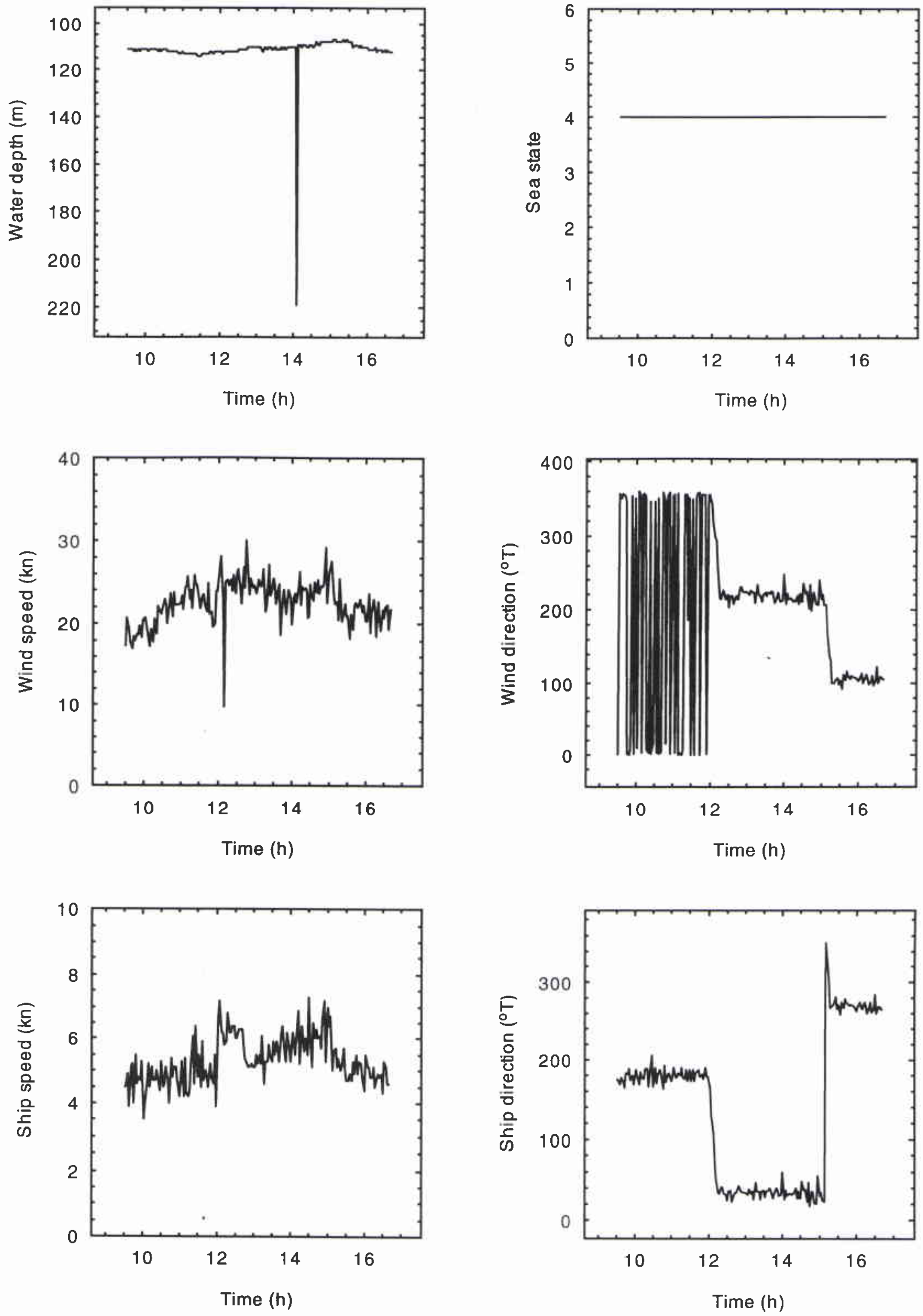

Figure B-28 *Environmental information for Alliance Run C2.*

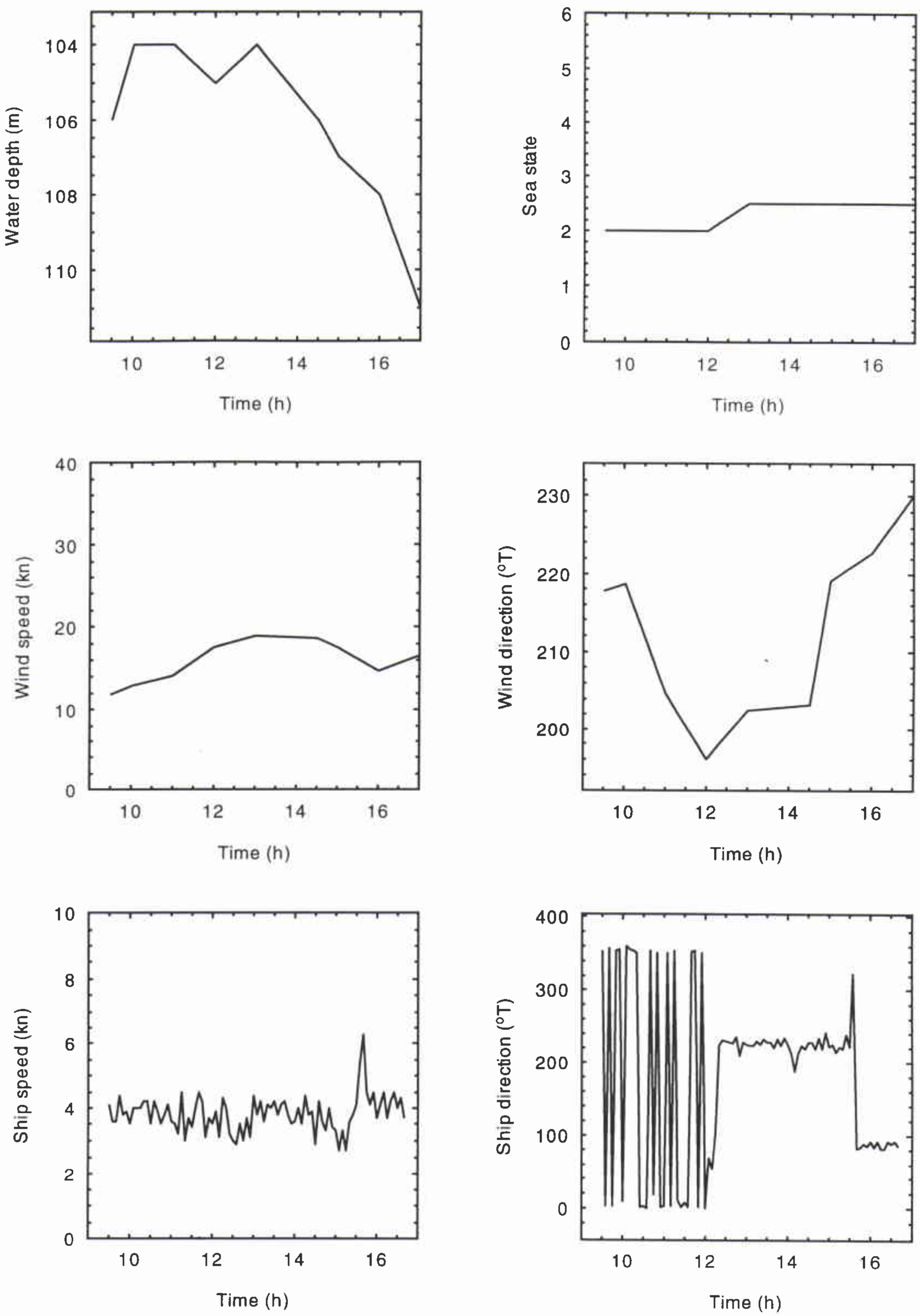

Figure B-29 *Environmental information from Bartlett for Alliance Run C2.*

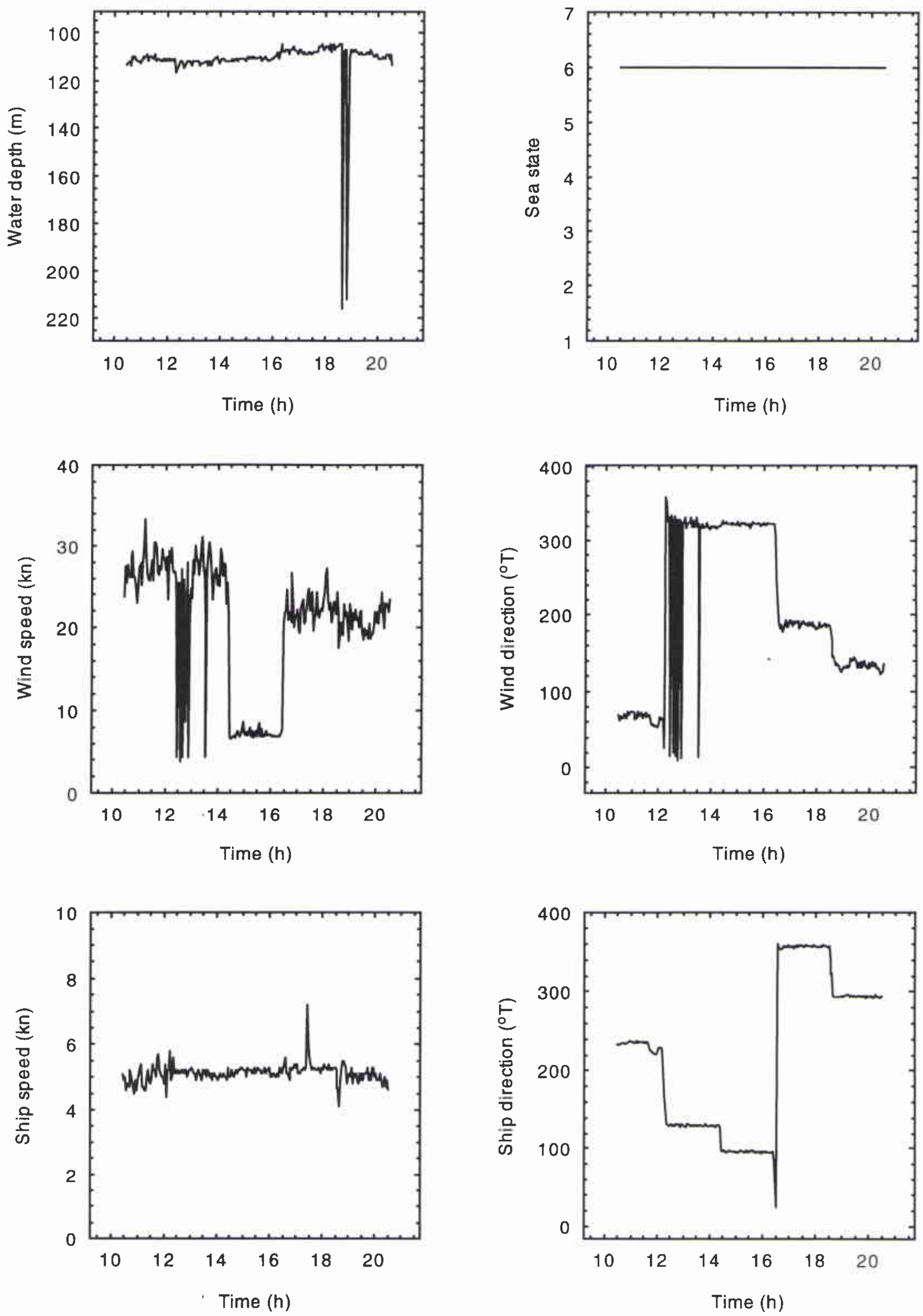

Figure B-30 *Environmental information for Alliance Run C3.*

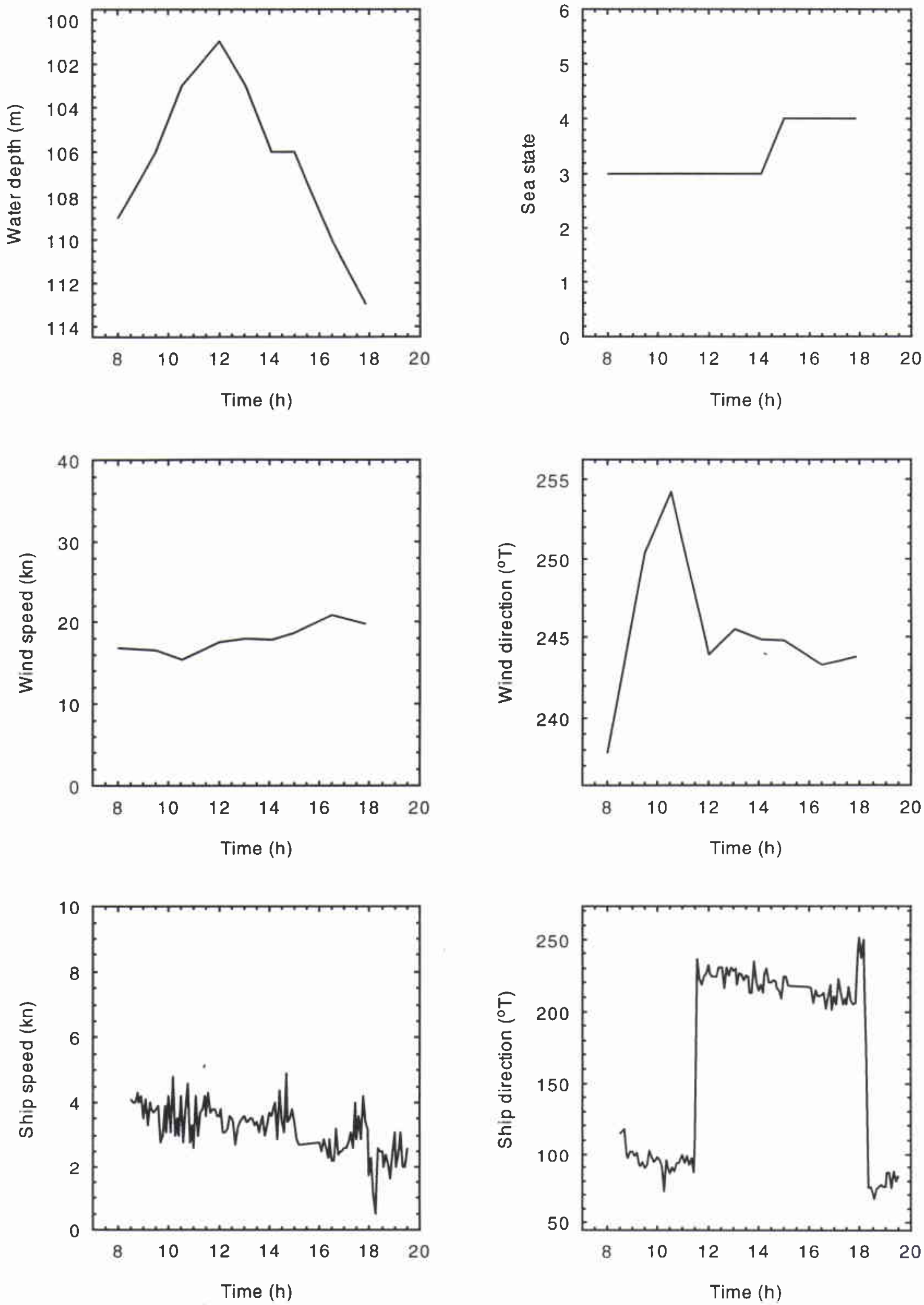

Figure B-31 *Environmental information from Bartlett for Alliance Run C3.*

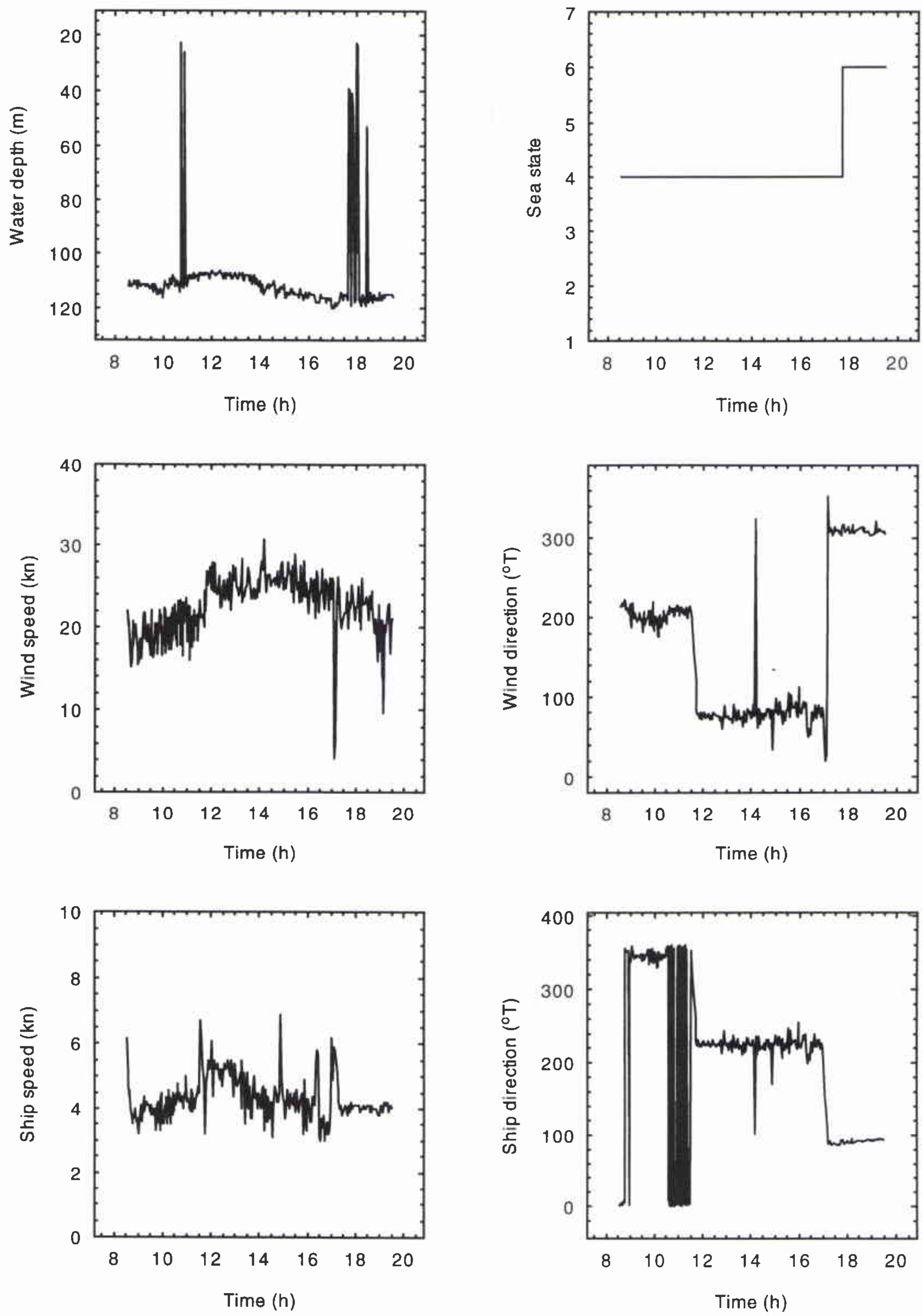

Figure B-32 *Environmental information for Alliance Run POLYG1.***Figure B-33** *Environmental information for Alliance Run POLYG2.***Figure B-34** *Environmental information for Alliance Run UNIBOOM.*

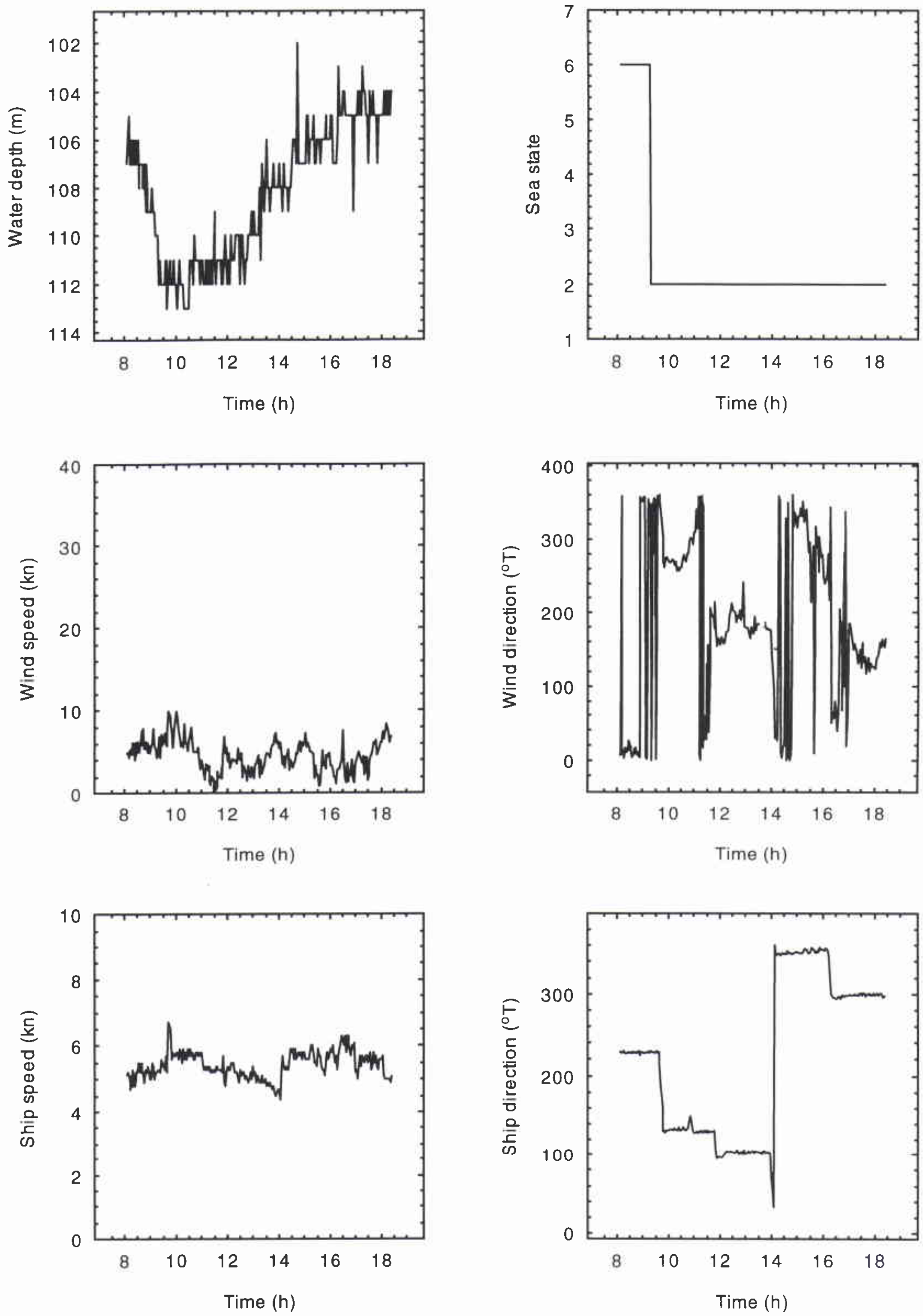

Figure B-33 *Environmental information for Alliance Run POLYG2.*

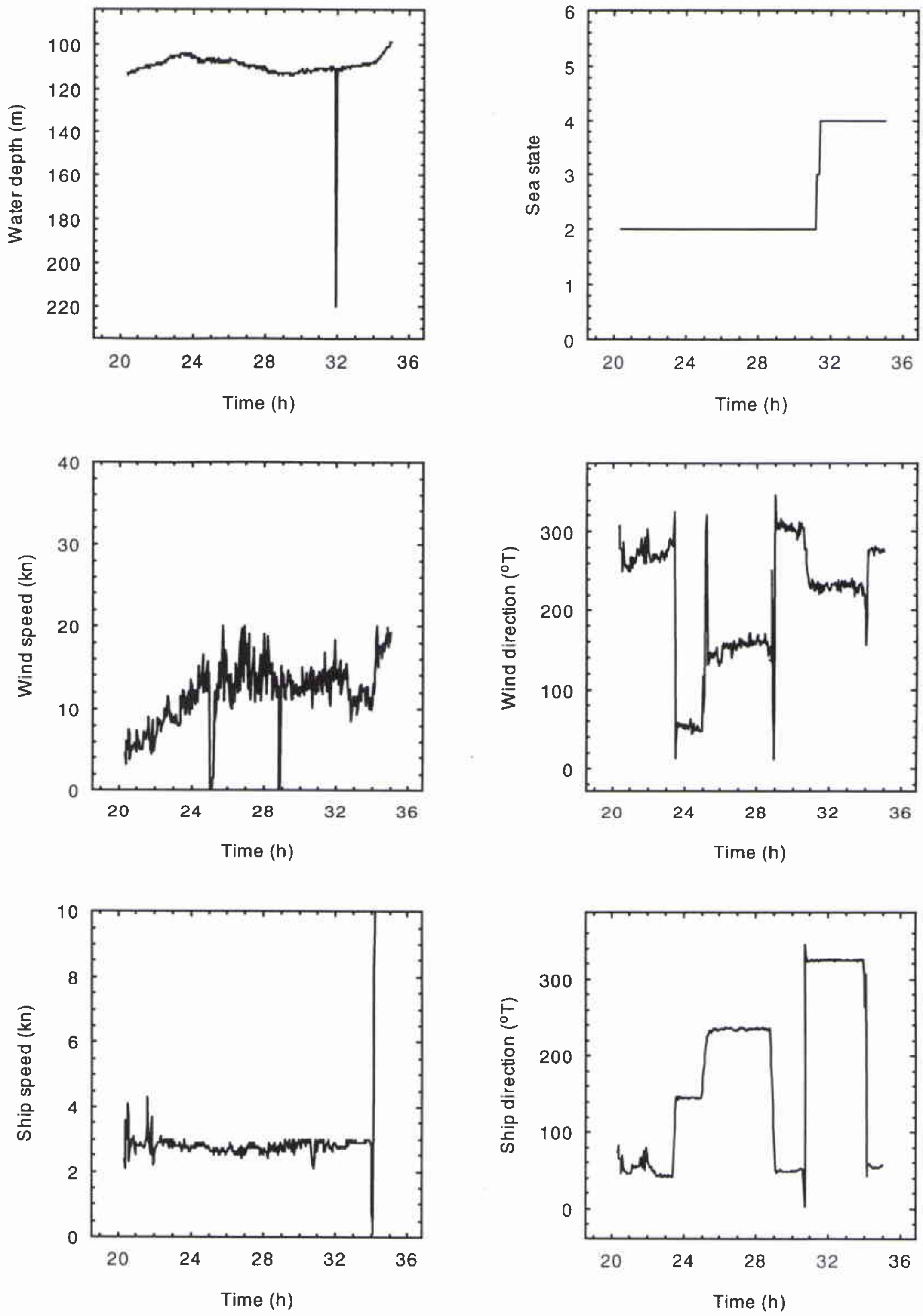

Figure B-34 *Environmental information for Alliance Run UNIBOOM.*

intentionally blank page

Appendix C
Sound speed profiles

This appendix contains information on the sound-speed profiles for the trial Celtic Duet. It begins with tables of the times and locations of CTDs and XBTs from *Alliance*, and the XBTs from *Bartlett*. These are followed by figures of the profiles themselves, grouped as indicated in Table 2 in the main part of the report.

XCTDs - *ALLIANCE*

XBT#	DATE	TIME	DEPTH	LATITUDE	LONGITUDE	SITE
1	06-JUL-1992	16:10	110.00	49. 29.8 N	6. 21.7 W	A

CTDs - *ALLIANCE*

CTD#	DATE	TIME	DEPTH	LATITUDE	LONGITUDE	SITE
1	04-JUL-1992	20:36	108.00	49. 30.7 N	5. 52.1 W	A
2	05-JUL-1992	20:09	120.00	49. 10.5 N	6. 01.0 W	A
3	06-JUL-1992	21:11	108.00	49. 30.2 N	5. 48.8 W	A
4	08-JUL-1992	07:47	155.00	49. 02.7 N	8. 05.1 W	B
6	08-JUL-1992	14:34	158.00	49. 00.4 N	8. 06.4 W	B
7	09-JUL-1992	17:28	151.00	48. 59.7 N	8. 08.3 W	B
8	10-JUL-1992	19:59	153.00	48. 01.8 N	8. 02.2 W	B
9	11-JUL-1992	20:44	136.00	49. 01.7 N	8. 00.7 W	B
10	13-JUL-1992	19:15	126.00	49. 06.9 N	7. 32.6 W	B
11	14-JUL-1992	21:19	110.00	50. 08.2 N	7. 13.3 W	C
12	15-JUL-1992	09:15	109.00	50. 08.9 N	7. 03.7 W	C
13	16-JUL-1992	06:50	115.00	50. 02.9 N	7. 12.7 W	C
14	17-JUL-1992	06:58	114.00	50. 04.7 N	7. 09.1 W	C
15	17-JUL-1992	20:01	116.00	50. 04.6 N	7. 14.1 W	C
16	18-JUL-1992	09:09	108.00	50. 20.4 N	7. 03.9 W	C
17	18-JUL-1992	21:06	115.00	50. 21.5 N	7. 05.2 W	C
18	20-JUL-1992	06:32	100.00	49. 39.1 N	5. 52.7 W	A
19	20-JUL-1992	18:49	106.00	49. 37.8 N	6. 01.8 W	A

XBTs - *ALLIANCE*

XBT#	DATE	TIME	DEPTH	LATITUDE	LONGITUDE	SITE
1	08-JUL-1992	16:15	150.00	48. 58.9 N	7. 56.5 W	B
2	08-JUL-1992	17:15	149.00	48. 56.9 N	7. 50.9 W	B
3	08-JUL-1992	18:17	145.00	48. 57.7 N	7. 52.6 W	B
4	08-JUL-1992	19:13	152.00	49. 02.5 N	8. 03.8 W	B
5	08-JUL-1992	20:14	144.00	49. 07.0 N	8. 15.4 W	B
6	08-JUL-1992	21:14	146.00	49. 11.2 N	8. 26.9 W	B
7	08-JUL-1992	22:19	140.00	49. 15.9 N	8. 39.1 W	B
8	08-JUL-1992	23:15	148.00	49. 20.0 N	8. 49.8 W	B
9	08-JUL-1992	23:45	133.00	49. 22.0 N	8. 55.5 W	B
10	09-JUL-1992	09:05	154.00	49. 03.0 N	8. 05.5 W	B
11	09-JUL-1992	12:05	148.00	49. 09.2 N	8. 18.9 W	B
12	09-JUL-1992	14:53	144.00	49. 10.4 N	8. 02.3 W	B
13	10-JUL-1992	13:41	153.00	49. 03.2 N	8. 02.5 W	B
14	10-JUL-1992	14:15	150.00	48. 59.4 N	8. 05.2 W	B
15	10-JUL-1992	15:14	142.00	48. 58.9 N	8. 13.8 W	B
16	10-JUL-1992	16:15	144.00	49. 05.0 N	8. 15.2 W	B
17	10-JUL-1992	17:15	143.00	49. 12.9 N	8. 07.7 W	B
18	10-JUL-1992	18:15	147.00	49. 07.9 N	7. 58.0 W	B
19	11-JUL-1992	09:03	148.00	49. 01.3 N	7. 59.0 W	B
20	11-JUL-1992	11:34	134.00	48. 56.2 N	7. 44.8 W	B
21	11-JUL-1992	14:35	138.00	49. 06.0 N	7. 49.5 W	B
22	11-JUL-1992	16:26	136.00	49. 12.3 N	7. 52.6 W	B
23	12-JUL-1992	08:43	143.00	48. 58.1 N	7. 55.8 W	B
24	12-JUL-1992	10:35	142.00	49. 03.6 N	8. 10.0 W	B
25	12-JUL-1992	12:55	153.00	49. 05.8 N	8. 03.5 W	B
26	12-JUL-1992	19:04	146.00	49. 04.8 N	8. 04.6 W	B
27	13-JUL-1992	08:53	146.00	48. 59.5 N	8. 04.0 W	B
28	13-JUL-1992	12:03	163.00	48. 53.3 N	8. 25.9 W	B
29	13-JUL-1992	14:00	153.00	48. 57.9 N	8. 10.5 W	B
30	15-JUL-1992	12:03	113.00	50. 07.0 N	7. 21.4 W	C
31	15-JUL-1992	14:34	114.00	50. 04.7 N	7. 39.3 W	C
32	15-JUL-1992	16:27	114.00	50. 05.8 N	7. 24.6 W	C
33	15-JUL-1992	20:23	113.00	50. 03.1 N	7. 07.3 W	C
34	16-JUL-1992	10:30	111.00	50. 02.8 N	7. 10.8 W	C
35	16-JUL-1992	12:00	112.00	49. 55.2 N	7. 10.7 W	C
36	16-JUL-1992	14:00	110.00	50. 03.1 N	7. 00.0 W	C
37	16-JUL-1992	15:08	104.00	50. 08.9 N	6. 53.9 W	C
38	16-JUL-1992	16:17	112.00	50. 09.6 N	7. 02.3 W	C
39	17-JUL-1992	10:04	111.00	50. 15.1 N	7. 08.2 W	C
40	17-JUL-1992	11:29	106.00	50. 20.9 N	7. 09.0 W	C
41	17-JUL-1992	14:17	114.00	50. 12.3 N	7. 23.9 W	C
42	17-JUL-1992	17:00	117.00	50. 04.7 N	7. 35.6 W	C
43	17-JUL-1992	19:00	118.00	50. 04.8 N	7. 21.1 W	C

44	20-JUL-1992	08:57	100.00	49. 31.7 N	6. 05.5 W	A
45	20-JUL-1992	11:09	112.00	49. 22.6 N	6. 01.1 W	A
46	20-JUL-1992	13:20	107.00	49. 18.3 N	5. 45.5 W	A
47	20-JUL-1992	15:23	106.00	49. 25.1 N	5. 42.4 W	A
48	20-JUL-1992	17:27	105.00	49. 33.9 N	5. 53.0 W	A

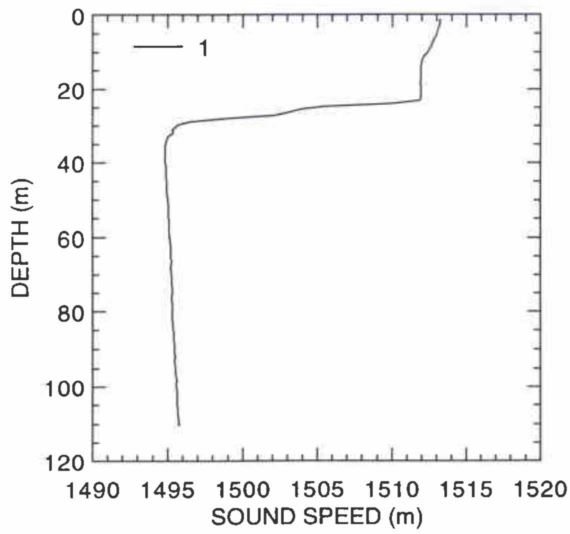

Figure C-1 *Sound speed profile from Alliance XCTD #1 at Site A.*

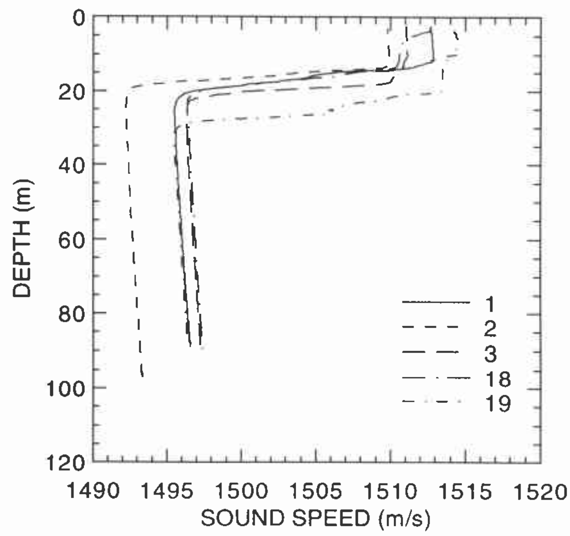

Figure C-2 *Sound speed profiles from Alliance CTDs #1–3, 18 and 19 at Site A.*

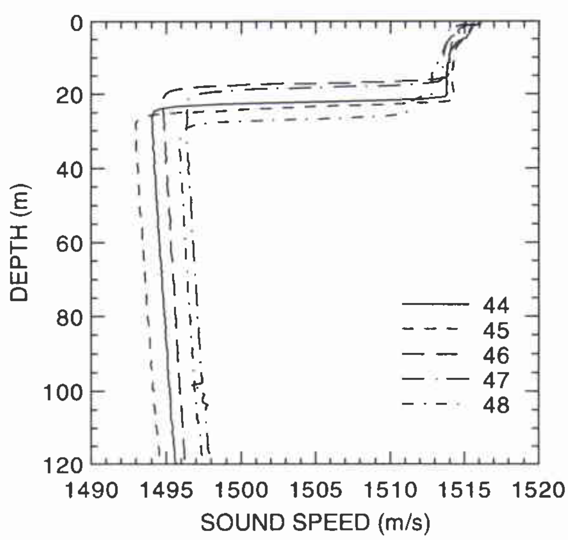

Figure C-3 *Sound speed profiles from Alliance XBTs #44–48 at Site A.*

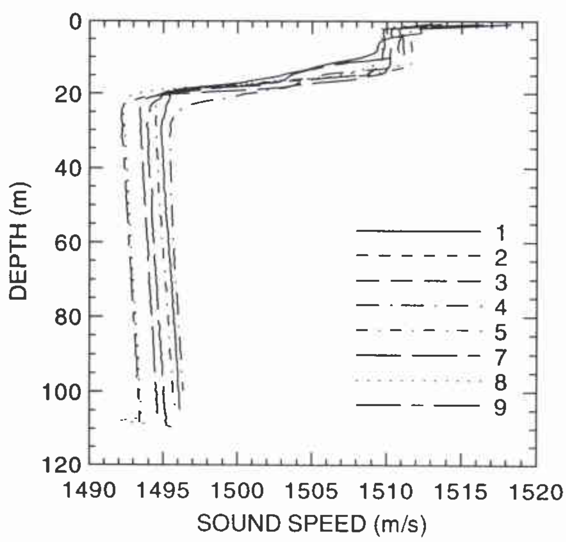

Figure C-4 *Sound speed profiles from Bartlett XBTs #1-9 at Site A.*

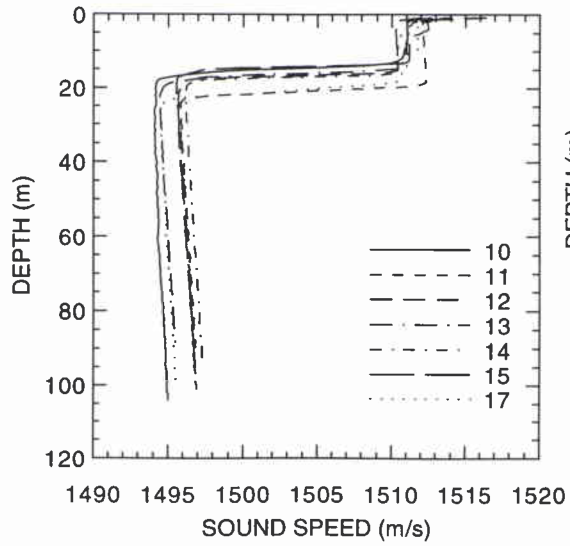

Figure C-5 *Sound speed profiles from Bartlett XBTs #10-17 at Site A.*

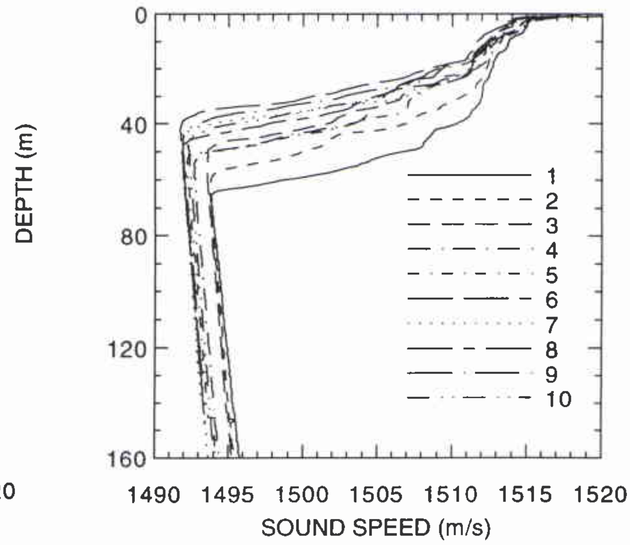

Figure C-6 *Sound speed profiles from Alliance XBTs #1-10 at Site B.*

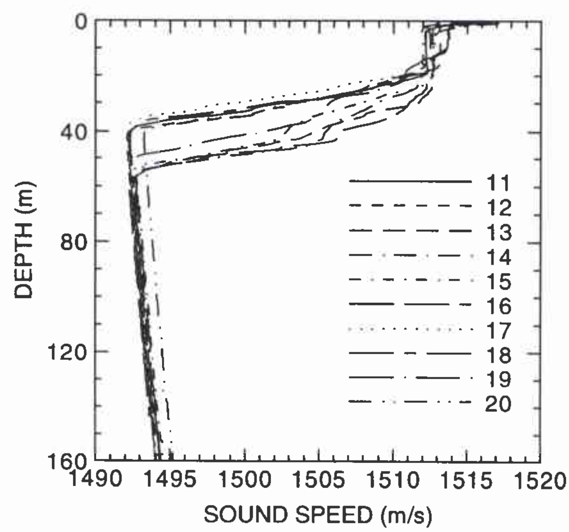

Figure C-7 *Sound speed profiles from Alliance XBTs #11-20 at Site B.*

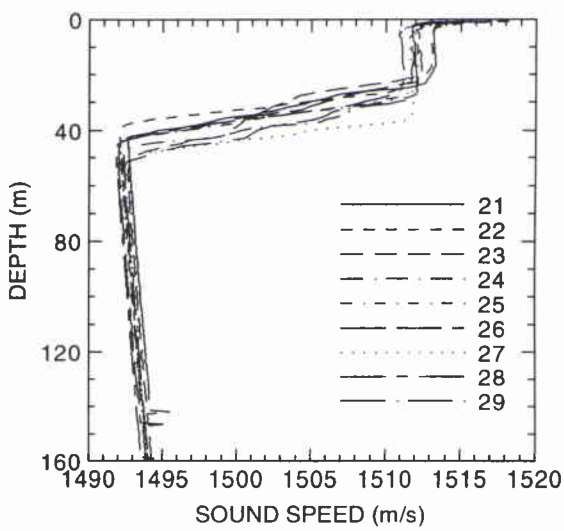

Figure C-8 *Sound speed profiles from Alliance XBTs #21-29 at Site B.*

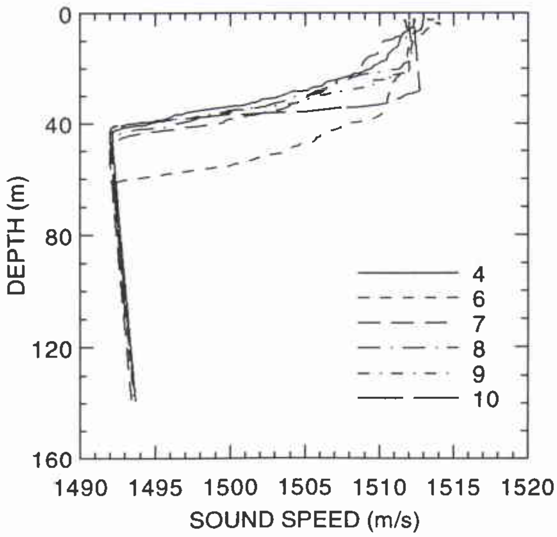

Figure C-9 *Sound speed profiles from Alliance CTDs #4–10 (except 5) at Site B.*

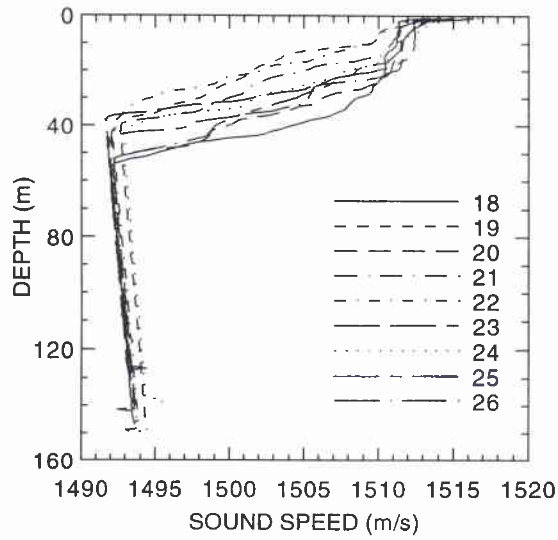

Figure C-10 *Sound speed profiles from Bartlett XBTs #18-26 at Site B.*

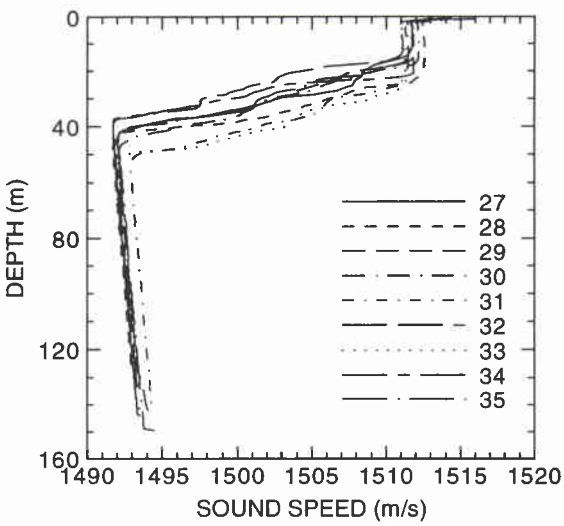

Figure C-11 *Sound speed profiles from Bartlett XBTs #27-35 at Site B.*

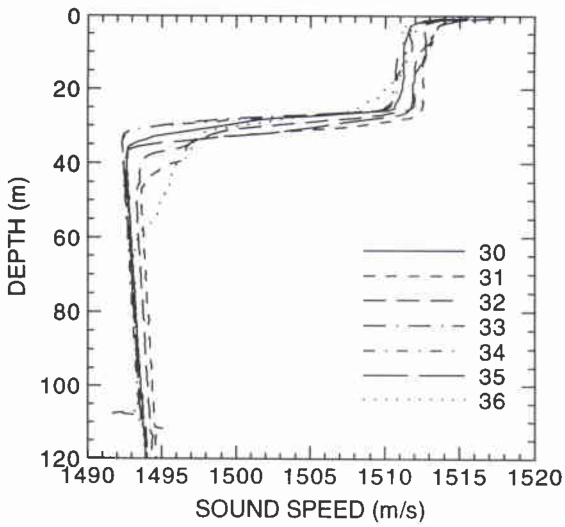

Figure C-12 *Sound speed profiles from Alliance XBTs #30-36 at Site C.*

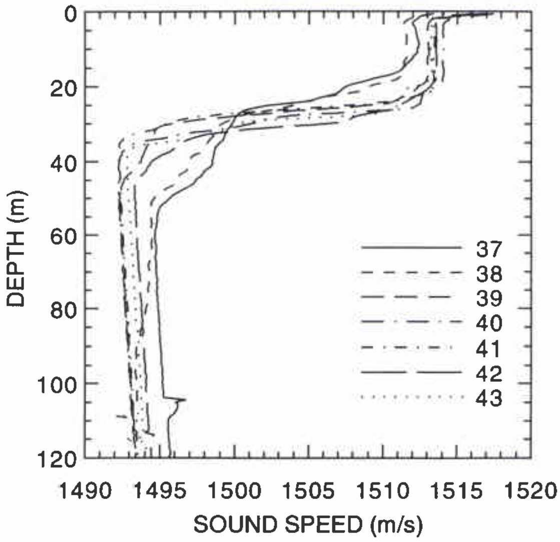

Figure C-13 *Sound speed profiles from Alliance XBTs #37-43 at Site C.*

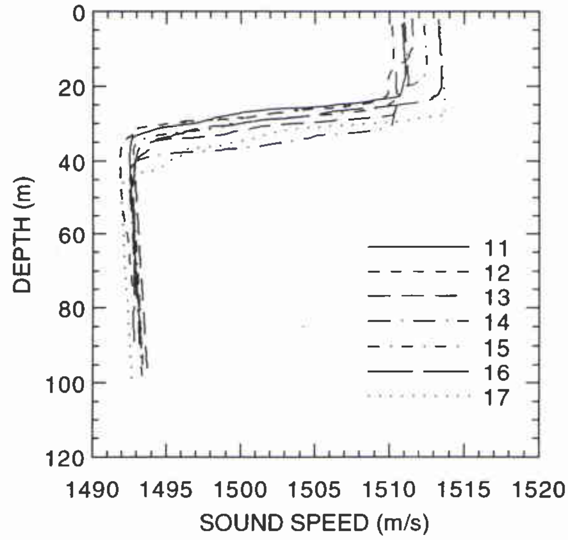

Figure C-14 *Sound speed profiles from Alliance CTDs #11–17 at Site C.*

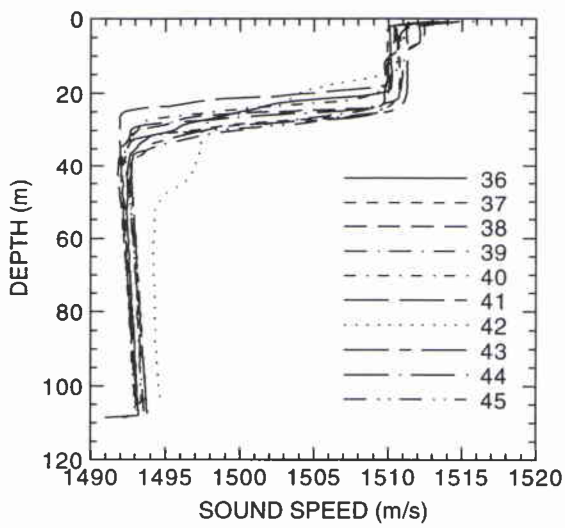

Figure C-15 *Sound speed profiles from Bartlett XBTs #36–45 at Site C.*

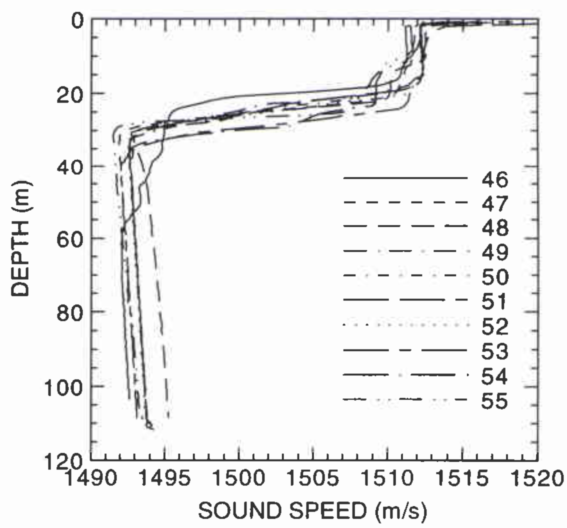

Figure C-16 *Sound speed profiles from Bartlett XBTs #46-55 at Site C.*

intentionally blank page

Appendix D
The Complex-Band-Shifting Procedure

A complex-band-shifting (CBS) procedure was developed for the Celtic Duet sea trial to support data reduction from the pulse data. The basic idea is to shift the signal down to zero frequency, apply a low-pass filter, and decimate the data. The CBS procedure and filters are implemented digitally using FFT techniques, described in Harris [19] and Vaidyanathan [20]. Harris [19, p. 224] uses a time series. The procedure developed in the SACLANTCEN Real-Time Group uses a frequency rotation of the spectrum of the input data; this is equivalent, but faster. The following examples illustrate the approach.

Figure D-1 shows the filter F60, designed with a Kaiser window, using the approach of Vaidyanathan [20]. For the sampling frequency of 6000 Hz (Nyquist frequency 3000 Hz) it has a pass band of 40 Hz, a cutoff frequency of 50 Hz (normalized frequency 0.01667), a transition band of 20 Hz (normalized frequency 0.0066), and a rejection band attenuation of 50 dB. The resultant filter has 439 (complex) coefficients. The amplitude response in dB is shown in the upper part of the figure, and the phase response (linear in the pass band), is shown in the lower part of the figure (modulo 360°).

Figure D-2 shows the replica of a 2.4-second HFM pulse (called H1) of 60 Hz bandwidth between 300 and 360 Hz, at sampling frequency of 3000 Hz. The first 0.1 s is plotted, together with the frequency response of the entire pulse. (The dB axis of the frequency response is arbitrary.)

Figure D-3 shows the CBS replica for H1, shifted from the centre frequency 330 Hz, for a sampling frequency of 3000 Hz, and FFT size of 2048. The decimation rate is 25, giving a resultant sampling frequency of 120 Hz. Note that the filter response F60 has been applied, so the replica ramps up from 0 during the 439 samples at the beginning and end of the pulse (~0.15 s); the solid line is the real part and the dotted line is the imaginary part of the shifted replica. The frequency response (arbitrary scale) is shown in the lower part of the figure; note that the negative frequencies are folded into the spectrum from 120 to 60 Hz.

The CBS procedure illustrated for H1 can be applied to the received signals from the actual transmitted pulses H1. An example is shown in Fig. 19. Note the main arrival (overloaded), the decaying reverberation, and scattering from some features. The replica needs only to be calculated once, and applied to each of the H1 pulses.

The matched filter can be applied using the CBS time series, and the CBS replica. Figure 20a shows how the higher signal near 70 s in Fig. 19 has become quite peaked, indicating a compact scattering feature.

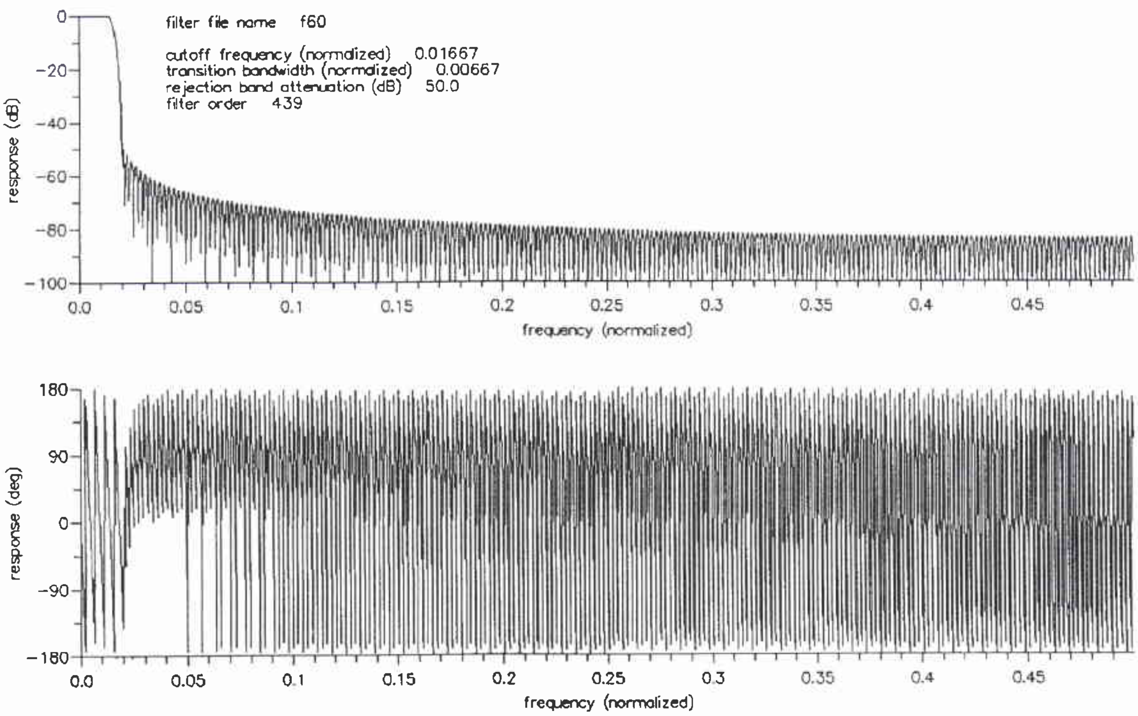

Figure D-1 *Amplitude and phase response for low-pass filter F60.*

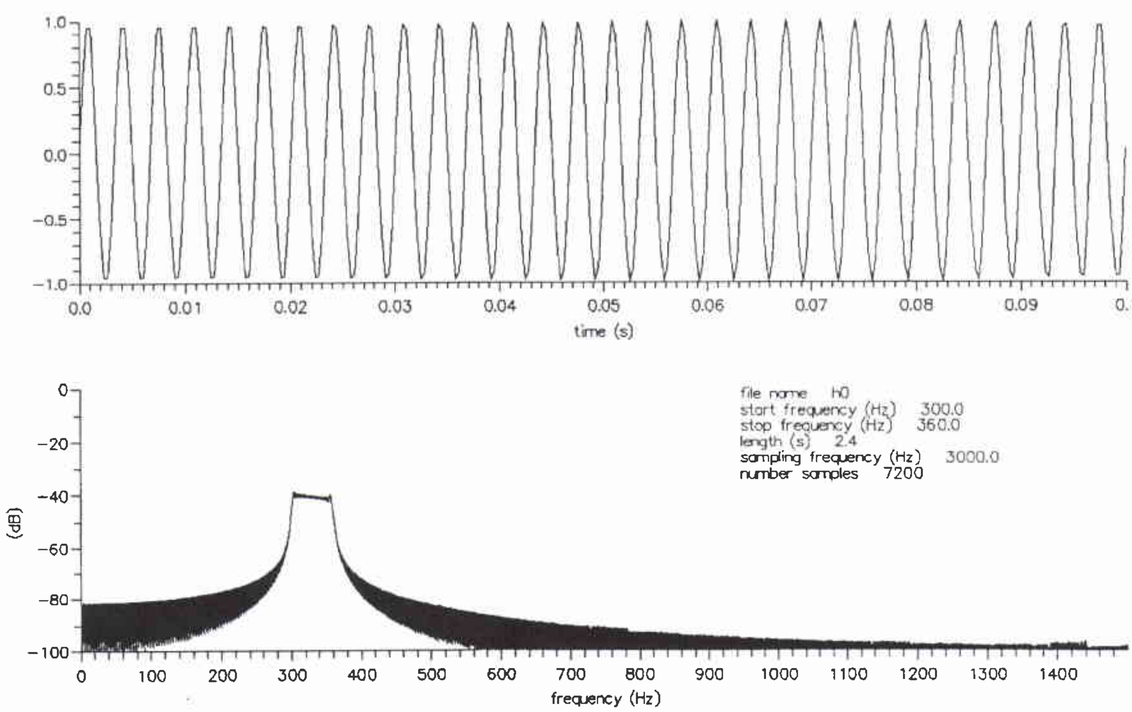

Figure D-2 *Portion of waveform for pulse H1 and frequency response for the full pulse.*

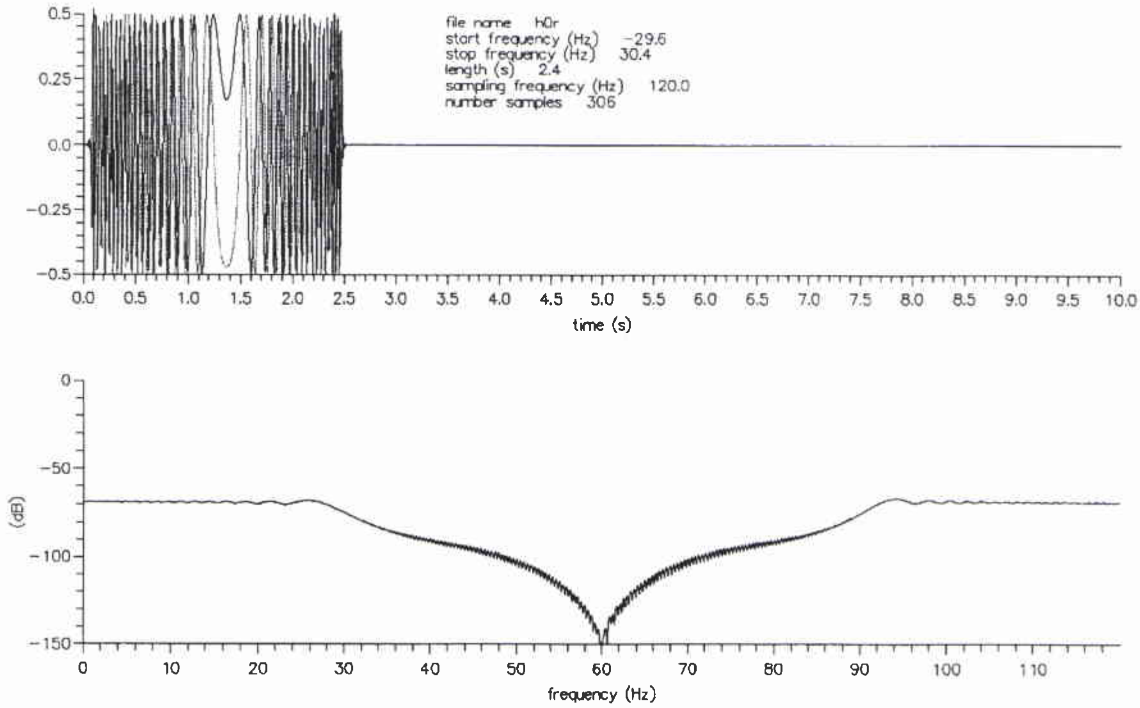

Figure D-3 *Complex-band-shifted replica and frequency response of pulse H1.*

intentionally blank page

Appendix E
Archival Data

During the trial the raw data were saved on HDDR tapes and the processed data from the WARP system were saved on optical disks. There were 120 HDDR tapes used and 7 optical disks recorded. Information was received from NRL on Exabyte tapes, part of which was copied to optical disks.

Table E-1 is intended to be a partial guide to where various files can be found. It refers to the data stored on SACLANTCEN's RV-20 optical disks in VAX/VMS BACKUP format. For the large data files, the file name and saveset name are usually the same except for the extension .DAT for the file name, and .SAV or .BCK for the saveset name. An asterisk denotes many files with similar names.

SACLANTCEN data are backed up on optical disks OD123, OD124, OD126, OD127, OD130, OD131, and OD150. Some data from NRL are stored on optical disks 105, OD125, OD149, and OD151. Hydrophone data for Run C1 were played back post-cruise from HDDR tapes for Kirsteins [17].

The raw data from the towed and vertical arrays are stored on 120 HDDR tapes. The numbers are not listed here. They can be found in the Cruise Log and Cruise Report.

Table E-1 *Cross reference between optical disks and file names for the various runs. An asterisk denotes many files with similar names.*

Alliance Run #	Optical Disk	File or SaveSet Names
BATHY1	OD150A	See IMS files below
A1	OD131A / B	A*
A2	OD131A / B	A*
CW1	OD131B	PROP01-PROP10
	OD237A	T_*
BATHY2	OD150A	See IMS files below
TLB		
CW2	OD130A	PROP10-PROP13
	OD123B	
	OD237A	V_*
B1	OD130A	BH*, BV*
B2SUS	OD130B	B2SUS*
	OD126A	B2VSUS*
B2	OD126A	B2T*, B2V*
	OD130A	B2*_WM1
	OD130B	B2_*
CW3	OD237A	V_*
B3	OD126A	B3_*
B4	OD126A	B4_*
BATHY3	OD150A	See IMS files below
C1	OD124A	C1_*
BATHY4	OD150A	See IMS files below
C2	OD124A	C2_*
C3	OD124B	C3_*
POLYG1	OD124B	P_1*
	OD123A	P_2* to P_5*
POLYG2	OD127A	P2_1*, P2_*
	OD127B	P3_* to P2_5*
UNIBOOM	n/a	
IMS	OD150A	IMSVAXG.SAV, IMSSIRENA.SAV
XBT	OD150A	CTDXBT.SAV
Waverider	OD237	WAVERIDER.BCK

Report no. changed (Mar 2006): SM-307-UU

Document Data Sheet

NATO UNCLASSIFIED

Security Classification		Project No.
NATO UNCLASSIFIED		05
Document Serial No.	**Date of Issue**	**Total Pages**
SM-307	October 1996	104 pp.

Author(s)

D.D. Ellis, F. Desharnais, R.H. Clarke, R. Hollett, E. Baglioni, A. Legner

Title

CELTIC DUET A Joint SACLANTCEN/NRL Shallow-Water Sea Trial in the Celtic Sea during July 1992: Data Summary

Abstract

In July 1992 a joint shallow-water sea trial was conducted in the Celtic Sea by the SACLANT Undersea Research Centre and the US Naval Research Laboratory. The purpose was to obtain monostatic and bistatic reverberation measurements, with supporting transmission loss and environmental measurements. Three sites were chosen: one where small sand waves were deemed to be present, a second where there were large sand ridges, and a third where thin sediment over a chalk bottom was expected. Two ships were used, the NRV *Alliance*, and the USNS *Bartlett*. Both ships were equipped with towed arrays and towed projectors. Both ships had vertical arrays and supporting equipment for environmental measurements. A follow-up sea trial obtained additional propagation and geo-acoustic measurements. The report describes the experiments, the ship tracks, and environmental inputs. Some results are shown, including a summary of the waverider analysis carried out at Imperial College in the UK. A few acoustic results are shown, describing checks on the data quality and illustrating representative data for propagation, ambient noise and reverberation.

Keywords

reverberation – ambient noise – propagation – sea-surface spectra – sound speed profiles

Issuing Organization

North Atlantic Treaty Organization
SACLANT Undersea Research Centre
Viale San Bartolomeo 400, 19138 La Spezia, Italy

[From N. America: SACLANTCEN (New York) APO AE 09613]

Tel: +39 (0)187 540 111
Fax:+39 (0)187 524 600

E-mail: library@saclantc.nato.int

NATO UNCLASSIFIED

Report no. changed (Mar 2006): SM-307-UU

Initial Distribution for SM-307

SCNR for SACLANTCEN		*National Liaison Officers*	
SCNR Belgium	1	NLO Canada	1
SCNR Canada	1	NLO Denmark	1
SCNR Denmark	1	NLO Germany	1
SCNR Germany	1	NLO Italy	2
SCNR Greece	2	NLO Netherlands	1
SCNR Italy	1	NLO UK	3
SCNR Netherlands	1	NLO US	4
SCNR Norway	1		
SCNR Portugal	1		
SCNR Spain	1		
SCNR Turkey	1		
SCNR UK	1		
SCNR US	2		
French Delegate	1		
SECGEN Rep. SCNR	1	Total external distribution	34
NAMILCOM Rep. SCNR	1	SACLANTCEN Library	26
SACLANT	3	Total number of copies	60